Supporting Information

Recyclable rhodium catalyst anchored onto bipyridine covalent triazine framework for transfer hydrogenation of N-heteroarenes in water

Jonas Everaert,[a] Karen Leus,[b] Hannes Rijckaert,[c] Maarten Debruyne,[a] Kristof Van Hecke,[c] Rino Morent,[b] Nathalie De Geyter,[b] Veronique Van Speybroeck,[d] Pascal Van Der Voort,[c] Christian V. Stevens*[a]

[a] SynBioC Research Group, Department of Green Chemistry and Technology, Faculty of Bioscience Engineering, Ghent University, Coupure Links 653, B-9000 Ghent, Belgium. E-mail: Chris.Stevens@UGent.be

[b] Department of Applied Physics, Faculty of Engineering and Architecture, Ghent University, Sint-Pietersnieuwstraat 41-B4, B-9000 Ghent, Belgium.

[c] Department of Chemistry, Faculty of Sciences, Ghent University, Krijgslaan 281-S3, B-9000 Ghent, Belgium.

[d] Center for Molecular Modeling (CMM), Ghent University, Technologiepark 46, B-9052 Zwijnaarde, Belgium.

Table of Contents

1 General methods

Solvents and reagents were purchased from commercial suppliers and used without further purification, unless otherwise stated. Thin layer chromatography (TLC) was performed using glass-backed 0.25 mm Merck silica gel 60 F_{254} TLC plates, and spots were visualized by UV light (254 nm). Column chromatography was performed using silica gel (particle size 35–70 µm, pore diameter 6 nm). ^{1}H NMR and ^{13}C NMR spectra were recorded at 400 and 101 MHz, respectively, using a Bruker Avance III HD 400 spectrometer equipped with a ^{1}H/BB z-gradient probe (BBO, 5 mm). The spectra were recorded at 25 °C and were processed using TopSpin 3.6.2. Chemical shifts (δ) are reported in parts per million (ppm) downfield of tetramethylsilane (internal reference) and coupling constants (*J*) are reported in hertz (Hz). Peaks were assigned with the aid of 2D spectra (COSY, HSQC, H2BC and HMBC). The atom numbering used in the assignment of peaks is in accordance with the IUPAC Nomenclature of Organic Chemistry. Infrared spectra (FT-IR) of discrete compounds were recorded from samples in neat form on a Shimadzu IRAFFINITY-1S FT-IR spectrophotometer with an ATR (Attenuated Total Reflectance) accessory. Only selected absorbances (ν_{max}, cm^{-1}) are reported. HPLC-MS analyses were performed on an Agilent 1200 Series HPLC system equipped with a Supelco Ascentis Express C18 column (3 cm × 4.6 mm, 2.7 µm fused-core particles, 90 Å) and connected to a UV-DAD detector and an Agilent 1100 Series LC/MSD-type SL mass spectrometer with electrospray ionization (ESI, capillary voltage 4 kV, fragmentor voltage 70 V) and with a mass-selective single-quadrupole detector.

Infrared (DRIFT) spectra of CTFs were recorded in the region 650–4000 cm^{-1} with a Thermo Nicolet 6700 FT-IR spectrophotometer equipped with a nitrogen-cooled MCT detector and a KBr beam splitter. Samples were measured within KBr powder. Nitrogen sorption measurements were carried out on a BELSORP-mini II apparatus at 77 K. Prior to measurements, samples were degassed at 120 °C under vacuum for 16 h. Specific surface areas were calculated using the Brunauer–Emmett–Teller (BET) method. For the BET calculations, pressure ranges were chosen in accordance with the criteria described by Rouquerol *et al*.[1] The pore size distribution was determined using the quenched solid density functional theory (QSDFT) model for N_2 adsorbed on carbons with cylindrical pores, implemented in Quantachrome's ASiQwin software (v4.0). Total pore volumes were determined at P/P_0 = 0.99. Elemental analysis was performed on a Thermo Scientific Flash 2000 CHNS/O analyzer equipped with a TCD detector. Powder X-ray diffraction (PXRD) spectra were collected using a Bruker D8 Advance diffractometer with a Cu Kα radiation source (λ = 1.5418 Å) at 40 kV and 45 mA and a scanning speed of 1° min^{-1}. X-ray photoelectron spectroscopy (XPS) was performed using the PHI 5000 VersaProbe II spectrometer equipped with a monochromatic Al Kα X-ray source (hv = 1486.6 eV). The samples were excited with an X-ray beam (size 200 µm) over an area of 500 x 500 $µm^2$ at a power of 50 W. Wide range survey scans and high-resolution spectra were recorded with a pass energy of 187.85 eV and 23.5 eV and a step size of 0.8 eV and 0.1 eV, respectively. All spectra were acquired at a take-off angle of 45° relative

to the sample surface in the XPS chamber, where the pressure was constantly maintained below 10^{-6} Pa. The survey scans were used to determine and quantify the surface elemental composition and were analyzed using the MultiPak (v9.6) software by utilizing a Shirley background and applying the relative sensitivity factors supplied by the instrument's manufacturer. The detailed high-resolution spectra were also analyzed using the same software package via their curve fitting into different peaks to identify the corresponding chemical bonds. The energy scale of all acquired spectra was calibrated with respect to the hydrocarbon component of the C 1s spectrum (285.0 eV). The reported quantitative results are the mean values obtained from six independent analysis points measured on each sample. Scanning transmission electron microscopy (STEM) images were taken with a high-angle annular dark-field (HAADF) detector on a JEOL JEM-2200FS TEM with a field emission gun at 200 kV. ICP-OES analyses were carried out on a Thermo Scientific iCAP 7400 Duo ICP-OES instrument. Prior to analysis, the samples were subjected to microwave-assisted (Mars 6 – CEM) digestion in a closed vessel using nitric acid (67%). Thermo Scientific™ Qtegra™ Intelligent Scientific Data Solution™ (ISDS) software was used to process the results.

2 Synthesis of building block and CTFs

2.1 Synthesis of 2,2'-bipyridine-5,5'-dicarbonitrile (1)

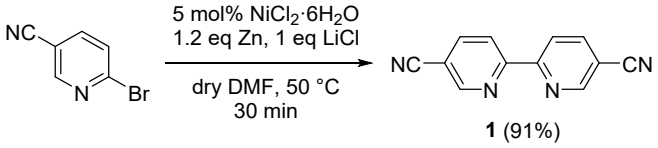

1 (91%)

2,2'-Bipyridine-5,5'-dicarbonitrile **1** was synthesized via a Ni-catalyzed reductive homocoupling of 2-bromo-5-cyanopyridine, as previously reported by us.[2]

2,2'-bipyridine-5,5'-dicarbonitrile (1)

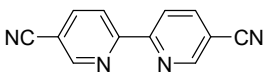

Yield 91%. Beige solid, mp >260 °C. **^{1}H NMR** (400 MHz, $CDCl_3$): δ 8.14 (2H, dd, *J* = 8.3, 2.0 Hz, $H^{4,4'}$), 8.64 (2H, dd, *J* = 8.3, 0.8 Hz, $H^{3,3'}$), 8.97 (2H, dd, *J* = 2.0, 0.8 Hz, $H^{6,6'}$). **^{13}C NMR** (101 MHz, $CDCl_3$): δ 110.7 ($C^{5,5'}$), 116.5 (2 x C≡N), 121.7 ($C^{3,3'}$), 140.5 ($C^{4,4'}$), 152.1 ($C^{6,6'}$), 157.0 ($C^{2,2'}$). **IR** (ATR, cm^{-1}): ν_{max} = 2239 (C≡N), 1591, 1535, 1460, 1369, 1236, 1028, 947, 845, 733, 650, 550, 488. **MS** (ESI): m/z (%) 207 ($[M + H]^+$, 100). Anal. Calcd for $C_{12}H_6N_4$: C, 69.90; H, 2.93; N, 27.17. Found: C, 70.04; H, 3.04; N, 27.90. The data are in accordance with those reported in the literature.[3]

2.2 Synthesis of bpyCTF

bpyCTF was synthesized under ionothermal conditions using $ZnCl_2$, which was dried overnight at 120 °C under vacuum prior to use. Typically, a quartz ampule was charged with 2,2'-bipyridine-2,2'-dicarbonitrile **1** (320 mg, 1.55 mmol, 1 eq) and $ZnCl_2$ (1.06 g, 7.76 mmol, 5 eq). The ampule was placed under vacuum, flame-sealed and heated to 400 °C in a Nabertherm furnace oven with a heating rate of 1 °C min^{-1}. After 48 h at 400 °C, the temperature was brought to room temperature and the obtained crude solid was ground with pestle and mortar. The black powder was subsequently stirred overnight in a HCl solution (1 M) under reflux conditions to remove $ZnCl_2$ and unreacted monomer. Afterward, the solid was filtered and successively washed with water until neutral pH was reached (3 x 200 mL), THF (3 x 200 mL), ethanol (3 x 100 mL) and acetone (3 x 200 mL). The obtained black powder was dried overnight under vacuum at 120 °C before further use.

2.3 Preparation of Rh@bpyCTF

$[Cp^*RhCl_2]_2$ complex (22.5 mg, 0.04 mmol) was dissolved in a mixture of anhydrous MeOH/$CHCl_3$ (1/1, 30 mL) under argon atmosphere. bpyCTF (300 mg, Rh/bpy molar ratio 0.05) was added, and the black suspension was heated to reflux temperature for 24 h. After cooling to room temperature, the solid was filtered and successively washed with MeOH (3 x 100 mL), CH_2Cl_2 (3 x 100 mL) and Et_2O (3 x 100 mL). The obtained solid was dried overnight under vacuum at 120 °C. ICP-OES analysis was performed to quantify the actual loading of Rh metal in the bpyCTF.

3 Characterization data for CTFs

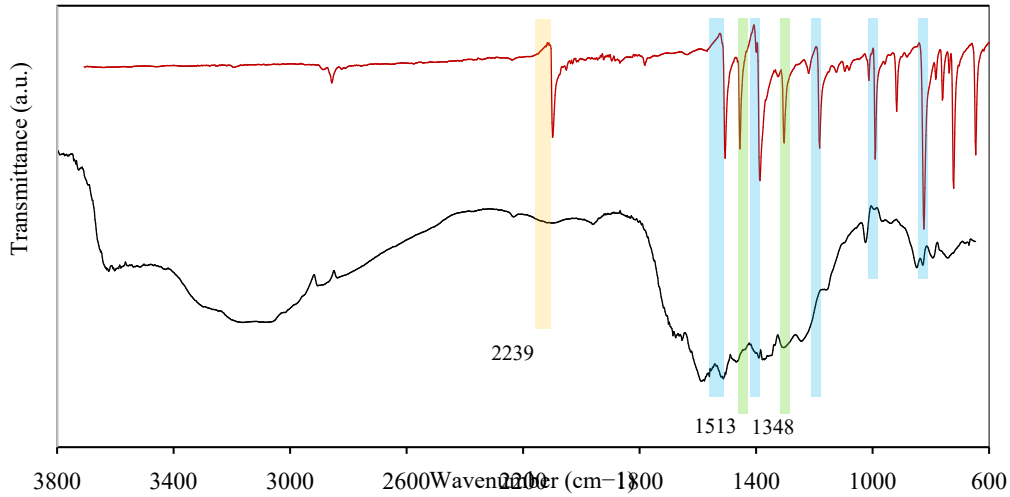

Figure S1. FT-IR spectral comparison between the monomer, 2,2'-bipyridine-5,5'-dicarbonitrile **1** (red) and bpyCTF (black). The characteristic band of the cyano group is highlighted in yellow, the triazine ring in green and bipyridine moiety in blue.

Table S1. Elemental analysis (C/H/N) of bpyCTF.

	Measured	Theoretical
C (wt%)	60.3	69.9
H (wt%)	3.1	2.9
N (wt%)	15.5	27.2
Residue (wt%)	21.1	–
C/N molar ratio	5.1	3.0

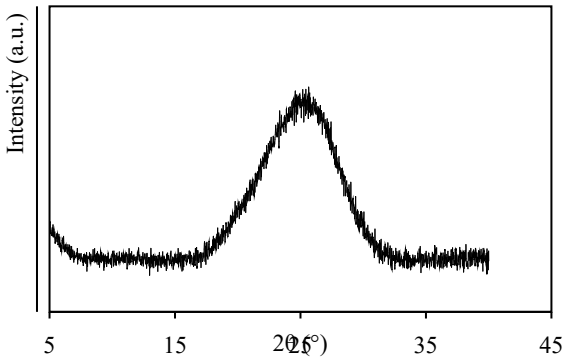

Figure S2. Powder X-ray diffraction pattern of bpyCTF.

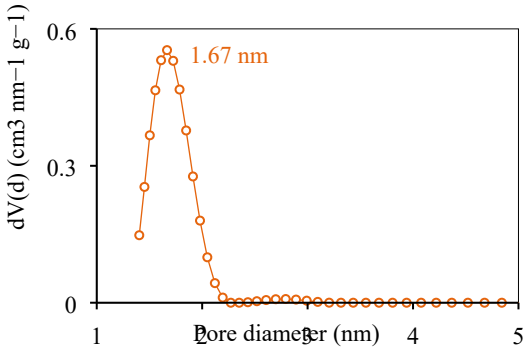

Figure S3. Pore size distribution of bpyCTF.

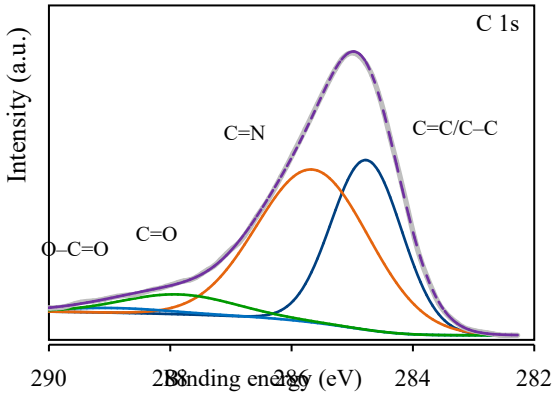

Figure S4. High-resolution C 1s XPS spectrum of bpyCTF.

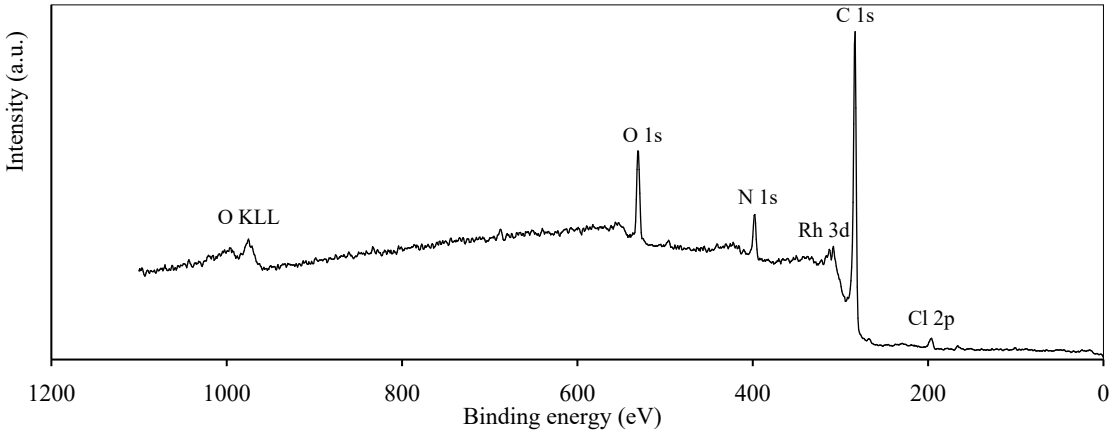

Figure S5. XPS survey spectrum of Rh@bpyCTF.

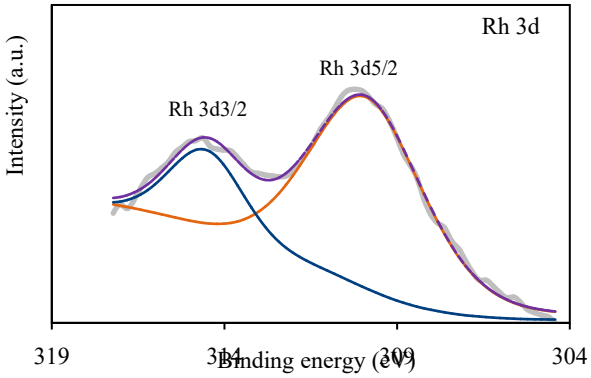

Figure S6. High-resolution Rh 3d XPS spectrum of Rh@bpyCTF after six reaction cycles.

4 Transfer hydrogenation reactions

4.1 General procedure in the reaction conditions optimization

The stirring speed was fixed (800 rpm) in all transfer hydrogenation reactions to improve the repeatability and to allow a comparison between reactions. Aqueous formate solutions were prepared by dissolving HCOOH and HCOONa in HPLC-grade water. The quantities needed were calculated using Equation 1. The pH of the solution was verified at 21 °C with a pH meter.

$$pH = pK_a + \log\left(\frac{[HCOONa]}{[HCOOH]}\right) \quad (1)$$

$$pK_a\,(HCOOH) = 3.6$$

In a 12 mL test tube, an aqueous HCOOH/HCOONa buffer (2 M, pH 4.5, 5 mL) was preheated to 80 °C, after which 2-methylquinoxaline **2a** (0.5 mmol) and Rh@bpyCTF (5.6 mg, 0.25 mol% Rh) were sequentially added. The test tube was provided with a cap which was not screwed tight to ensure CO_2 could still be released. The reaction mixture was vigorously stirred (fixed at 800 rpm) to ensure sufficient mixing. Aliquots (300 µL) were taken basified (pH > 10) with NaOH and extracted with Et_2O (3 x 500 µL). The combined organic phases were evaporated to dryness and the residue was analyzed by ^{1}H NMR spectroscopy ($CDCl_3$).

4.2 Catalyst recycling experiments

Catalyst recycling experiments were performed in a 100 mL test tube with a 4 M HCOOH/HCOONa buffer solution (pH 4.5, 25 mL) and with 2-methylquinoxaline **2a** (322 µL, 2.5 mmol) in 1 mL EtOAc, and Rh@bpyCTF (28 mg, 0.25 mol% Rh). An aliquot was taken after 3 h reaction to determine the conversion by ^{1}H NMR spectroscopy ($CDCl_3$). After each run, the catalyst was recovered by filtration, whereupon it was successively washed with water, acetone and diethyl ether, and subsequently dried under vacuum at 100 °C for 5 h. The dried catalyst was then applied in the next reaction run.

4.3 Synthesis of [Cp*Rh(bpy)Cl]Cl

$[Cp^*Rh(\mu\text{-}Cl)Cl]_2$ dimer (30 mg, 48 µmol) and 2,2'-Bipyridine (15 mg, 96 µmol) were dissolved in $CHCl_3$ (1 mL) and stirred at room temperature. Within a few minutes, an orange suspension started to form. After 1 h, the orange precipitate was collected by filtration, rinsed with cold $CHCl_3$, and dried *in vacuo*, yielding [Cp*Rh(bpy)Cl]Cl as pale orange solid (38 mg, 84%). The formation of a complex with bipyridine was confirmed by ^{1}H NMR analysis (Figure S7). A downfield shift of the NMR signals was observed upon binding of the ligand with Rh.

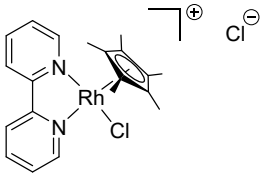

(2,2'-bipyridine-κ*N,N'*)chlorido(η^5-pentamethylcyclopentadienyl)rhodium(III) chloride

Pale orange solid. Yield 84%. **^{1}H NMR** (400 MHz, $CDCl_3$): δ 1.73 (15H, s, $C_5(C\underline{H}_3)_5$), 7.82 (2H, ddd, *J* = 7.8, 5.7, 1.1 Hz, $H^{5,5'}$), 8.26 (2H, td, *J* = 7.8, 1.3 Hz, $H^{4,4'}$), 8.85 (2H, dd, *J* = 5.7, 1.3 Hz, $H^{6,6'}$), 9.08 (2H, d, *J* = 7.8 Hz, $H^{3,3'}$). **^{13}C NMR** (101 MHz, $CDCl_3$): δ 9.2 ($C_5(\underline{C}H_3)_5$), 97.1 (d, $J_{Rh,C}$ = 8.1 Hz, $\underline{C}_5(CH_3)_5$), 125.7 ($C^{3,3'}$), 128.4 ($C^{5,5'}$), 140.8 ($C^{4,4'}$), 151.1 ($C^{6,6'}$), 154.7 ($C^{2,2'}$). **IR** (ATR, cm^{-1}): ν_{max} = 3541, 3283, 1603, 1443, 1302, 1024, 766. **MS** (ESI): m/z (%) 429/431 ($[C_{20}H_{23}N_2ClRh]^+$, 100), 197 ($[C_{20}H_{23}N_2ClRh - Cl]^{2+}$, 53).

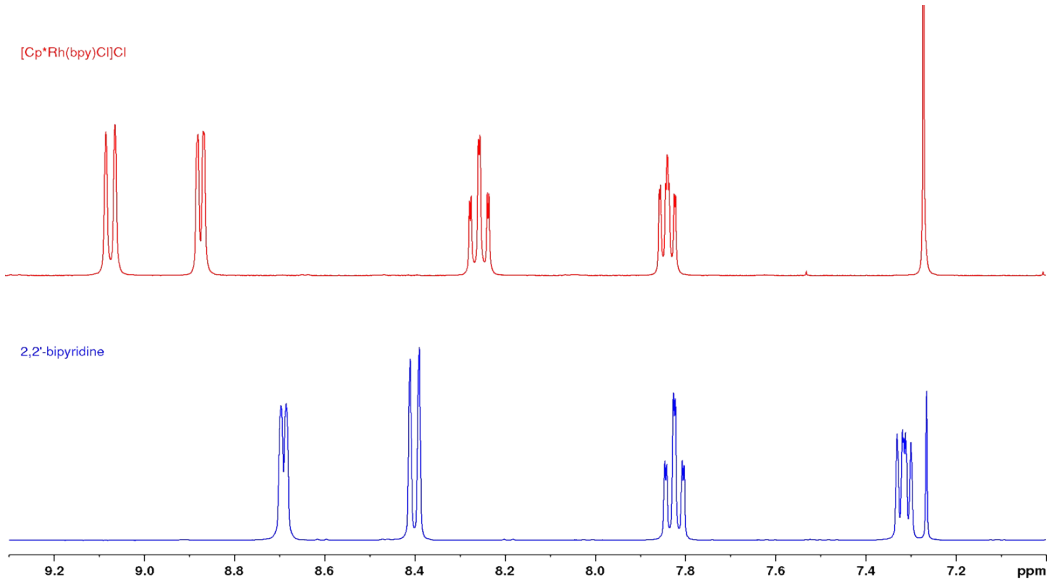

Figure S7. ^{1}H NMR spectra ($CDCl_3$) of free 2,2'-bipyridine (bottom) and 2,2'-bipyridine coordinated in [Cp*Rh(bpy)Cl]Cl (top). A downfield shift of the NMR signals was observed upon binding of the ligand with Rh.

4.4 Continuous flow transfer hydrogenation

The continuous flow setup was constructed as follows (Figure S8): A solution of 2-methylquinoxaline in EtOAc and an aqueous HCOOH/HCOONa buffer solution were introduced into the system by means of two ReaXus 6010R high-performance reciprocating pumps (Teledyne Isco). The applied concentrations and flow rates (FR) of the solutions are given in Table 5 of the main article. The liquid streams were brought into contact by using a PEEK Y-connector (IDEX Health &Science, part No. P-512), creating a segmented flow regime before entering the packed-bed reactor column. The packed-bed reactor column was assembled by filling a PTFE tubing (BOLA, cat. No. S1810-33, I.D. 2.4 mm, O.D. 3.2 mm) with 215 mg Rh@bpyCTF (containing 2.3 wt% Rh) mixed with 750 mg glass beads (Ø 750 µm). The packed bed had a length of 15 cm and was held in place by a cotton plug of about 2 cm at each end (Figure S8). The column was mounted vertically in a GC oven at 80 °C and the liquid flow was directed upward through the column. A 6.9 bar back pressure regulator (IDEX Health & Science, part No. P-763) was connected to the end of the reactor column, after which the reaction mixture was flown through an ice–water bath. At the end of the setup, the liquid stream was passed through a Zaiput Flow Technologies SEP-10 liquid–liquid separator with PTFE membrane to separate the organic phase from the aqueous phase. Samples were collected and the solvent was evaporated by a stream of nitrogen gas. The conversion of 2-methylquinoxaline **2a** to 2-methyl-1,2,3,4-tetrahydroquinoxaline **3a** was determined by integration of the methyl signal of **2a** (2.79 ppm) and **3a** (1.19 ppm) in the ^{1}H NMR spectra ($CDCl_3$) of the crude reaction product.

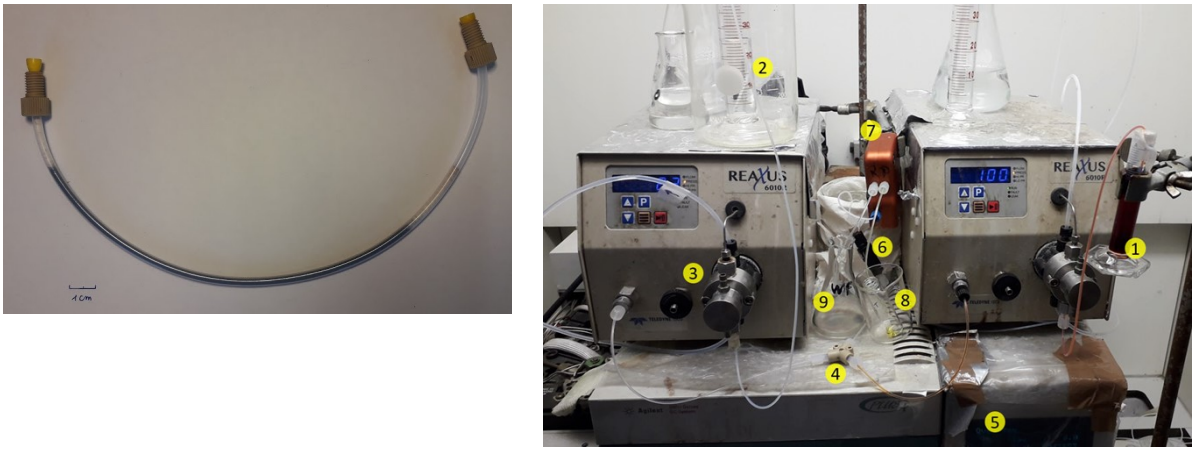

Figure S8. Picture of the packed-bed reactor column (left) and the continuous flow setup (right).

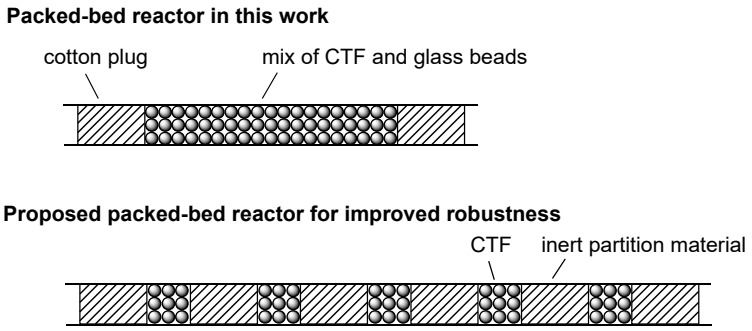

Figure S9. Proposed reactor design to prevent displacement of the CTF particles and channel formation.

4.5 Synthetic procedures and spectral data for substrates

4.5.1 Synthesis of 2-(*tert*-butyl)quinoxaline (2b)

2-(*tert*-Butyl)quinoxaline **2b** was synthesized through C–H alkylation of quinoxaline via the classical Minisci-type reaction.[4] A mixture of quinoxaline (300 mg, 2.30 mmol, 1 eq), pivalic acid (423 mg, 4.14 mmol, 1.8 eq), H_2SO_4 (123 µl, 2.30 mmol, 1 eq), silver nitrate (31 mg, 0.18 mmol, 8 mol%) and ammonium persulfate (1.05 g, 4.60 mmol, 2 eq) in CH_2Cl_2/H_2O (1/1, 30 mL) was refluxed at 50 °C. After 2 h, the reaction mixture was basified to pH 9–10 by the addition of NaOH (1 M) and the organic phase was separated. The aqueous phase was extracted with CH_2Cl_2 (2 x 10 mL), and the combined organic phases were dried over $MgSO_4$, filtered and concentrated *in vacuo*. The crude product was purified by column chromatography on silica gel and petroleum ether/ethyl acetate 9/1 as eluent to yield 2-(*tert*-butyl)quinoxaline **2b** as a colorless oil (312 mg, 73%).

2-(*tert*-Butyl)quinoxaline (2b)

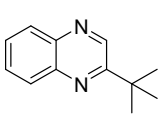

Yield 73%. Colorless oil, R_f = 0.32 (PE/EtOAc 9/1). **^{1}H NMR** (400 MHz, $CDCl_3$): δ 1.52 (9H, s, 3 x CH_3), 7.67–7.76 (2H, m, $H^{6,7}$), 8.03–8.09 (2H, m, $H^{5,8}$), 8.99 (1H, s, H^3). **^{13}C NMR** (101 MHz, $CDCl_3$): δ 29.7 (3 x CH_3), 37.2 ($\underline{C}_{quat}(CH_3)_3$), 128.9 ($C^6$), 128.9 ($C^8$), 129.3 ($C^5$), 129.6 ($C^7$), 140.8 ($C^{4a}$), 141.6 ($C^{8a}$), 143.4 ($C^3$), 163.7($C^2$). **IR** (ATR, cm^{-1}): ν_{max} = 2965, 1557, 1493, 1479, 1462, 1364, 1163, 1096, 1016, 968, 773, 424. **MS** (ESI): m/z (%) 187 ($[M + H]^+$, 100). The data are in accordance with those reported in the literature.[5]

4.5.2 Synthesis of 2-phenylquinoxaline (2c)

To as solution of benzene-1,2-diamine (300 mg, 2.77 mmol, 1 eq) in THF (10 mL), 2-bromoacetophenone (552 mg, 2.77 mmol, 1 eq) and pyridine (22 µL, 0.28 mmol, 10 mol%) were added and the mixture was stirred in open air at room temperature for 2 h. Subsequently, water (10 mL) was added, and the reaction mixture was extracted with EtOAc (3 x 15 mL). The combined organic phases were dried over $MgSO_4$, filtered and concentrated under reduced pressure.

Purification of the crude product by flash column chromatography on silica gel and petroleum ether/ethyl acetate 19/1 as eluent afforded 2-phenylquinoxaline **2c** as a yellow solid (345 mg, 60%).

2-Phenylquinoxaline (2c)

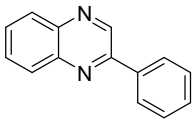

Yield 60%. Yellow solid, R_f = 0.18 (PE/EtOAc 19/1). **^{1}H NMR** (400 MHz, $CDCl_3$): δ 7.50–7.61 (3H, m, $CH_{phenyl,para}$, 2 x $CH_{phenyl,meta}$), 7.72–7.83 (2H, m, $H^{6,7}$), 8.11–8.18 (2H, m, $H^{5,8}$), 8.18–8.22 (2H, m, 2 x $CH_{phenyl,ortho}$), 9.34 (1H, s, H^3). **^{13}C NMR** (101 MHz, $CDCl_3$): δ 127.6 (2 x $CH_{phenyl,ortho}$), 129.2 (C^5, 2 x $CH_{phenyl,meta}$), 129.5 (C^6), 129.7 (C^8), 130.2 ($CH_{phenyl,para}$), 130.3 (C^7), 136.8 ($C_{quat,phenyl}$), 141.6 (C^{4a}), 142.3 (C^{8a}), 143.4 (C^3), 151.9 (C^2). **IR** (ATR, cm^{-1}): ν_{max} = 1545, 1487, 1312, 1028, 955, 764, 748, 685, 669, 550, 407. **MS** (ESI): m/z (%) 207 ($[M + H]^+$, 100). The data are in accordance with those reported in the literature.[6]

4.5.3 Synthesis of 2,3-disubstitued quinoxalines 2d–2k

As a representative example, the synthesis of 2,3-dimethylquinoxaline **2d** is described. To a stirred solution of benzene-1,2-diamine (324 mg, 3 mmol, 1 eq) in methanol (20 mL) was added butane-2,3-dione (263 µL, 3 mmol, 1 eq). The reaction mixture was stirred at room temperature for 1 h, after which the solvent was removed *in vacuo*. Diethyl ether (25 mL) was added to the residue and the mixture was washed with water (3 x 10 mL). The organic phase was dried over $MgSO_4$, filtered and the solvent was evaporated under reduced pressure to obtain 2,3-dimethylquinoxaline **2d** as white crystals (433 mg, 91%). No further purification was necessary for all the derivatives, unless otherwise stated.

2,3-Dimethylquinoxaline (2d)

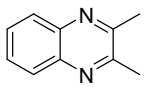

Yield 91%. White crystals. **^{1}H NMR** (400 MHz, $CDCl_3$): δ 2.73 (6H, s, 2 x CH_3), 7.63–7.68 (2H, m, $H^{6,7}$), 7.94–8.00 (2H, m, $H^{5,8}$). **^{13}C NMR** (101 MHz, $CDCl_3$): δ 23.3 (2 x CH_3), 128.5 ($C^{5,8}$), 129.0 ($C^{6,7}$), 141.2 ($C^{4a,8a}$), 153.6 ($C^{2,3}$). **IR** (ATR, cm^{-1}): ν_{max} = 1489, 1435, 1395, 1363, 1317, 1209, 1165, 988, 976, 904, 758, 669, 611. **MS** (ESI): m/z (%) 159 ($[M + H]^+$, 100). The data are in accordance with those reported in the literature.[7]

2-Ethyl-3-methylquinoxaline (2e)

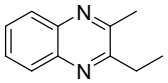

Yield 99%. Off-white solid. **^{1}H NMR** (400 MHz, $CDCl_3$): δ 1.42 (3H, t, *J* = 7.5 Hz, $CH_2C\underline{H}_3$), 2.77 (3H, s, $C^3C\underline{H}_3$), 3.04 (2H, q, *J* = 7.5 Hz, $C\underline{H}_2CH_3$), 7.63–7.69 (2H, m, $H^{6,7}$), 7.95–8.05 (2H, m, $H^{5,8}$). **^{13}C NMR** (101 MHz, $CDCl_3$): δ 12.0 ($CH_2\underline{C}H_3$), 22.7 ($C^3\underline{C}H_3$), 29.0

($\underline{C}H_2CH_3$), 128.3 (C^8), 128.6 (C^5), 128.7(C^6), 128.8 (C^7), 141.0 and 141.2 ($C^{4a,8a}$), 153.1 (C^3), 157.6 (C^2). **IR** (ATR, cm^{-1}): ν_{max} = 1487, 1369, 1381, 1304, 1204, 1152, 1126, 903, 754, 660, 608, 422. **MS** (ESI): m/z (%) 173 ($[M + H]^+$, 100). The data are in accordance with those reported in the literature.[8]

2-Methyl-3-phenylquinoxaline (2f)

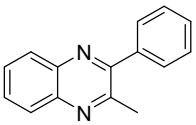

Yield 93%. White solid. **^{1}H NMR** (400 MHz, $CDCl_3$): δ 2.78 (3H, s, CH_3), 7.46–7.56 (3H, m, $CH_{phenyl,para}$, 2 x $CH_{phenyl,meta}$), 7.64–7.68 (2H, m, 2 x $CH_{phenyl,ortho}$), 7,69–7.77 (2H, m, $H^{6,7}$), 8.09–8.14 (1H, m, H^5), 8.03–8.09 (1H, m, H^8). **^{13}C NMR** (101 MHz, $CDCl_3$): δ 24.4 (CH_3), 128.3 (C^5), 128.6 (2 x $CH_{phenyl,meta}$), 128.9 (2 x $CH_{phenyl,ortho}$), 129.0 ($CH_{phenyl,para}$), 129.2 (C^7), 129.3 (C^8), 129.7 (C^6), 139.1 ($C_{quat,phenyl}$), 141.0 (C^{8a}), 141.3 (C^{4a}), 152.5 (C^2), 154.9 (C^3). **IR** (ATR, cm^{-1}): ν_{max} = 1486, 1443, 1395, 1341, 1005, 993, 756, 698, 608, 577, 478, 436. **MS** (ESI): m/z (%) 221 ($[M + H]^+$, 100). The data are in accordance with those reported in the literature.[9]

2,3-Diphenylquinoxaline (2g)

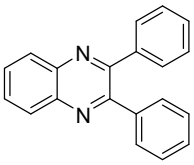

Yield 82%. White solid. **^{1}H NMR** (400 MHz, $CDCl_3$): δ 7.31–7.40 (6H, m, 4 x $CH_{phenyl,meta}$, 2 x $CH_{phenyl,para}$), 7.50–7.55 (4H, m, 4 x $CH_{phenyl,ortho}$), 7.75–7.81 (2H, m, $H^{5,8}$), 8.16–8.21 (2H, m, $H^{6,7}$). **^{13}C NMR** (101 MHz, $CDCl_3$): δ 128.4 (4 x $CH_{phenyl,meta}$), 128.9 (2 x $CH_{phenyl,para}$), 129.4 ($C^{6,7}$), 130.0 (4 x $CH_{phenyl,ortho}$), 130.1 ($C^{5,8}$), 139.3 (2 x $C_{quat,phenyl}$), 141.4 ($C^{4a,8a}$), 153.6 ($C^{2,3}$). **IR** (ATR, cm^{-1}): ν_{max} = 1477, 1443, 1396, 1346, 1059, 978, 930, 761, 696, 669, 598, 538. **MS** (ESI): m/z (%) 283 ($[M + H]^+$, 100). The data are in accordance with those reported in the literature.[9]

6-Methoxy-2,3-dimethylquinoxaline (2h)

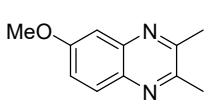

Yield 72%, after automated column chromatography (SiO_2). White solid, R_f = 0.21 (PE/EtOAc 3/2). **^{1}H NMR** (400 MHz, $CDCl_3$): δ 2.69 (3H, s, CH_3), 2.71 (3H, s, CH_3), 3.94 (3H, s, CH_3O), 7.28–7.33 (2H, m, $H^{5,7}$), 7.86 (1H, d, *J* = 8.8 Hz, H^8). **^{13}C NMR** (101 MHz, $CDCl_3$): δ 22.8 (CH_3), 23.1 (CH_3), 55.7 (CH_3O), 106.2 (C^5), 121.7 (C^7), 129.3 (C^8), 137.0 (C^{8a}), 142.5 (C^{4a}), 150.6 and 153.4 ($C^{2,3}$), 160.0 (C^6). **IR** (ATR, cm^{-1}): ν_{max} = 1616, 1493, 1443, 1375, 1215, 1153, 1110, 1016, 947, 824, 598, 436. **MS** (ESI): m/z (%) 189 ($[M + H]^+$, 100). The data are in accordance with those reported in the literature.[10]

6-Chloro-2,3-dimethylquinoxaline (2i)

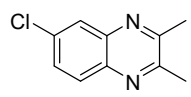

Yield 99%. Beige-brown solid. **^{1}H NMR** (400 MHz, $CDCl_3$): δ 2.72 (3H, s, CH_3), 2.73 (3H, s, CH_3), 7.60 (1H, dd, *J* = 8.9, 2.3 Hz, H^7), 7.90 (1H, d, *J* = 8.9 Hz, H^8), 7.97 (1H, d, *J* = 2.3 Hz, H^5). **^{13}C NMR** (101 MHz, $CDCl_3$): δ 23.15 (CH_3), 23.21 (CH_3), 127.4 (C^5), 129.6 (C^8), 129.8 (C^7), 134.4 (C^6), 139.6 (C^{8a}), 141.4 (C^{4a}), 153.8 and 154.6 ($C^{2,3}$). **IR** (ATR, cm^{-1}): ν_{max} = 1601, 1479, 1439, 1395, 1368, 1323, 1159, 1063, 924, 887, 831, 781, 723, 577, 428. **MS** (ESI): m/z (%) 193/195 ($[M + H]^+$, 100). The data are in accordance with those reported in the literature.[7]

2,3-Dimethylquinoxaline-6-carbonitrile (2j)

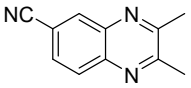

Yield 99%. Salmon pink solid. **^{1}H NMR** (400 MHz, $CDCl_3$): δ 2.77 (3H, s, CH_3), 2.78 (3H, s, CH_3), 7.81 (1H, dd, *J* = 8.6, 1.7 Hz, H^7), 8.60 (1H, d, *J* = 8.6 Hz, H^8), 8.35 (1H, d, *J* = 1.7 Hz, H^5). **^{13}C NMR** (101 MHz, $CDCl_3$): δ 23.3 (CH_3), 23.5 (CH_3), 112.2 (C^6), 118.3 (C≡N), 129.8 (C^7), 130.0 (C^8), 134.4 (C^5), 140.3 (C^{4a}), 142.7 (C^{8a}), 155.9 and 156.7 ($C^{2,3}$). **IR** (ATR, cm^{-1}): ν_{max} = 2224, 1603, 1574, 1439, 1396, 1368, 1323, 1167, 908, 835, 611, 577, 419. **MS** (ESI): m/z (%) 184 ($[M + H]^+$, 100). The data are in accordance with those reported in the literature.[10]

2,3-Dimethyl-6-nitroquinoxaline (2k)

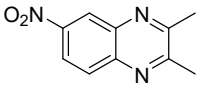

Quantitative yield. Light brown solid. **^{1}H NMR** (400 MHz, $CDCl_3$): δ 2.80 (6H, s, 2 x CH_3), 8.11 (1H, d, *J* = 9.1 Hz, H^8), 8.44 (1H, dd, *J* = 9.1, 2.4 Hz, H^7), 8.90 (1H, d, *J* = 2.4 Hz, H^5). **^{13}C NMR** (101 MHz, $CDCl_3$): δ 23.3 (CH_3), 23.5 (CH_3), 122.3 (C^7), 124.8 (C^5), 129.9 (C^8), 139.9 (C^{4a}), 143.7 (C^{8a}), 147.1 (C^6), 156.3 and 157.2 ($C^{2,3}$). **IR** (ATR, cm^{-1}): ν_{max} = 1616, 1578, 1524, 1398, 1341, 1196, 1165, 895, 845, 822, 743, 712, 420. **MS** (ESI): *m/z* (%) 204 ($[M + H]^+$, 100). The data are in accordance with those reported in the literature.[7]

4.6 Synthetic procedure and spectral data for products

General procedure for the transfer hydrogenation toward N-heteroarenes **3** and **5**:

In a 12 mL test tube, an aqueous HCOOH/HCOONa buffer (4 M, pH 4.5, 7 mL) was preheated to 80 °C, after which N-heteroarene substrate (0.7 mmol) dissolved in EtOAc (0.7 mL), and Rh@bpyCTF (7.9 mg, 0.25 mol% Rh) were sequentially added. The test tube was provided with a cap which was not screwed tight to ensure CO_2 could still be released. The reaction mixture was vigorously stirred (fixed at 800 rpm) to ensure sufficient mixing. Upon complete conversion of the substrate (monitored by LC-MS), the catalyst was filtered and rinsed with water and Et_2O. After basifying the filtrate (pH > 10) with NaOH (1 M), the organic phase was separated, and the aqueous phase was extracted twice with Et_2O (2 x 15 mL). The combined organic phases were dried over $MgSO_4$, filtered and evaporated *in vacuo*. The product was purified by normal-phase column chromatography on silica gel and petroleum ether/ethyl acetate as eluent.

2-Methyl-1,2,3,4-tetrahydroquinoxaline (3a)

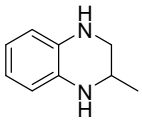

Yield 94%. Pale orange solid, R_f = 0.15 (PE/EtOAc 4/1). **^{1}H NMR** (400 MHz, $CDCl_3$): δ 1.19 (3H, d, *J* = 6.3 Hz, CH_3), 3.04 (1H, dd, *J* = 10.7, 8.2 Hz, H^{3a}), 3.32 (1H, dd, *J* = 10.7, 2.9 Hz, H^{3b}), 3.47–3.56 (1H, m, H^2), 3.60 (2H, br s, 2 x NH), 6.47–6.53 (2H, m, $H^{5,8}$), 6.55–6.62 (2H, m, $H^{6,7}$). **^{13}C NMR** (101 MHz, $CDCl_3$): δ 19.9 (CH_3), 45.7 (C^2),48.3 (C^3), 114.4 and 114.5 ($C^{5,8}$), 118.69 and 118.71 ($C^{6,7}$), 133.2 and 133.6 ($C^{4a,8a}$). **IR** (ATR, cm^{-1}): ν_{max} = 3358, 3310, 2957, 2845, 1595, 1499, 1362, 1304, 1269, 1070, 922, 741. **MS** (ESI): m/z (%) 149 ($[M + H]^+$, 100). The data are in accordance with those reported in the literature.[11]

2-*tert*-Butyl-1,2,3,4-tetrahydroquinoxaline (3b)

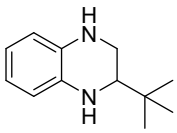

Yield 80%. Pale yellow crystals, R_f = 0.18 (PE/EtOAc 9/1). **^{1}H NMR** (400 MHz, $CDCl_3$): δ 0.99 (9H, s, 3 x CH_3), 3.10–3.18 (2H, m, $H^{2,3a}$), 3.31–3.39 (1H, m, H^{3b}), 3.64 (2H, br s, 2 x NH), 6.48–6.62 (4H, m, $H^{5,6,7,8}$). **^{13}C NMR** (101 MHz, $CDCl_3$): δ 26.0 (3 x CH_3), 32.8 ($\underline{C}_{quat}(CH_3)_3$), 42.5 ($C^3$), 59.0 ($C^2$), 114.25 and 114.32 ($C^{5,8}$), 118.2 and 118.9 ($C^{6,7}$), 133.3 and 134.6 ($C^{4a,8a}$). **IR** (ATR, cm^{-1}): ν_{max} = 3368, 2957, 1595, 1503, 1472, 1300, 1119, 1076, 1032, 905, 733. **MS** (ESI): m/z (%) 191 ($[M + H]^+$, 100). The data are in accordance with those reported in the literature.[5]

2-Phenyl-1,2,3,4-tetrahydroquinoxaline (3c)

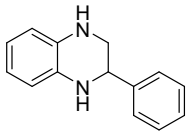

Yield 85%. Yellow solid, R_f = 0.13 (PE/EtOAc 19/1). **^{1}H NMR** (400 MHz, $CDCl_3$): δ 3.33 (1H, dd, *J* = 11.0, 8.2 Hz, H^{3a}), 3.46 (1H, dd, *J* = 11.0, 3.1 Hz, H^{3b}), 3.86 (2H, br s, 2 x NH), 4.48 (1H, dd, *J* = 8.2, 3.1 Hz), 6.55–6.61, (2H, m, $H^{5,8}$), 6.61–6.67, (2H, m, $H^{6,7}$), 7.28–7.34 (1H, m, $CH_{phenyl,para}$), 7.28–7.41 (1H, m, 2 x $CH_{phenyl,ortho}$, 2 x $CH_{phenyl,meta}$). **^{13}C NMR** (101 MHz, $CDCl_3$): δ 49.2 (C^3), 54.7 (C^2), 114.4 and 114.7 ($C^{5,8}$), 118.8 and 118.9 ($C^{6,7}$), 127.0 (2 x $CH_{phenyl,ortho}$), 127.9 ($CH_{phenyl,para}$), 128.6 (2 x $CH_{phenyl,meta}$), 132.8 and 134.1 ($C^{4a,8a}$), 141.9 ($C_{quat,phenyl}$). **IR** (ATR, cm^{-1}): ν_{max} = 3337, 2849, 1593, 1506, 1491, 1452, 1302, 1271, 1119, 743, 698. **MS** (ESI): m/z (%) 211 ($[M + H]^+$, 100). The data are in accordance with those reported in the literature.[12]

2,3-Dimethyl-1,2,3,4-tetrahydroquinoxaline (3d)

Spectral data derived from the mixture of *cis*- and *trans*-isomers (*cis*/*trans* = 55/45).

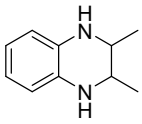

Yield 76%. White crystals, R_f = 0.20 and 0.24 (PE/EtOAc 4/1). *cis*-Isomer: **^{1}H NMR** (400 MHz, $CDCl_3$): δ 1.12 (6H, d, *J* = 6.4 Hz, 2 x CH_3), 3.45–3.52 (2H, m, $H^{2,3}$), 3.52 (2H, br s, 2 x NH), 6.46–6.52 (2H, m, $H^{5,8}$), 6.55–6.60 (2H, m, $H^{6,7}$). **^{13}C NMR** (101 MHz, $CDCl_3$): δ 17.2 (2 x CH_3), 49.0 ($C^{2,3}$), 114.4 ($C^{5,8}$), 118.5 ($C^{6,7}$), 133.5 ($C^{4a,8a}$). *trans*-Isomer: **^{1}H NMR** (400 MHz, $CDCl_3$): δ 1.17 (6H, ~d, *J* = 5.8 Hz, 2 x CH_3), 2.98–3.06 (2H, m, $H^{2,3}$), 3.52 (2H, br s, 2 x NH), 6.46–6.52 (2H, m, $H^{5,8}$), 6.55–6.60 (2H, m, $H^{6,7}$). **^{13}C NMR** (101 MHz, $CDCl_3$): δ 19.0 (2 x CH_3), 52.0 ($C^{2,3}$), 113.9 ($C^{5,8}$), 118.6 ($C^{6,7}$), 132.7 ($C^{4a,8a}$). **IR** (ATR, cm^{-1}): ν_{max} = 3335, 2968, 1597, 1503, 1439, 1373, 1285, 1152, 1082, 916, 737. **MS** (ESI): m/z (%) 163 ($[M + H]^+$, 100). The data are in accordance with those reported in the literature.[13]

***cis*-2-Ethyl-3-methyl-1,2,3,4-tetrahydroquinoxaline (*cis*-3e)**

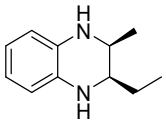

Yield 82% (*cis* + *trans*). White solid, R_f = 0.25 (PE/EtOAc 17/3). **^{1}H NMR** (400 MHz, $CDCl_3$): δ 0.98 (3H, t, *J* = 7.3 Hz, $CH_2C\underline{H}_3$), 1.12 (3H, d, *J* = 6.5 Hz, $CHC\underline{H}_3$), 1.45 (2H, quint, *J* = 7.3 Hz, $C\underline{H}_2CH_3$), 3.24 (1H, td, *J* = 7.3, 2.8 Hz, H^2), 3.52 (1H, qd, *J* = 6.5, 2.8 Hz, H^3), 3.63 (2H, br s, 2 x NH), 6.46–6.52 (2H, m, $H^{5,8}$), 6.55–6.60 (2H, m, $H^{6,7}$). **^{13}C NMR** (101 MHz, $CDCl_3$): δ 10.3 ($CH_2\underline{C}H_3$), 16.7 ($CH\underline{C}H_3$), 23.9 ($\underline{C}H_2CH_3$), 48.3 (C^3), 55.1 (C^2), 114.2 and 114.4 ($C^{5,8}$), 118.4 and 118.5 ($C^{6,7}$), 132.7 (C^{4a}), 132.8 (C^{8a}). **IR** (ATR, cm^{-1}): ν_{max} = 3374, 3345, 2961, 2932, 1595, 1503, 1460, 1437, 1371, 1281, 1169, 1119, 1040, 907, 731. **MS** (ESI): m/z (%) 177 ($[M + H]^+$, 100). The data are in accordance with those reported in the literature.[8]

trans-2-Ethyl-3-methyl-1,2,3,4-tetrahydroquinoxaline (_trans_-3e)

Spectral data derived from the mixture of *cis*- and *trans*-isomers (*cis*/*trans* = 71/28).

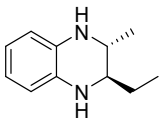

Colorless viscous oil. **^{1}H NMR** (400 MHz, $CDCl_3$): δ 0.98 (3H, t, *J* = 7.6 Hz, $CH_2C\underline{H}_3$), 1.12 (3H, d, *J* = 6.5 Hz, $CHC\underline{H}_3$), 1.45 (1H, quint, *J* = 7.6 Hz, $C\underline{H}_aH_bCH_3$), 1.69 (1H, dqd, *J* = 14.0, 7.6, 3.6 Hz, $CH_a\underline{H}_bCH_3$), 2.87 (1H, ddd, *J* = 7.6, 6.5, 3.6 Hz, H^2), 3.16 (1H, quint, *J* = 6.5 Hz, H^3), 3.40–3.70 (2H, br s, 2 x NH), 6.46–6.52 (2H, m, $H^{5,8}$), 6.55–6.60 (2H, m, $H^{6,7}$). **^{13}C NMR** (101 MHz, $CDCl_3$): 9.5 ($CH_2\underline{C}H_3$), 19.4 ($CH\underline{C}H_3$), 25.5 ($\underline{C}H_2CH_3$), 49.7 (C^3), 57.1 (C^2), 114.0 ($C^{5,8}$), 118.4 and 118.5 ($C^{6,7}$), 133.1 (C^{4a}), 133.3 (C^{8a}). **MS** (ESI): m/z (%) 177 ($[M + H]^+$, 100). The data are in accordance with those reported in the literature.[8]

cis-2-Methyl-3-phenyl-1,2,3,4-tetrahydroquinoxaline (_cis_-3f)

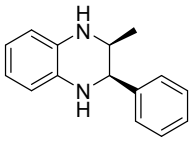

Yield 75%. Yellow viscous oil, R_f = 0.11 (PE/EtOAc 19/1). **^{1}H NMR** (400 MHz, $CDCl_3$): δ 0.94 (3H, d, *J* = 6.5 Hz, CH_3), 3.71 (1H, qd, *J* = 6.5, 3.2 Hz, H^2), 3.94 (2H, br s, 2 x NH), 4.50 (1H, d, *J* = 3.2 Hz, H^3), 6.53–6.59 (2H, m, $H^{5,8}$), 6.60–6.68 (2H, m, $H^{6,7}$), 7.24–7.34 (5H, m, 6 x CH_{phenyl}). **^{13}C NMR** (101 MHz, $CDCl_3$): δ 17.6 (CH_3), 49.5 (C^2), 58.5 (C^3), 113.9 and 114.8 ($C^{5,8}$), 118.4 and 119.3 ($C^{6,7}$), 127.3 ($CH_{phenyl,para}$), 127.6 (2 x $CH_{phenyl,ortho}$), 128.2 (2 x $CH_{phenyl,meta}$), 132.3 and 133.2 ($C^{4a,8a}$), 141.8 ($C_{quat,phenyl}$). **IR** (ATR, cm^{-1}): ν_{max} = 3362, 2968, 1595, 1503, 1452, 1368, 1277, 1146, 735, 698. **MS** (ESI): m/z (%) 225 ($[M + H]^+$, 100). The data are in accordance with those reported in the literature.[9]

cis-2,3-Diphenyl-1,2,3,4-tetrahydroquinoxaline (_cis_-3g)

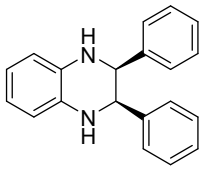

Yield 77%. White solid, R_f = 0.11 (PE/EtOAc 4/1). **^{1}H NMR** (400 MHz, $CDCl_3$): δ 4.08 (2H, br s, 2 x NH), 4.74 (2H, s, $H^{2,3}$), 6.60–6.67 (2H, m, $H^{5,8}$), 6.67–6.73 (2H, m, $H^{6,7}$), 6.85–6.91 (4H, m, 4 x $CH_{phenyl,ortho}$) 7.07–7.19 (6H, m, 4 x $CH_{phenyl,meta}$ 2 x $CH_{phenyl,para}$). **^{13}C NMR** (101 MHz, $CDCl_3$): δ 59.5 ($C^{2,3}$), 114.1 ($C^{5,8}$), 118.9 ($C^{6,7}$), 127.3 (2 x $CH_{phenyl,para}$), 127.7 (4 x $CH_{phenyl,meta}$), 127.9 (4 x $CH_{phenyl,ortho}$), 133.1 ($C^{4a,8a}$), 140.6 (2 x $C_{quat,phenyl}$). **IR** (ATR, cm^{-1}): ν_{max} = 3412, 3024, 2828, 1605, 1508, 1450, 1319, 1279, 1107, 735, 698. **MS** (ESI): m/z (%) 287 ($[M + H]^+$, 100). The data are in accordance with those reported in the literature.[9]

Crystals suitable for X-ray diffraction analysis were obtained from a saturated solution in chloroform by slow evaporation of the solvent at room temperature.

cis-6-Methoxy-2,3-dimethyl-1,2,3,4-tetrahydroquinoxaline (_cis_-3h)

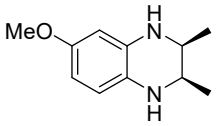

Yield 95% (*cis* + *trans*). Colorless oil, R_f = 0.23 (PE/EtOAc 3/2). **^{1}H NMR** (400 MHz, $CDCl_3$): δ 1.109 (3H, d, *J* = 6.4 Hz, CH_3), 1.110 (3H, d, *J* = 6.4 Hz, CH_3), 3.24 (2H, br s, 2 x NH), 3.38–3.51 (2H, m, $H^{2,3}$), 3.70 (3H, s, CH_3O) 6.11 (1H, d, *J* = 2.5 Hz, H^5), 6.17 (1H, dd, *J* = 8.4, 2.5 Hz, H^7), 6.45 (1H, d, *J* = 8.4 Hz, H^8). **^{13}C NMR** (101 MHz, $CDCl_3$): δ 17.1 (2 x CH_3), 49.19 and 49.24 ($C^{2,3}$), 55.6 (CH_3O), 100.9 (C^5), 103.2 (C^7), 115.6 (C^8), 126.1 (C^{8a}), 134.0 (C^{4a}), 153.5 (C^6). **IR** (ATR, cm^{-1}): ν_{max} = 3360, 2967, 2832, 1616, 1599, 1512, 1441, 1375, 1260, 1202, 1165, 1040, 829, 785. **MS** (ESI): m/z (%) 193 ($[M + H]^+$, 100). The data are in accordance with those reported in the literature.[14]

trans-6-Methoxy-2,3-dimethyl-1,2,3,4-tetrahydroquinoxaline (_trans_-3h)

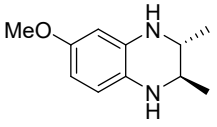

Colorless oil, R_f = 0.31 (PE/EtOAc 3/2). **^{1}H NMR** (400 MHz, $CDCl_3$): δ 1.155 (3H, d, *J* = 6.1 Hz, CH_3), 1.158 (3H, d, *J* = 6.1 Hz, CH_3), 2.89–3.08 (2H, m, $H^{2,3}$), 3.38 (2H, br s, 2 x NH), 3.70 (3H, s, CH_3O) 6.12 (1H, ~d, *J* = 2.5 Hz, H^5), 6.14–6.20 (1H, m, H^7), 6.45 (1H, d, *J* = 8.3 Hz, H^8). **^{13}C NMR** (101 MHz, $CDCl_3$): δ 18.9 (CH_3), 19.1 (CH_3), 52.2 and 52.4 ($C^{2,3}$), 55.6 (CH_3O), 100.4 (C^5), 103.1 (C^7), 115.1 (C^8), 127.2 (C^{8a}), 134.8 (C^{4a}), 153.4 (C^6). The data are in accordance with those reported in the literature.[14]

6-Chloro-2,3-dimethyl-1,2,3,4-tetrahydroquinoxaline (3i)

Spectral data derived from the mixture of *cis*- and *trans*-isomers (*cis*/*trans* = 81/19).

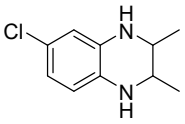

Yield 92%. White solid, R_f = 0.26 and 0.34 (PE/EtOAc 4/1). <u>*cis*-Isomer</u>: **^{1}H NMR** (400 MHz, $CDCl_3$): δ 1.11 (6H, d, *J* = 6.4 Hz, 2 x CH_3), 2.86–3.87 (2H, br s, 2 x NH), 3.42–3.51 (2H, m, $H^{2,3}$), 6.38 (1H, d, *J* = 8.2 Hz, H^8), 6.44 (1H, d, *J* = 2.3 Hz, H^5), 6.50 (1H, dd, *J* = 8.2, 2.3 Hz, H^7). **^{13}C NMR** (101 MHz, $CDCl_3$): δ 16.8 (CH_3), 17.0 (CH_3), 48.8 and 48.9 ($C^{2,3}$), 113.8 (C^5), 115.4 (C^8), 117.9 (C^7), 123.5 (C^6), 130.3 (C^{8a}), 133.8 (C^{4a}). <u>*trans*-Isomer</u>: **^{1}H NMR** (400 MHz, $CDCl_3$): δ 1.16 (3H, d, *J* = 5.9 Hz, CH_3), 1.17 (3H, d, *J* = 5.9 Hz, CH_3), 2.86–3.87 (2H, br s, 2 x NH), 2.93–3.05 (2H, m, $H^{2,3}$), 6.38 (1H, d, *J* = 8.2 Hz, H^8), 6.45 (1H, d, *J* = 2.3 Hz, H^5), 6.50 (1H, dd, *J* = 8.2, 2.3 Hz, H^7). **^{13}C NMR** (101 MHz, $CDCl_3$): δ 18.9 (CH_3), 18.9 (CH_3), 51.8 ($C^{2,3}$), 113.3 (C^5), 114.6 (C^8), 117.8 (C^7), 123.2 (C^6), 131.6 (C^{8a}), 134.5 (C^{4a}). **IR** (ATR, cm^{-1}): ν_{max} = 3358, 3283, 2970, 2928, 2860, 1595, 1503, 1439, 1375, 1287, 1242, 1180, 1088, 962, 853, 795. **MS** (ESI): m/z (%) 197/199 ($[M + H]^+$, 100). The data are in accordance with those reported in the literature.[8]

2,3-Dimethyl-1,2,3,4-tetrahydroquinoxaline-6-carbonitrile (3j)

Spectral data derived from the mixture of *cis*- and *trans*-isomers (*cis*/*trans* = 83/17).

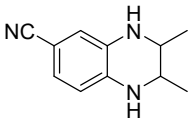

Yield 96%. Colorless viscous oil, R_f = 0.12 (PE/EtOAc 4/1). <u>*cis*-Isomer</u>: **^{1}H NMR** (400 MHz, $CDCl_3$): δ 1.12 (3H, d, *J* = 6.5 Hz, CH_3), 1.14 (3H, d, *J* = 6.5 Hz, CH_3), 3.47 (1H, d, *J* = 6.5, 3.0 Hz, H^3), 3.56 (1H, d, *J* = 6.5, 3.0 Hz, H^2), 3.96 (2H, br s, 2 x NH), 6.40 (1H, d, *J* = 8.1 Hz, H^8), 6.67 (1H, d, *J* = 1.8 Hz, H^5), 6.866 (1H, d, *J* = 8.1, 1.8 Hz, H^7). **^{13}C NMR** (101 MHz, $CDCl_3$): δ 17.0 (CH_3), 17.3 (CH_3), 48.3 (C^3), 49.0 (C^2), 99.29 (C^6), 112.9 (C^8), 116.3 (C^5), 120.9 (C≡N), 123.76 (C^7), 132.1 (C^{4a}), 137.1 (C^{8a}). <u>*trans*-Isomer</u>: **^{1}H NMR** (400 MHz, $CDCl_3$): δ 1.19 (6H, d, *J* = 6.3 Hz, 2 x CH_3), 2.96 (1H, quint, *J* = 6.3 Hz, H^3), 3.09 (1H, quint, *J* = 6.3 Hz, H^2), 3.96 (2H, br s, 2 x NH), 6.41 (1H, d, *J* = 8.1 Hz, H^8), 6.68 (1H, d, *J* = 1.8 Hz, H^5), 6.872 (1H, d, *J* = 8.1, 1.8 Hz, H^7). **^{13}C NMR** (101 MHz, $CDCl_3$): δ 18.8 (CH_3), 18.9 (CH_3), 51.2 (C^3), 52.0 (C^2), 99.26 (C^6), 112.5 (C^8), 115.9 (C^5), 120.9 (C≡N), 123.82 (C^7), 132.8 (C^{4a}), 137.7 (C^{8a}). **IR** (ATR, cm^{-1}): ν_{max} = 3354, 2970, 2207, 1599, 1522, 1443, 1377, 1296, 858, 802. **MS** (ESI): m/z (%) 188 ($[M + H]^+$, 100).

2,3-Dimethylquinoxalin-6-amine (3k)

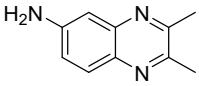

Yield 77%. Yellow solid, R_f = 0.22 (EtOAc). **^{1}H NMR** (400 MHz, $CDCl_3$): δ 2.65 (3H, s, CH_3), 2.66 (3H, s, CH_3), 4.06 (2H, br s, NH_2), 7.06–7.10 (2H, m, $H^{5,7}$), 7.76 (1H, dd, *J* = 8.3, 0.8 Hz, H^8). **^{13}C NMR** (101 MHz, $CDCl_3$): δ 22.7 (CH_3), 23.2 (CH_3), 108.2 (C^5), 120.6 (C^7), 129.3 (C^8), 136.0 (C^{8a}), 142.8 (C^{4a}), 147.0 (C^6), 149.3 and 153.4 ($C^{2,3}$). **IR** (ATR, cm^{-1}): ν_{max} = 3321, 3204, 1643, 1614, 1501, 1377, 1341, 1242, 1159, 1126, 995, 947, 827. **MS** (ESI): m/z (%) 174 ($[M + H]^+$, 100).

2-Methyl-1,2,3,4-tetrahydroquinoline (5a)

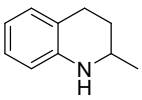

Yield 99%. Colorless oil, which turns bordeaux-brown upon standing, R_f = 0.36 (PE/EtOAc 9/1). **^{1}H NMR** (400 MHz, $CDCl_3$): δ 1.20 (3H, d, *J* = 6.3 Hz, CH_3), 1.58 (1H, dddd, 12.7, 11.4, 9.9, 5.2 Hz, H^{3a}), 1.92 (1H, dddd, 12.7, 5.6, 3.6, 2.9 Hz, H^{3b}), 2.72 (1H, ddd, 16.5, 5.2, 3.6 Hz, H^{4a}), 2.83 (1H, ddd, 16.5, 11.4, 5.6 Hz, H^{4b}), 3.40 (1H, dqd, *J* = 9.9, 6.3, 2.9 Hz, H^2), 3.68 (1H, br s, NH), 6.46 (1H, dd, *J* = 8.4, 0.9 Hz, H^8), 6.60 (1H, td, *J* = 7.4, 0.9 Hz, H^6), 6.93–6.98 (2H, m, $H^{5,7}$). **^{13}C NMR** (101 MHz, $CDCl_3$): δ 22.6 (CH_3), 26.6 (C^4), 30.2 (C^3), 47.2 (C^2), 114.0 (C^8), 117.0 (C^6), 121.1 (C^{4a}), 126.7 (C^7), 129.3 (C^5), 144.8 (C^{8a}). **IR** (ATR, cm^{-1}): ν_{max} = 3393, 2924, 1607, 1584, 1485, 1306, 1275, 1256, 1152, 743. **MS** (ESI): m/z (%) 148 ($[M + H]^+$, 100). The data are in accordance with those reported in the literature.[15]

1,2,3,4-Tetrahydro-1,5-naphthyridine (5b)

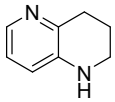

Yield 85%. White solid. **^{1}H NMR** (400 MHz, $CDCl_3$): δ 2.00-2.07 (2H, m, $NCH_2C\underline{H}_2$), 2.93 (2H, t, *J* = 6.5 Hz, $C_{quat}C\underline{H}_2$), 3.27–3.32 (2H, m, $NC\underline{H}_2$), 3.79 (1H, br s, NH), 6.72 (1H, dd, *J* = 8.0, 1.4 Hz, H^8), 6.88 (1H, dd, *J* = 8.0, 4.7 Hz, H^7), 7.86 (1H, dd, *J* = 4.7, 1.4 Hz, H^6). **^{13}C NMR** (101 MHz, $CDCl_3$): δ 21.8 (C^4), 30.4 (C^3), 41.5 (C^2), 120.2 (C^8), 121.9 (C^7), 138.0 (C^6), 140.9 (C^{8a}), 142.8 (C^{4a}). **IR** (ATR, cm^{-1}): ν_{max} = 3223, 2932, 1580, 1456, 1352, 1298, 1269, 1227, 1190, 1125, 1098, 1011, 791, 731. **MS** (ESI): m/z (%) 135 ($[M + H]^+$, 100). The data are in accordance with those reported in the literature.[16]

2,9-Dimethyl-1,2,3,4-tetrahydro-1,10-phenanthroline (5c)

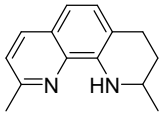

Yield 87%. Pale yellow solid, R_f = 0.52 (PE/EtOAc 17/3). **^{1}H NMR** (400 MHz, $CDCl_3$): δ 1.37 (3H, *J* = 6.1 Hz, C^2CH_3), 1.72 (1H, dddd, *J* = 12.8, 10.9, 9.5, 5.3 Hz, H^{3a}), 2.00–2.07 (1H, m, H^{3b}), 2.68 (3H, s, C^9CH_3), 2.85 (1H, ddd, *J* = 16.6, 5.3, 3.8 Hz, H^{4a}), 2.99 (1H, ddd, *J* = 16.6, 10.9, 5.7 Hz, H^{4b}), 3.58 (1H, dqd, *J* = 9.5, 6.1, 2.9 Hz, H^2), 5.85 (1H, br s, NH), 6.93 (1H, d, *J* = 8.2 Hz, H^6), 7.09 (1H, d, *J* = 8.2 Hz, H^5), 7.15 (1H, d, *J* = 8.3 Hz, H^8), 7.87 (1H, d, *J* = 8.3 Hz, H^7). **^{13}C NMR** (101 MHz, $CDCl_3$): δ 22.5 ($C^2\underline{C}H_3$), 25.1 ($C^9\underline{C}H_3$), 26.6 (C^4), 30.0 (C^3), 46.6 (C^2), 113.2 (C^6), 116.5 (C^{4a}), 121.2 (C^8), 125.3 (C^{6a}), 127.8 (C^5), 135.9 (C^7), 136.8 (C^{10a}), 140.0 (C^{10b}), 155.7 (C^9). **IR** (ATR, cm^{-1}): ν_{max} = 3362, 2968, 1595, 1503, 1452, 1368, 1277, 735, 698. **MS** (ESI): m/z (%) 213 ($[M + H]^+$, 100). The data are in accordance with those reported in the literature.[17]

1,2,3,4,7,8,9,10-Octahydro-1,10-phenanthroline (5d)

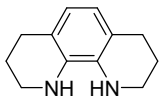

Yield 82%. Off-white crystals, R_f = 0.16 (PE/EtOAc 4/1). **^{1}H NMR** (400 MHz, $CDCl_3$): δ 1.83–1.92 (4H, m, 2 x $NCH_2C\underline{H}_2$), 2.73 (4H, t, *J* = 6.3 Hz, 2 x $C_{quat}CH_2$), 3.19 (2H, br s, 2 x NH), 3.29 (4H, m, 2 x NCH_2), 6.45 (2H, s, $H^{5,6}$). **^{13}C NMR** (101 MHz, $CDCl_3$): δ 22.5 (2 x $NCH_2\underline{C}H_2$), 26.9 (2 x $C_{quat}\underline{C}H_2$), 42.6 (2 x NCH_2), 119.1 ($C^{5,6}$), 120.5 ($C^{4a,6a}$), 132.8 ($C^{10a,10b}$). **IR** (ATR, cm^{-1}): ν_{max} = 3246, 2922, 2833, 1616, 1582, 1489, 1437, 1422, 1327, 1261, 1246, 1194, 1171, 1109, 1007, 779. **MS** (ESI): m/z (%) 189 ($[M + H]^+$, 100). The data are in accordance with those reported in the literature.[18]

9,10-Dihydroacridine (5e)

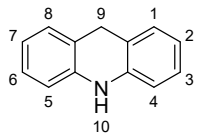

Yield 91%. White crystals, R_f = 0.36 (PE/EtOAc 9/1). **^{1}H NMR** (400 MHz, $CDCl_3$): δ 4.05 (2H, s, CH_2), 5.93 (1H, br s, NH), 6.66 (2H, dd, *J* = 7.9, 1.0 Hz, $H^{4,5}$), 6.84 (2H, td, *J* = 7.4, 1.0 Hz, $H^{2,7}$), 7.04–7.12 (4H, m, $H^{3,6,1,8}$). **^{13}C NMR** (101 MHz, $CDCl_3$): δ 31.4 (CH_2), 113.4 ($C^{4,5}$), 120.1 ($C^{8a,9a}$), 120.6 ($C^{2,7}$), 127.0 ($C^{3,6}$), 128.6 ($C^{1,8}$), 140.1 ($C^{4a,10a}$). **IR** (ATR, cm^{-1}): ν_{max} = 3372, 1599, 1582, 1454, 1294, 743, 714, 607, 532, 434. **MS** (ESI): m/z (%) 182 ($[M + H]^+$, 100). The data are in accordance with those reported in the literature.[19]

Phthalazine-2(1*H*)-carbaldehyde (5f)

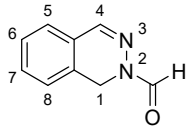

Yield 80%. Pale yellow crystals, R_f = 0.37 (PE/EtOAc 7/3). **^{1}H NMR** (400 MHz, $CDCl_3$): δ 4.94 (2H, s, CH_2), 7.17 (1H, d, *J* = 7.5 Hz, H^8), 7.25 (1H, dd, *J* = 7.5, 0.9 Hz, H^5), 7.35 (1H, t, *J* = 7.5 Hz, H^6), 7.44 (1H, td, *J* = 7.5, 0.9 Hz, H^7), 7.53 (1H, s, H^4), 8.72 (1H, s, N(C=O)H). **^{13}C NMR** (101 MHz, $CDCl_3$): δ 41.1 (CH_2), 124.3 (C^{4a}), 126.2 (C^8), 126.5 (C^5), 128.5 (C^6), 129.0 (C^{8a}), 132.0 (C^7), 143.0 (C^4), 164.7 (N(C=O)H). **IR** (ATR, cm^{-1}): ν_{max} = 2893, 1670, 1396, 1356, 1331, 1221, 1209, 1136, 1105, 912, 760, 642, 588. **MS** (ESI): m/z (%) 161 ($[M + H]^+$, 100). The data are in accordance with those reported in the literature.[20]

4.7 Deformylation of phthalazine-2(1*H*)-carbaldehyde (6)

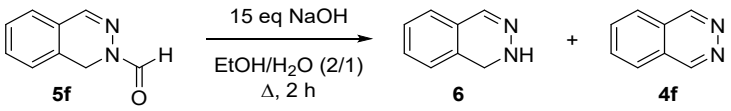

Scheme S1. NaOH-mediated cleavage of the *N*-formyl group.

The formyl group of phthalazine-2(1*H*)-carbaldehyde **5f** (64 mg, 0.40 mmol, 1 eq) was hydrolyzed by treatment with 1 M NaOH (240 µL, 6.00 mmol, 15 eq) under reflux conditions diluted in an ethanol/water mixture (2/1, 6 mL). After 2 h, the mixture was extracted with Et_2O (4 x 10 mL) and the combined organic layers were dried over $MgSO_4$, filtered and concentrated under vacuum to obtain the deformylated product. ^{1}H NMR analysis showed that the product obtained not only contained the targeted 1,2-dihydrophthalazine **6**, but also phthalazine **4f** to a minor extend (**6**/**4f** = 96/4). Over time, the fraction of phthalazine increased, suggesting that 1,2-dihydrophthalazine **6** spontaneously oxidizes on exposure to air.

1,2-Dihydrophthalazine (6)

Spectral data derived from the mixture of compound **6** and phthalazine **4f** (^{1}H NMR: **6**/**4f** = 96/4; ^{13}C NMR: **6**/**4f** = 79/21).

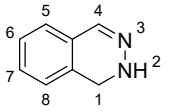

Yield 68%. White solid, R_f = 0.19 (PE/EtOAc 70/30). **^{1}H NMR** (400 MHz, $CDCl_3$): δ 4.23 (2H, s, CH_2), 5.91 (1H, br s, NH), 7.04–7.08 (1H, m, H^8), 7.10–7.15 (1H, m, H^5), 7.25–7.35 (2H, m, $H^{6,7}$), 7.49 (1H, s, H^4). **^{13}C NMR** (101 MHz, $CDCl_3$): δ 44.9 (CH_2), 124.4 (C^5), 125.2 (C^8), 126.2 (C^{4a}), 127.9 (C^6), 130.3 (C^7), 131.0 (C^{8a}), 140.3 (C^4). **IR** (ATR, cm^{-1}): ν_{max} = 3265, 1439, 1317, 1088, 1018, 912, 793, 725, 590. **MS** (ESI): m/z (%) 133 ([M + H]$^+$, 100). The data are in accordance with those reported in the literature.[21]

4.8 Single-crystal X-ray diffraction of compound *cis*-3g

The X-ray diffraction analysis was performed by Prof. Kristof Van Hecke (XStruct, Department of Chemistry, Faculty of Sciences, Ghent University). **CCDC 2226036** contains the supplementary crystallographic data for compound ***cis*-3g**. These data can be obtained free of charge from The Cambridge Crystallographic Data Centre via www.ccdc.cam.ac.uk/structures.

For the structure of compound ***cis*-3g**, single-crystal X-ray intensity data were collected at 100 K on a Rigaku Oxford Diffraction Supernova Dual Source (Cu at zero) diffractometer equipped with an Atlas CCD detector using ω scans and Cu Kα (λ = 1.54184 Å) radiation. The images were interpreted and integrated with the program CrysAlis^{Pro} (Rigaku Oxford Diffraction). Using Olex2,[22] the structure was solved with the SHELXT[23] structure solution program using intrinsic phasing and refined with the SHELXL[24] refinement package using least-squares minimization. Non-hydrogen atoms were anisotropically refined and the hydrogen atoms in the riding mode and isotropic temperature factors fixed at 1.2 times U(eq) of the parent atoms.

Crystal data for compound ***cis*-3g**

$C_{20}H_{18}N_2$, M = 286.36 g/mol, monoclinic, space group $P2_1/n$ (No. 14), a = 12.54957(13) Å, b = 5.45668(4) Å, c = 21.5051(3) Å, β = 100.0457(10)°, V = 1450.07(3) Å^3, Z = 4, T = 100(2) K, μ(Cu Kα) = 0.595 mm^{-1}, F(000) = 608, ρ_{calc} = 1.312 g cm^{-3}, 38566 reflections measured (7.628° ≤ 2Θ ≤ 147.574°), 2917 unique (R_{int} = 0.0278, R_{sigma} = 0.0107) which were used in all calculations. The final R_1 was 0.0351 ($I > 2\sigma(I)$) and wR_2 was 0.0962 (all data).

5 NMR spectra

^{1}H NMR ($CDCl_3$) compound **1**

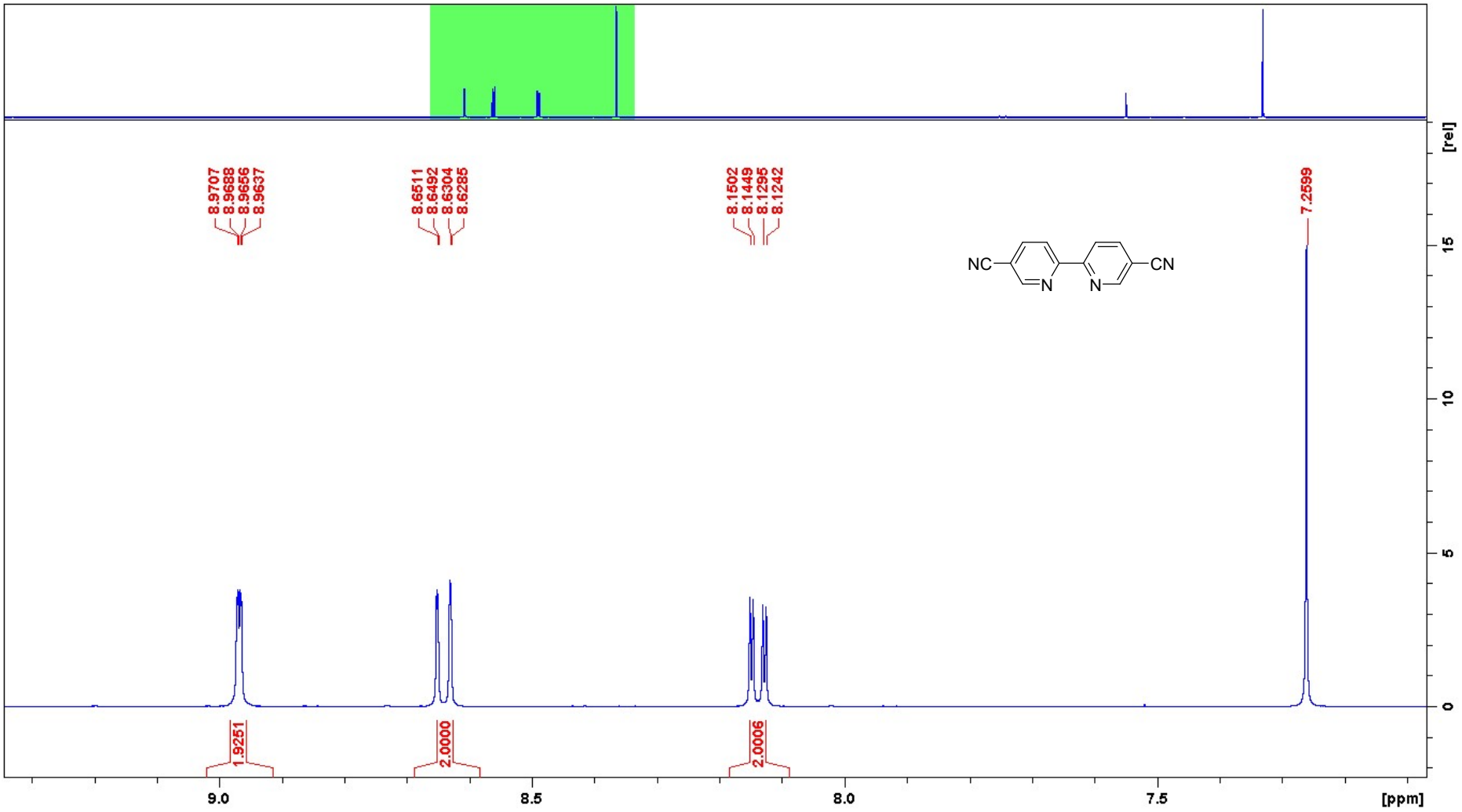

^{13}C NMR ($CDCl_3$) compound **1**

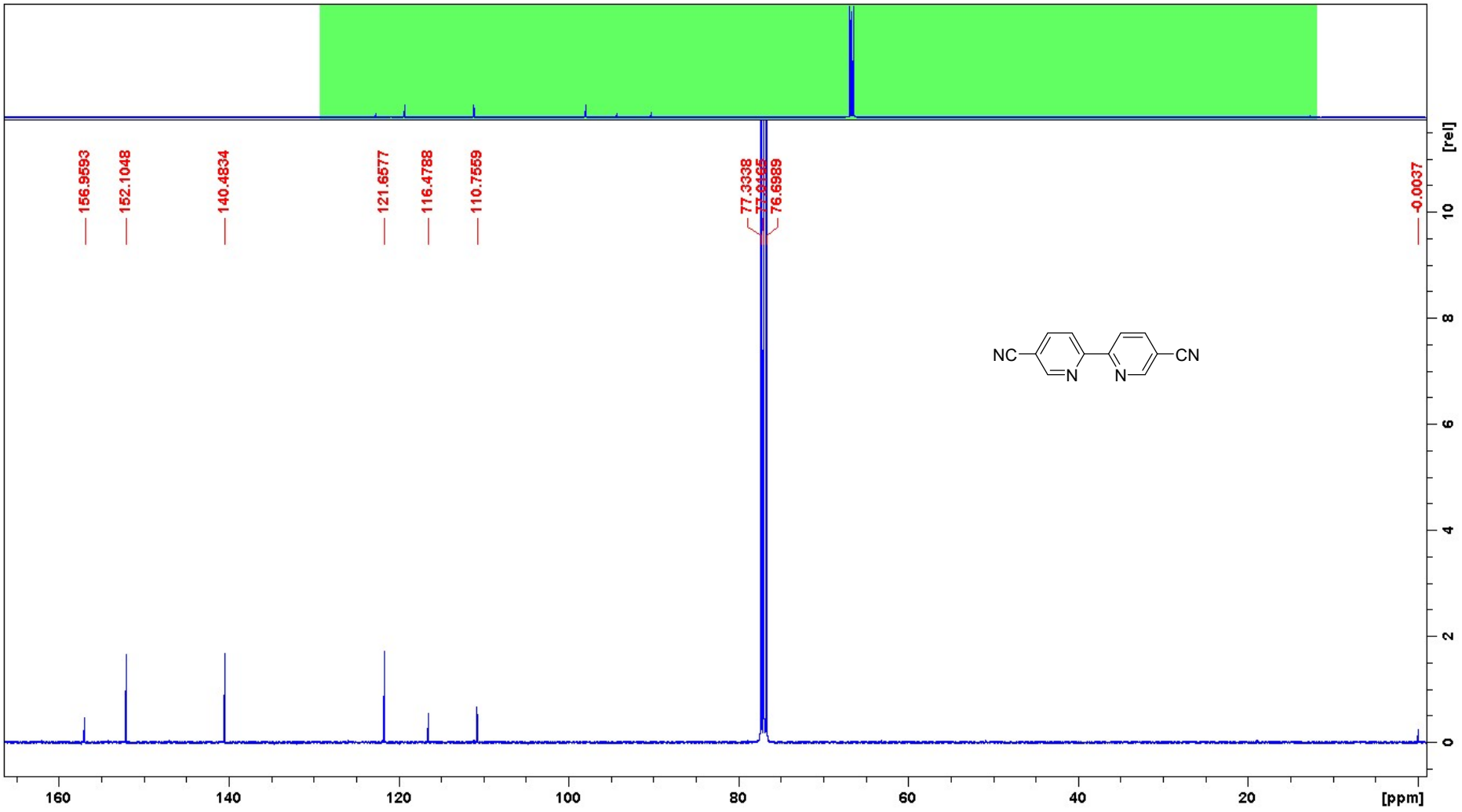

5.1 NMR spectra of transfer hydrogenation substrates

^{1}H NMR ($CDCl_3$) compound **2b**

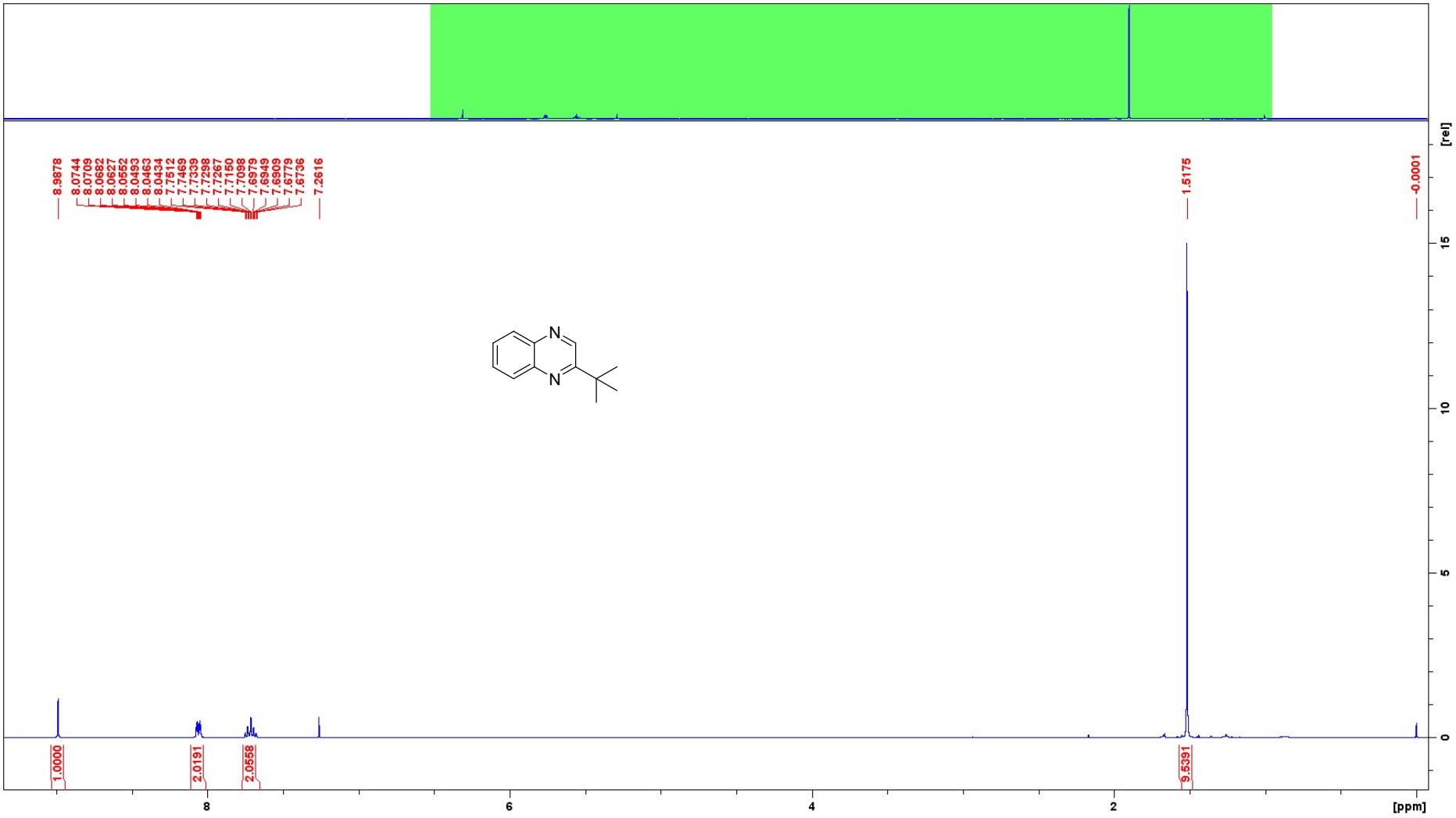

^{13}C NMR ($CDCl_3$) compound **2b**

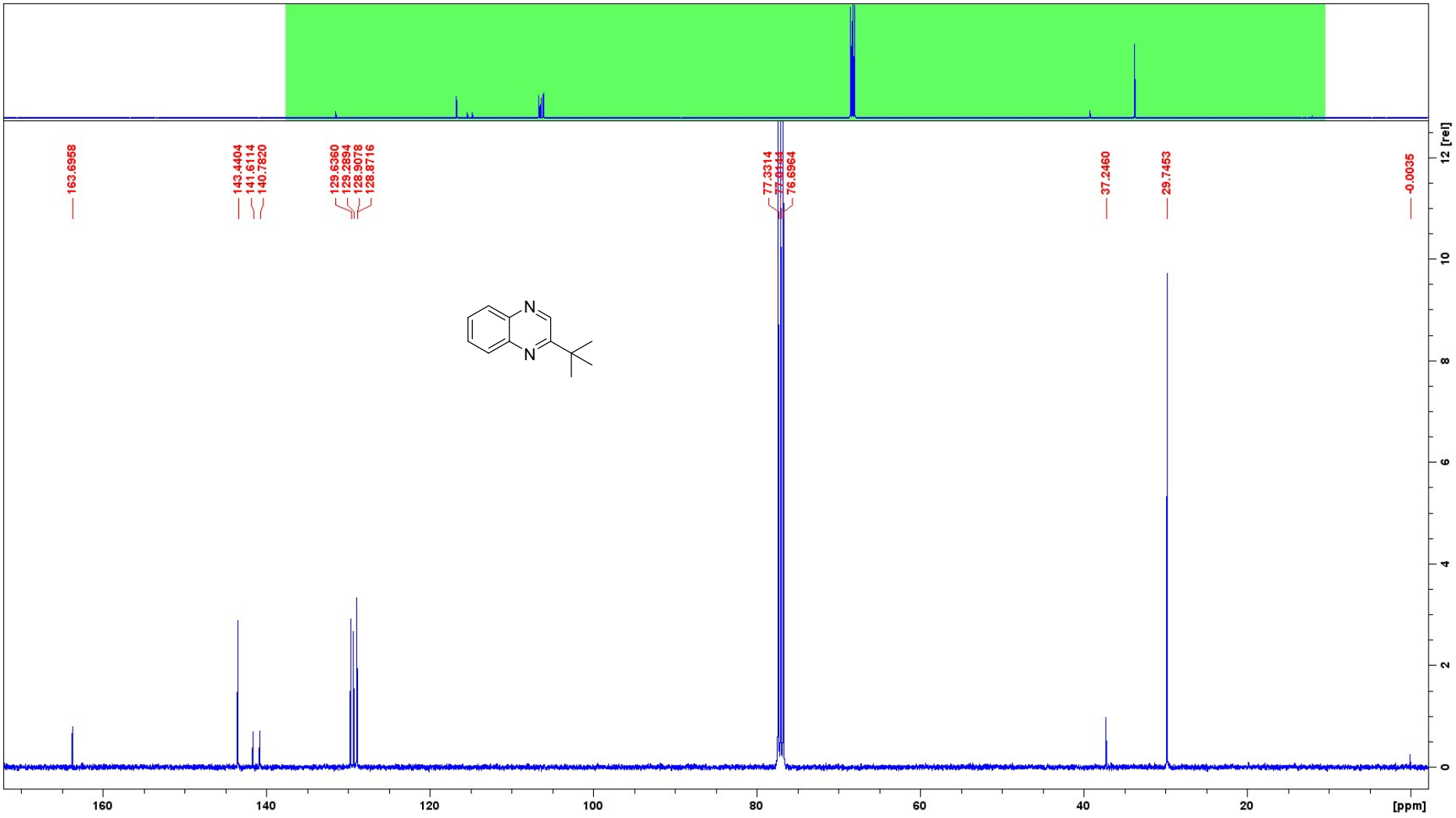

^{1}H NMR ($CDCl_3$) compound **2c**

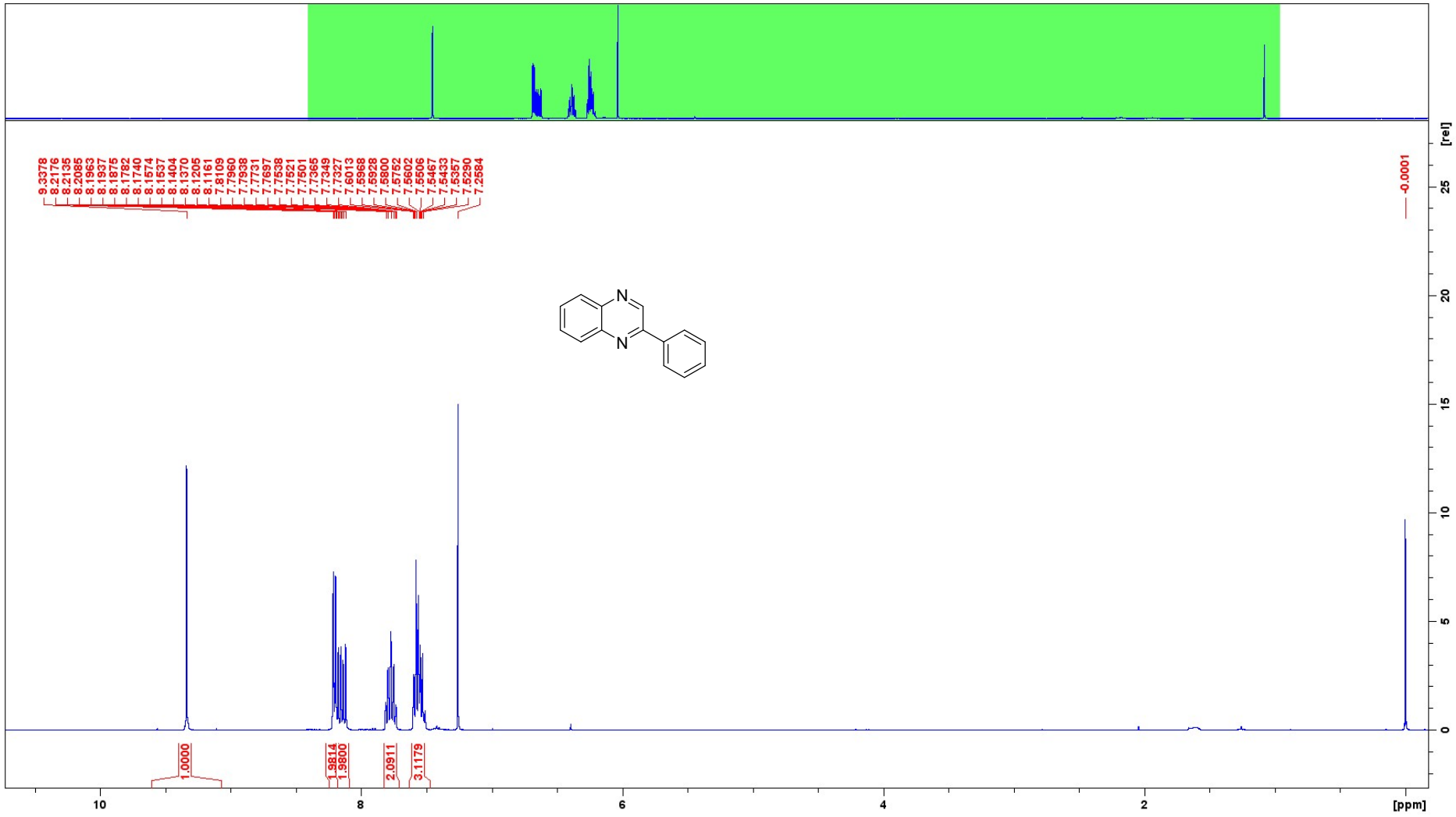

^{13}C NMR ($CDCl_3$) compound **2c**

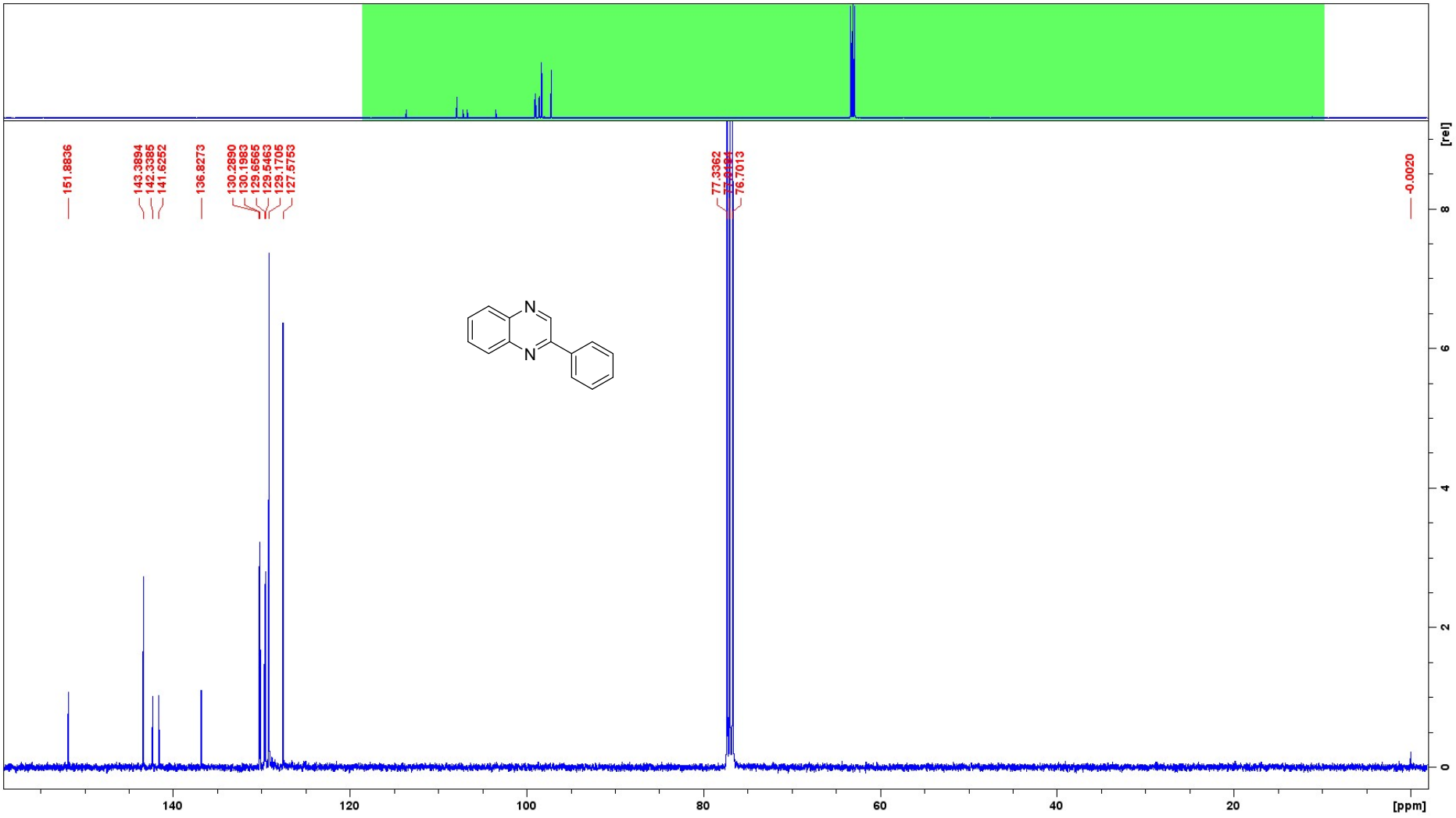

^{1}H NMR ($CDCl_3$) compound **2d**

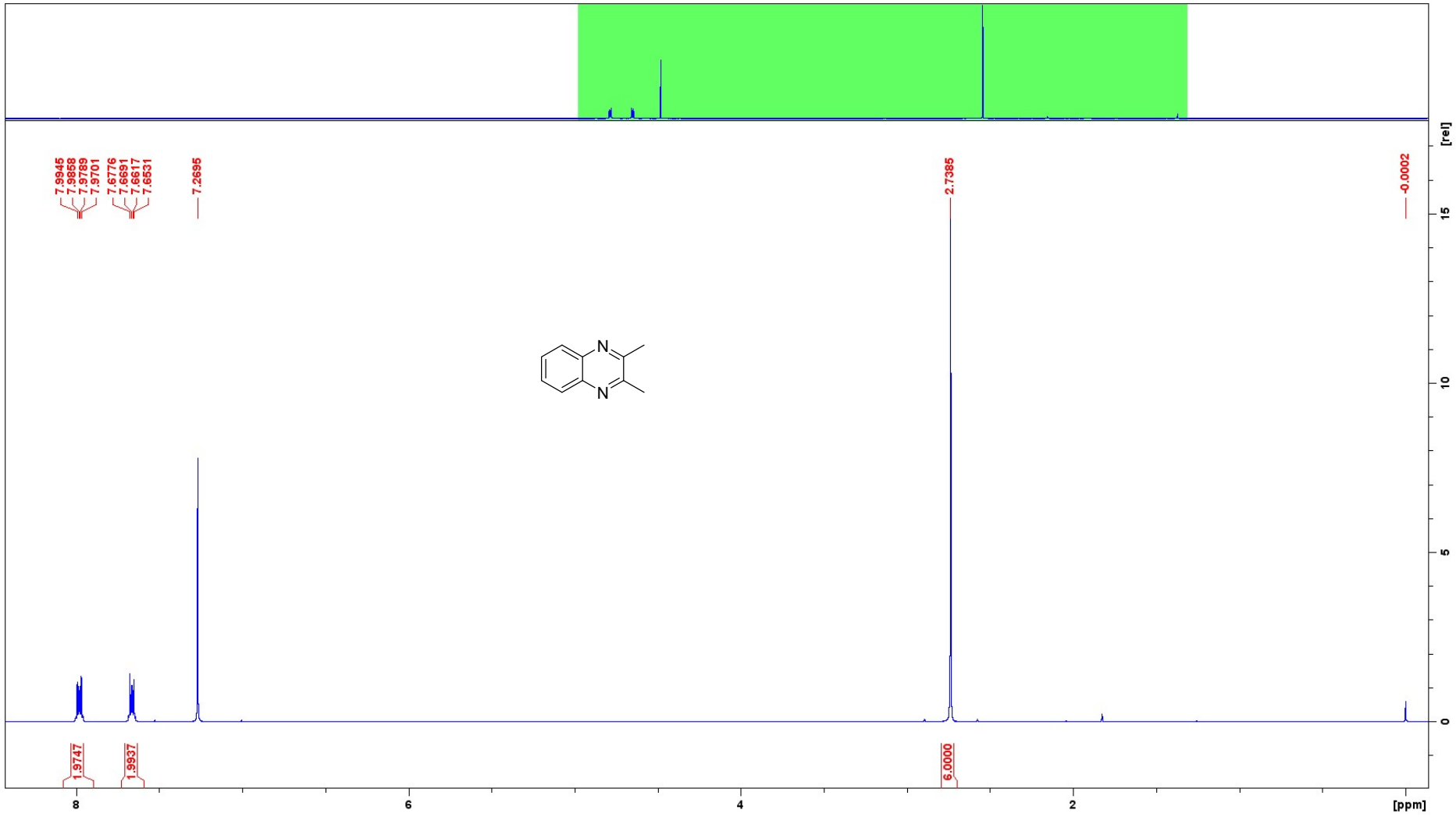

^{13}C NMR ($CDCl_3$) compound **2d**

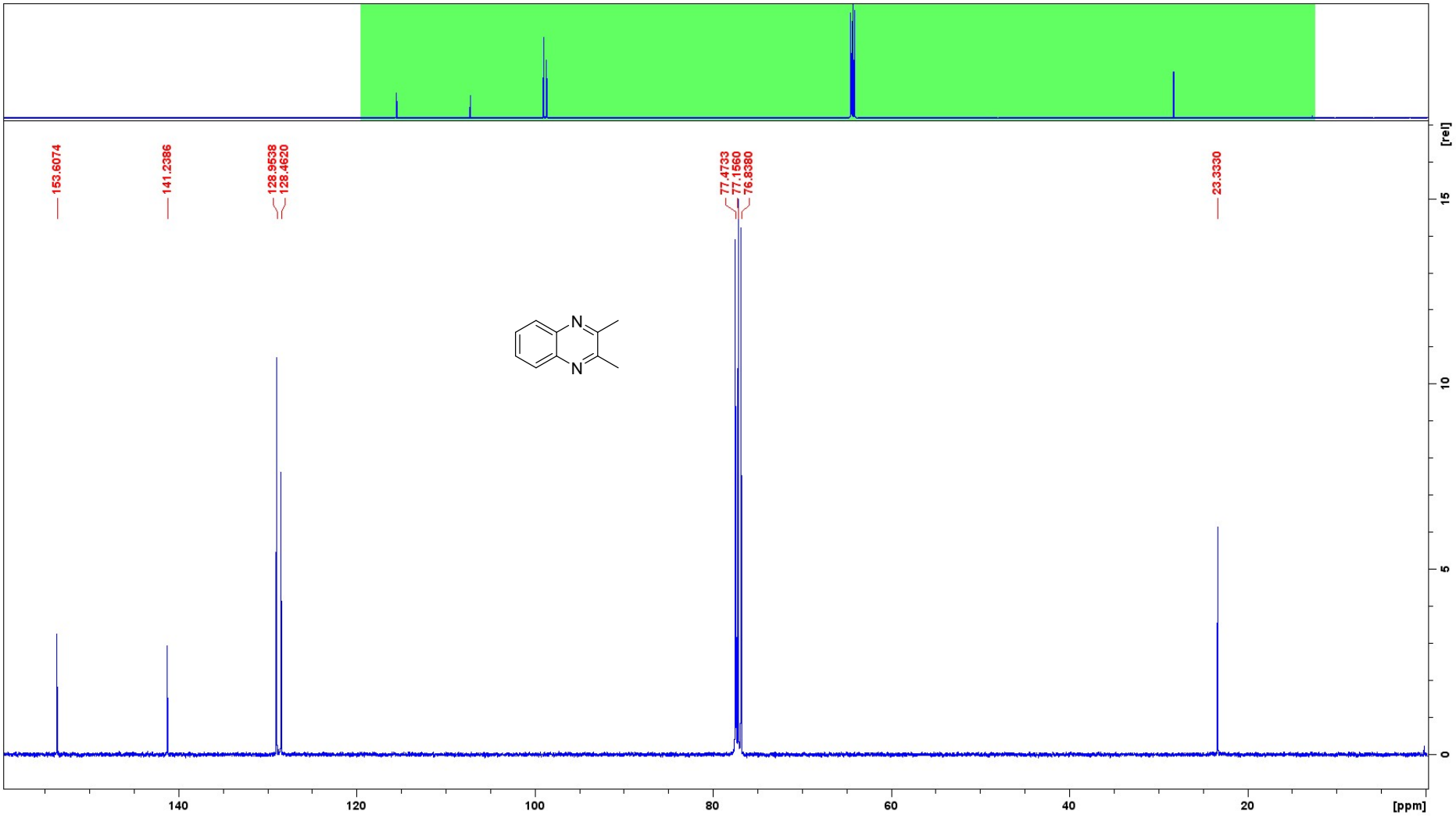

^{1}H NMR ($CDCl_3$) compound **2e**

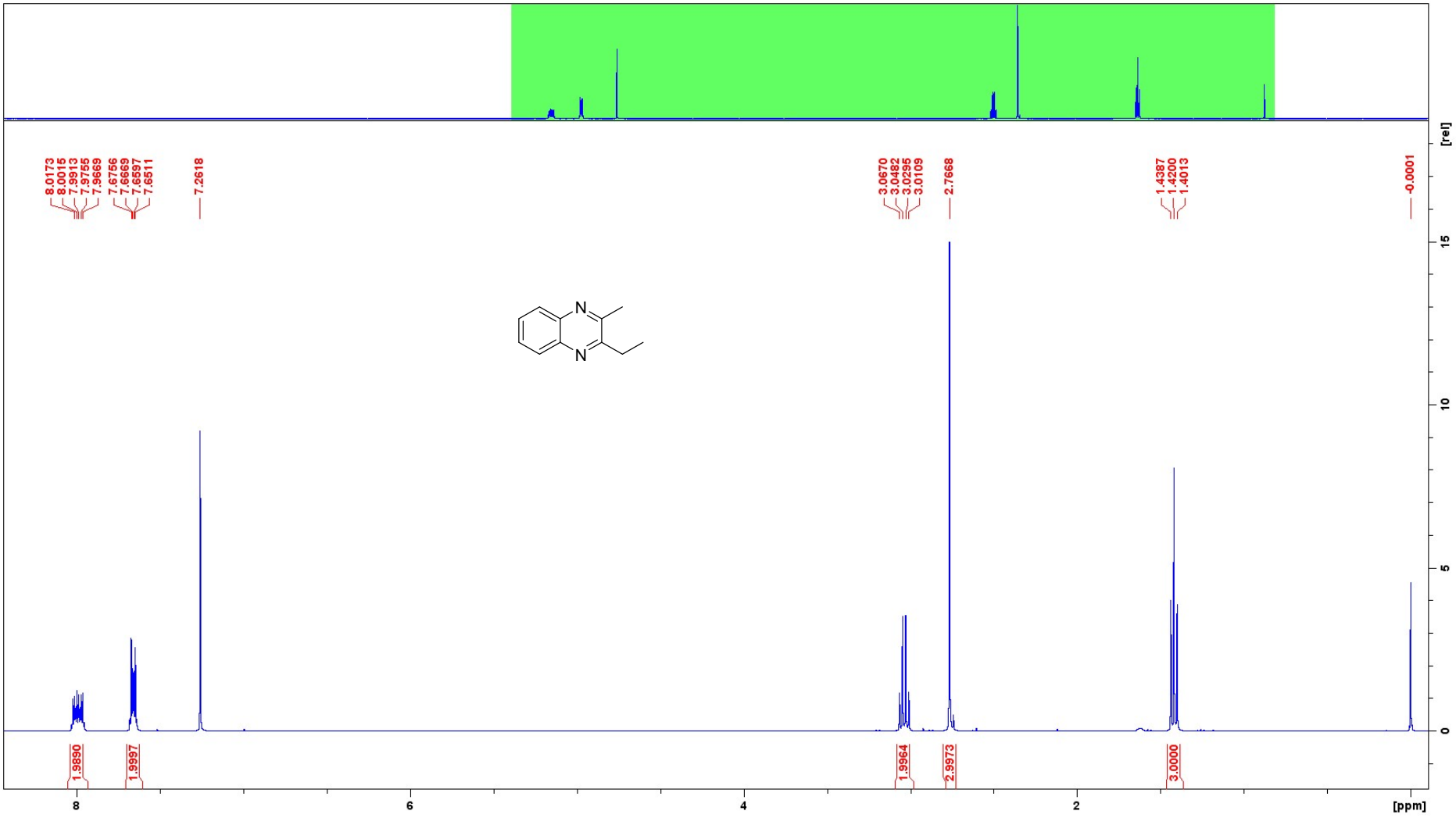

^{13}C NMR ($CDCl_3$) compound **2e**

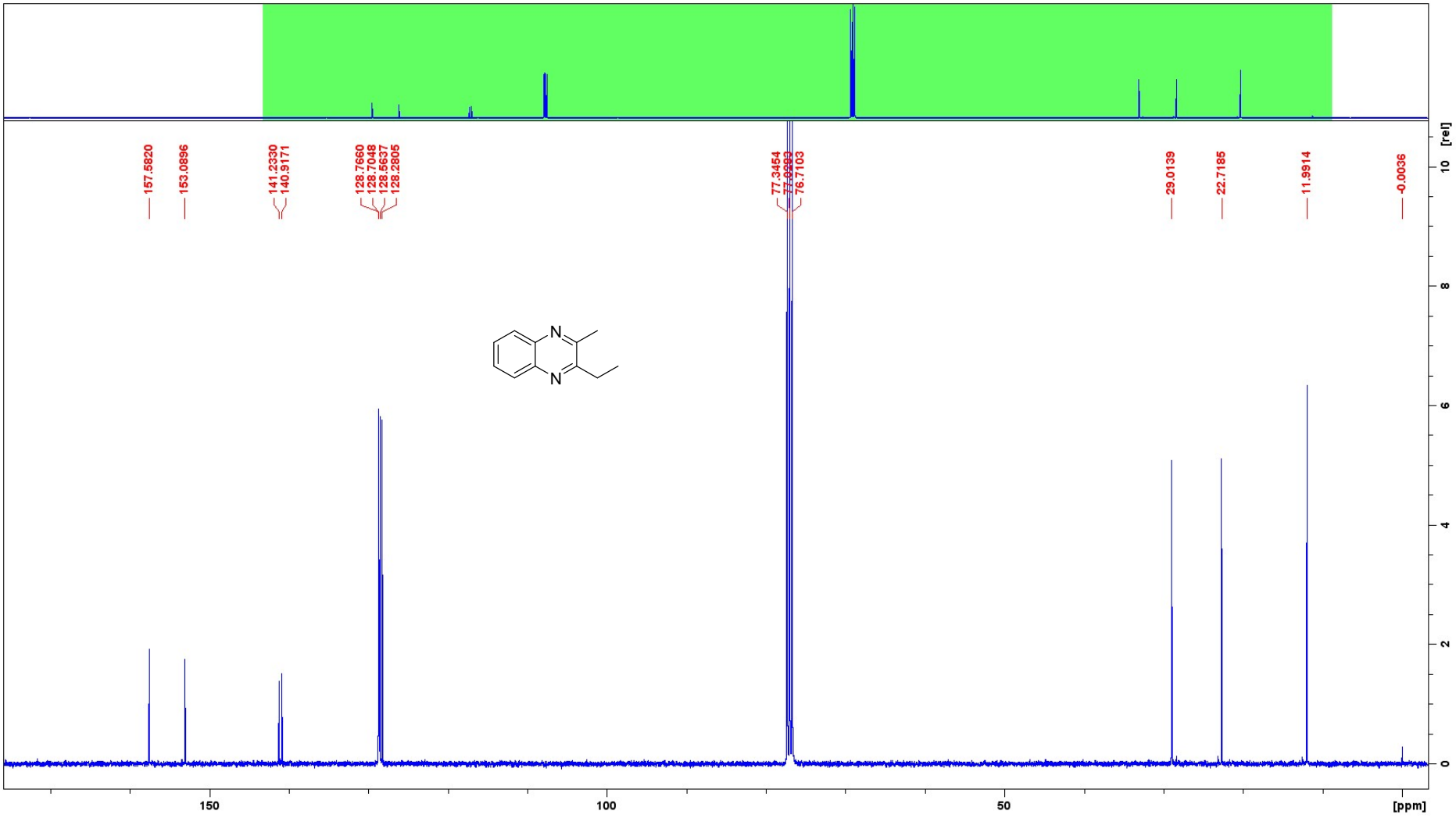

^{1}H NMR ($CDCl_3$) compound **2f**

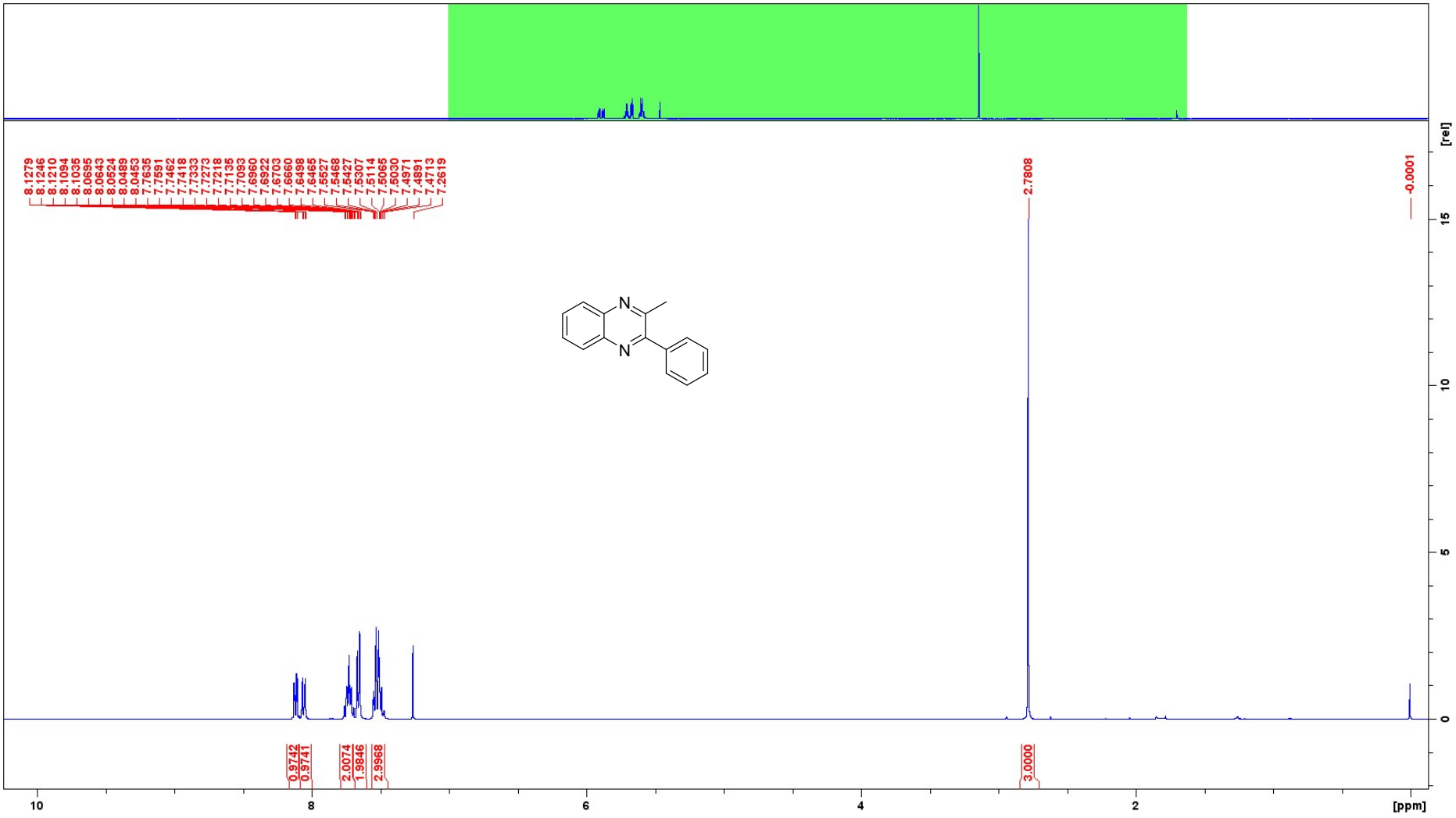

^{13}C NMR ($CDCl_3$) compound **2f**

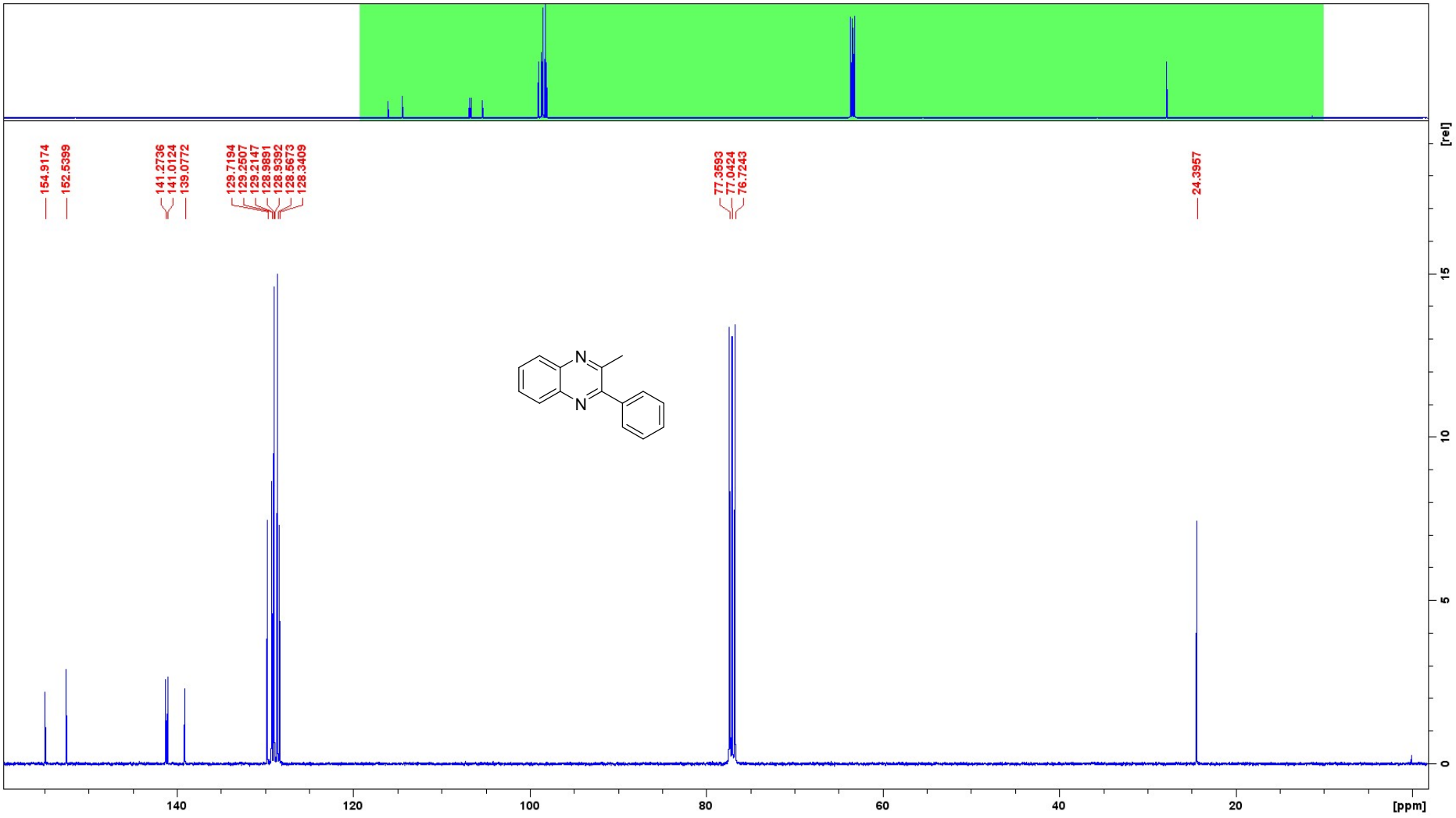

^{1}H NMR ($CDCl_3$) compound **2g**

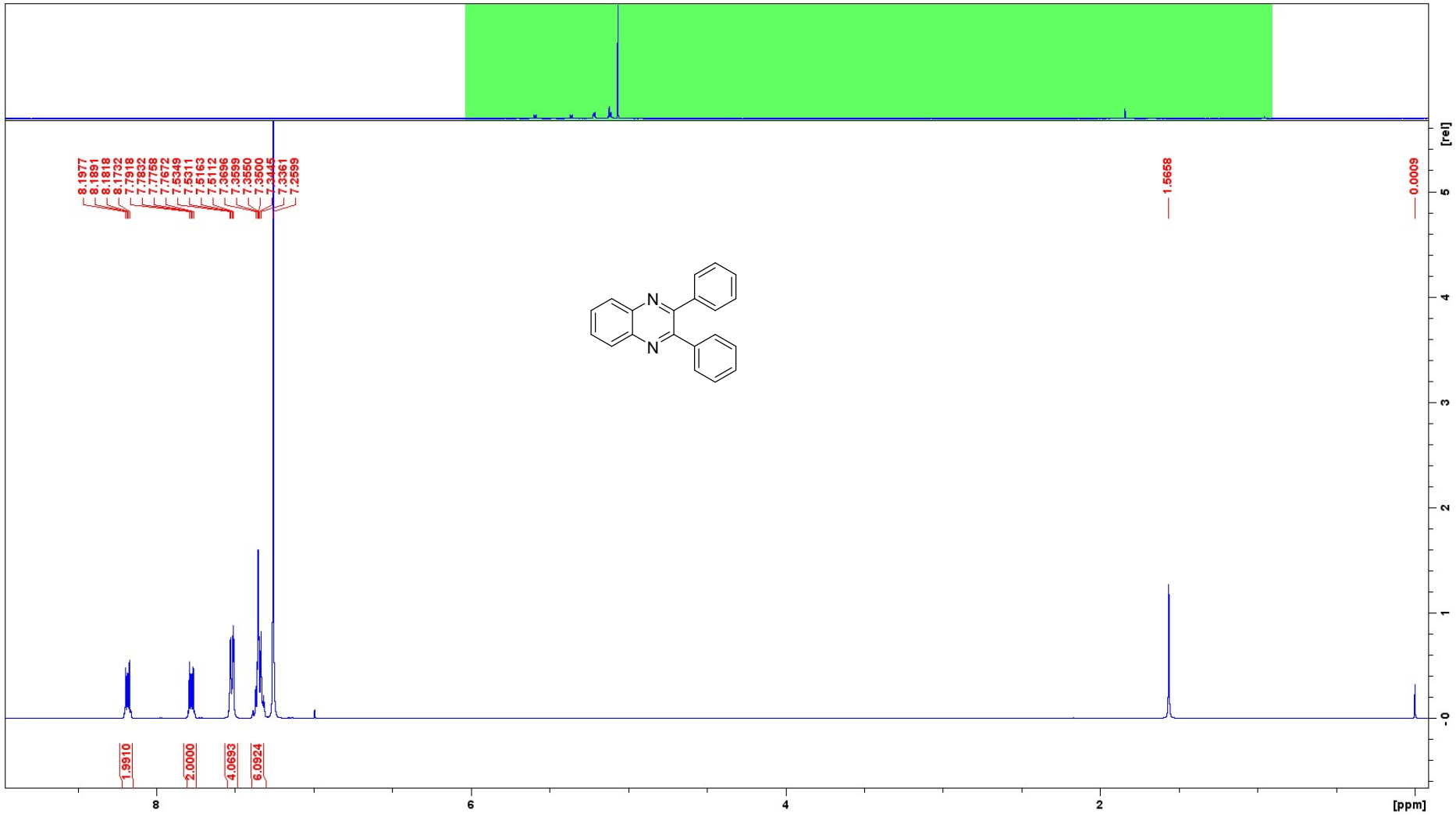

^{13}C NMR ($CDCl_3$) compound **2g**

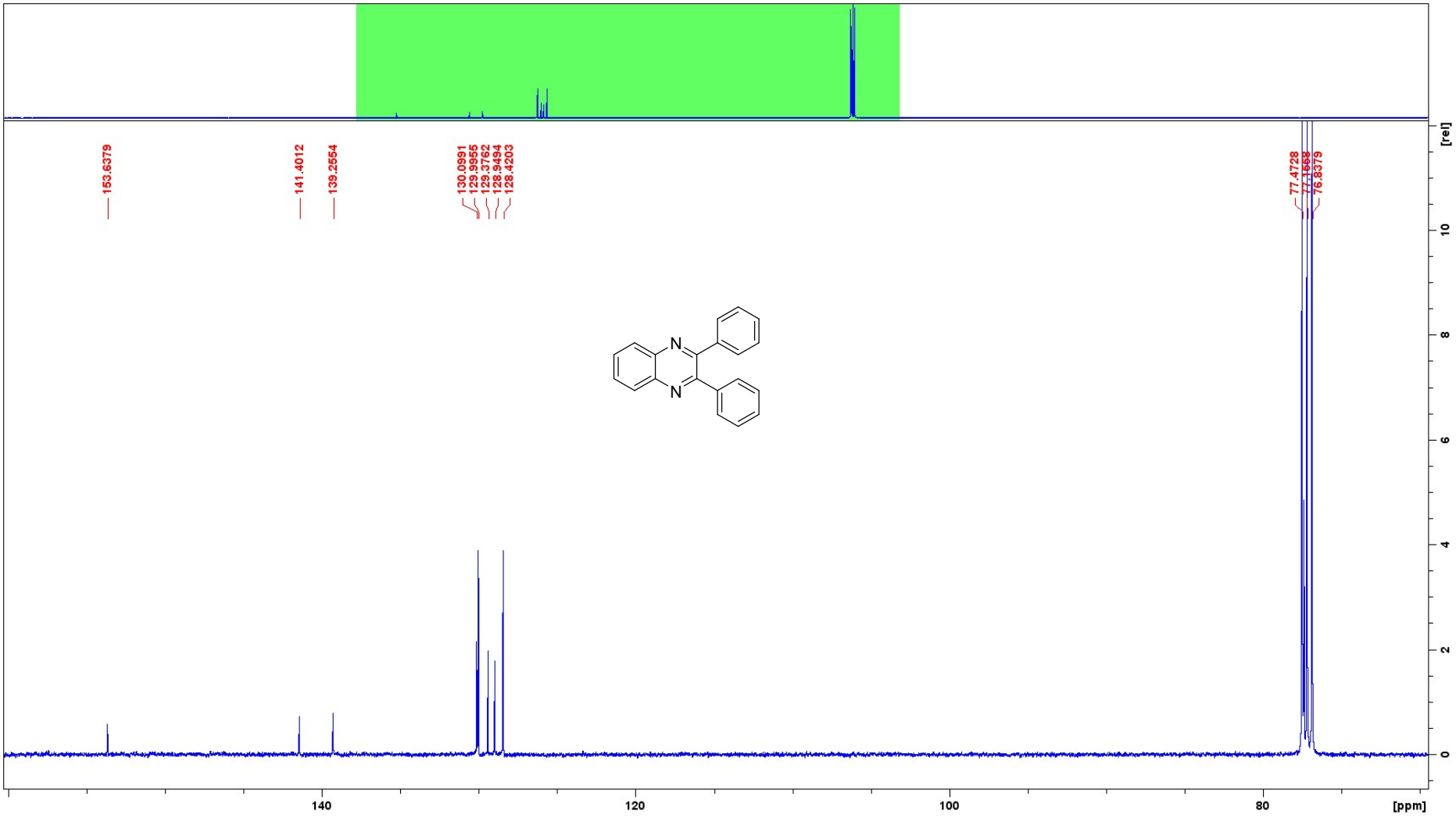

^{1}H NMR ($CDCl_3$) compound **2h**

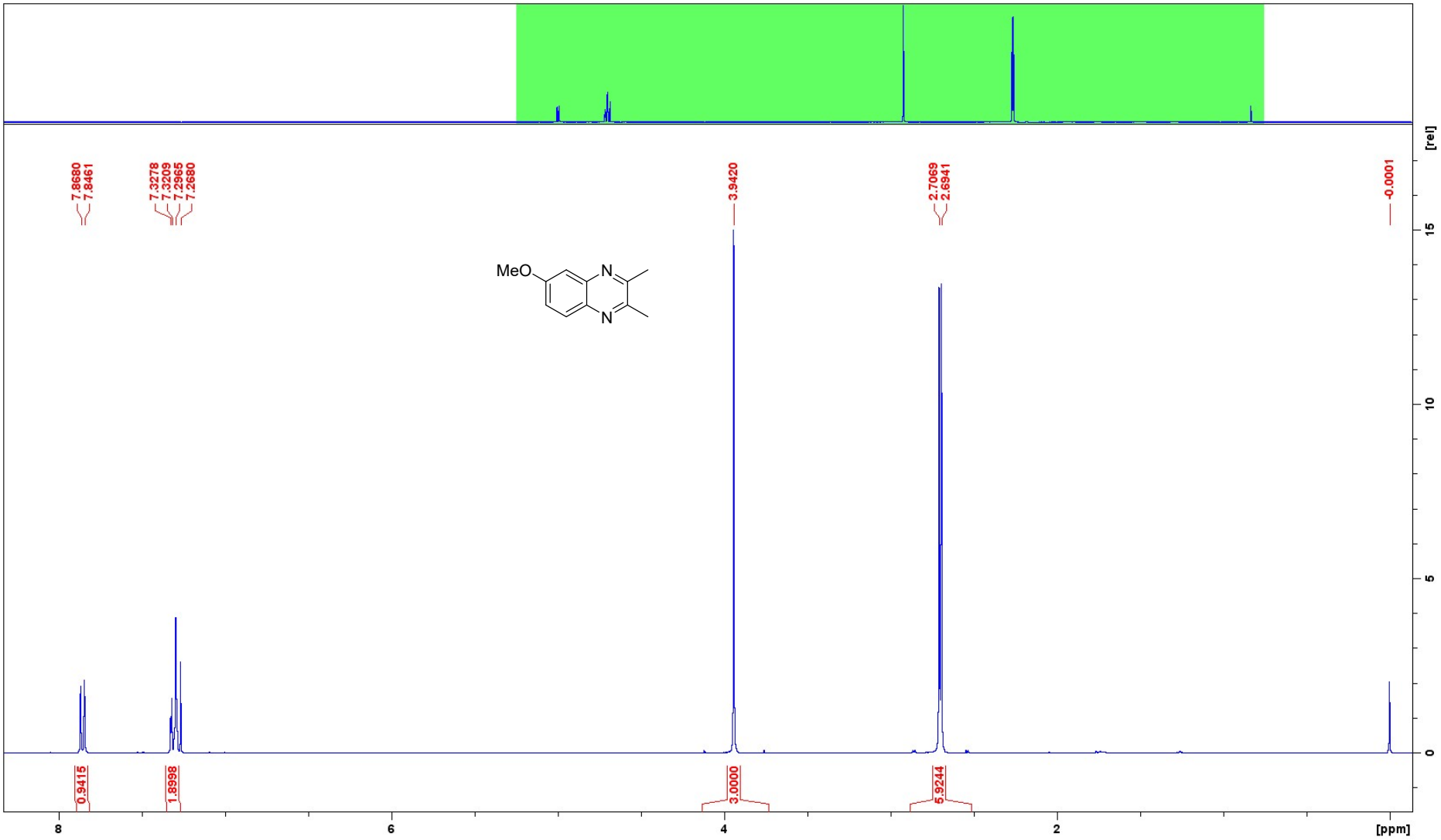

^{13}C NMR ($CDCl_3$) compound **2h**

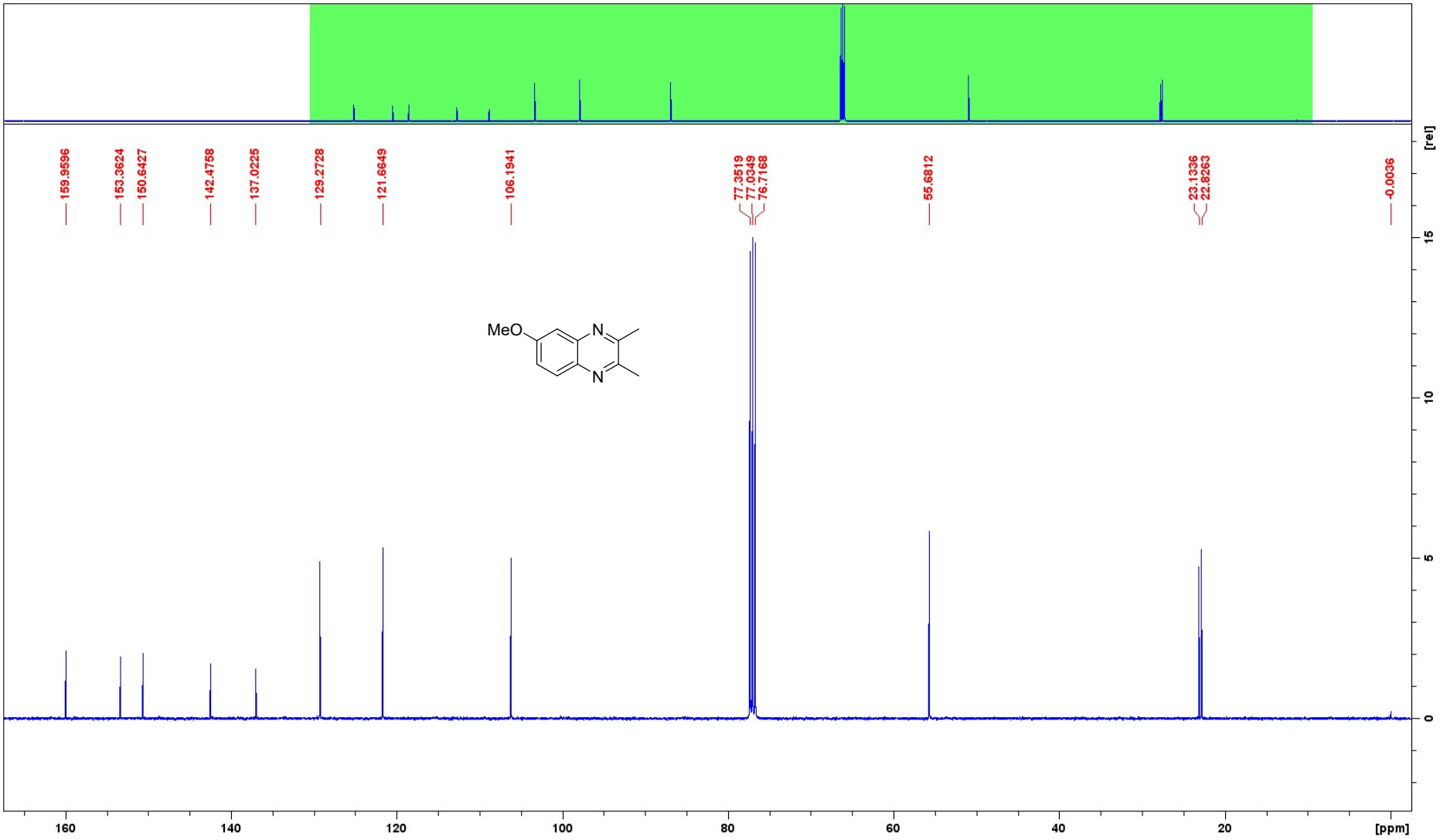

^{1}H NMR ($CDCl_3$) compound **2i**

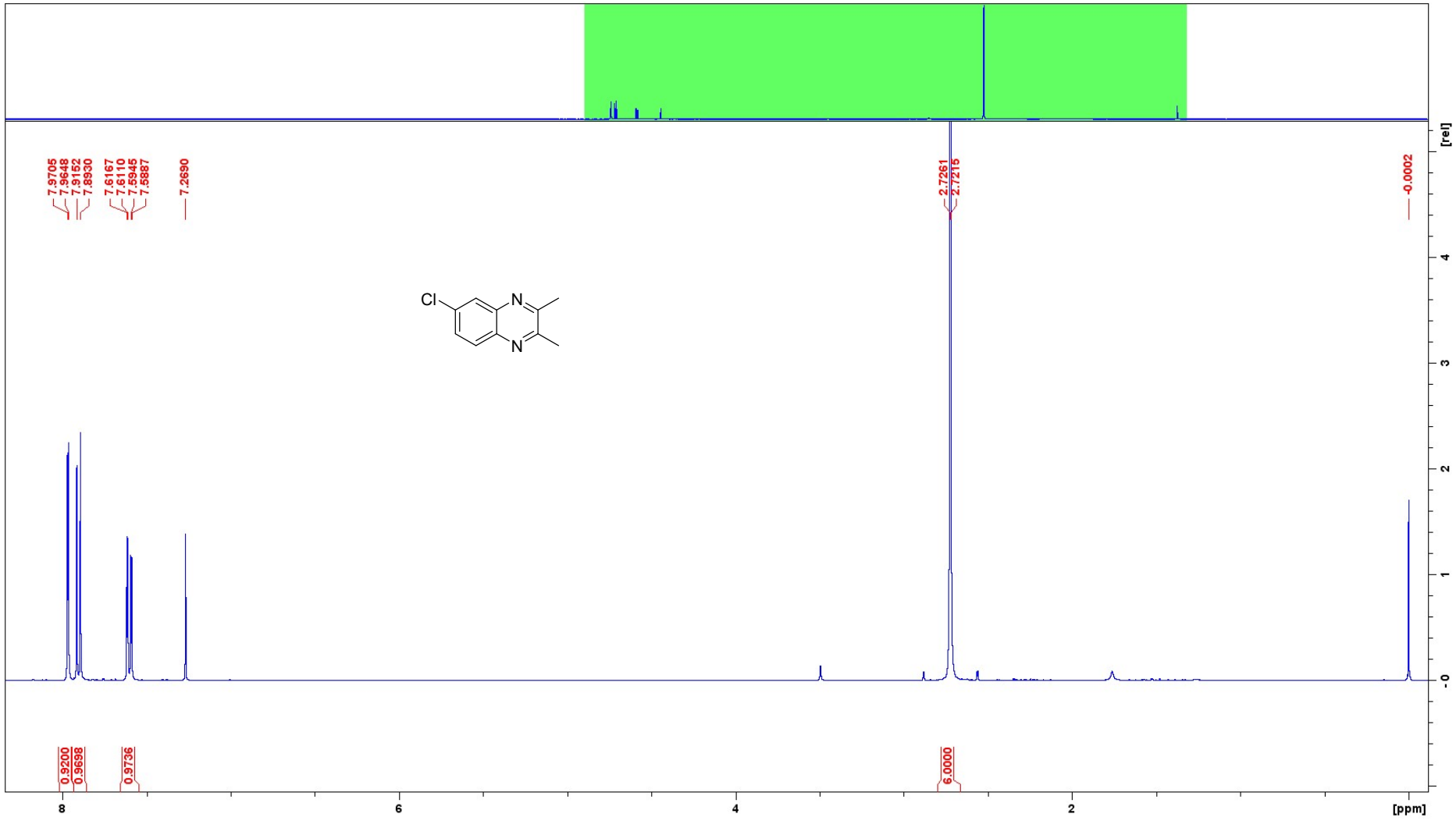

^{13}C NMR ($CDCl_3$) compound **2i**

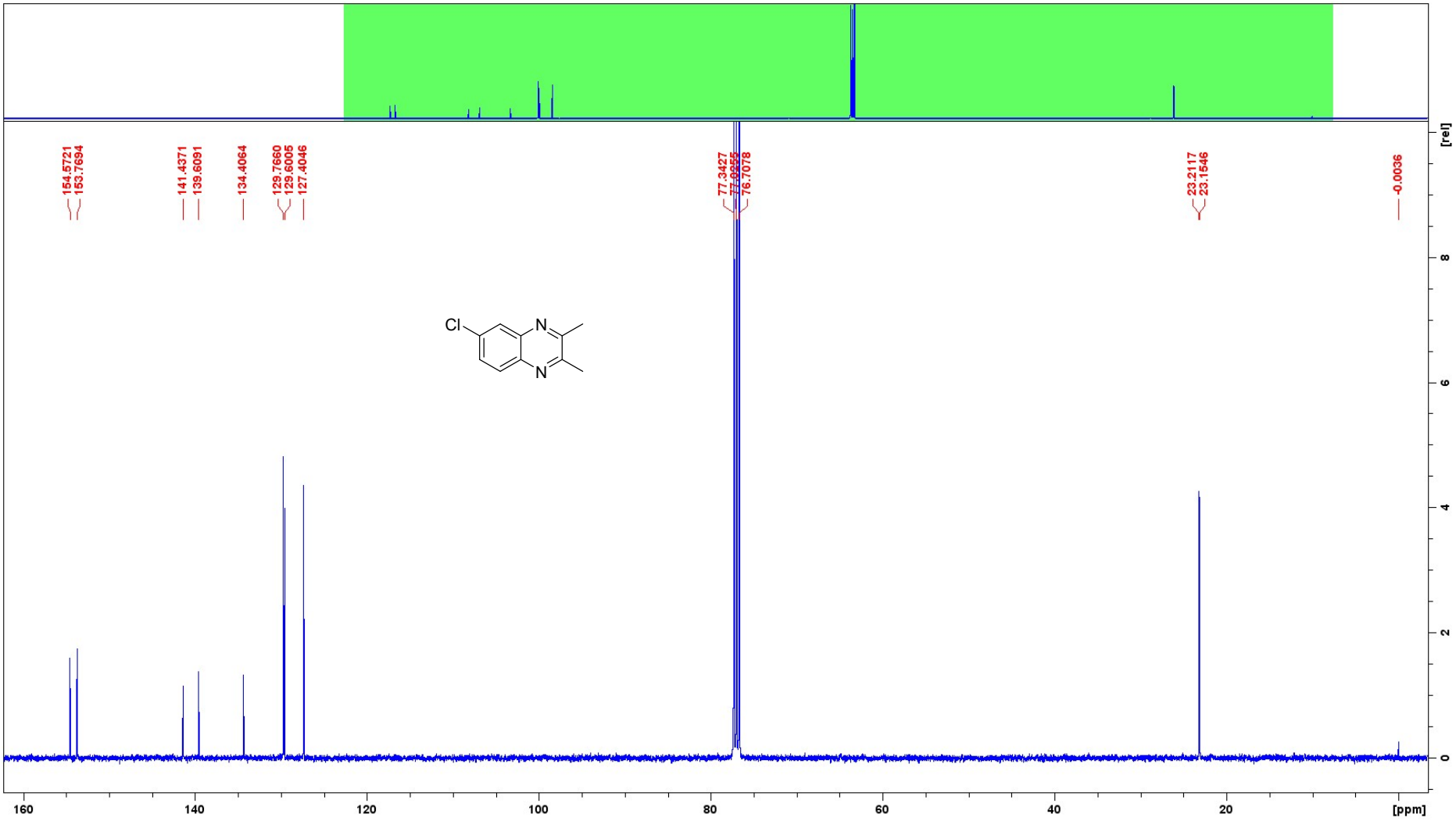

^{1}H NMR ($CDCl_3$) compound **2j**

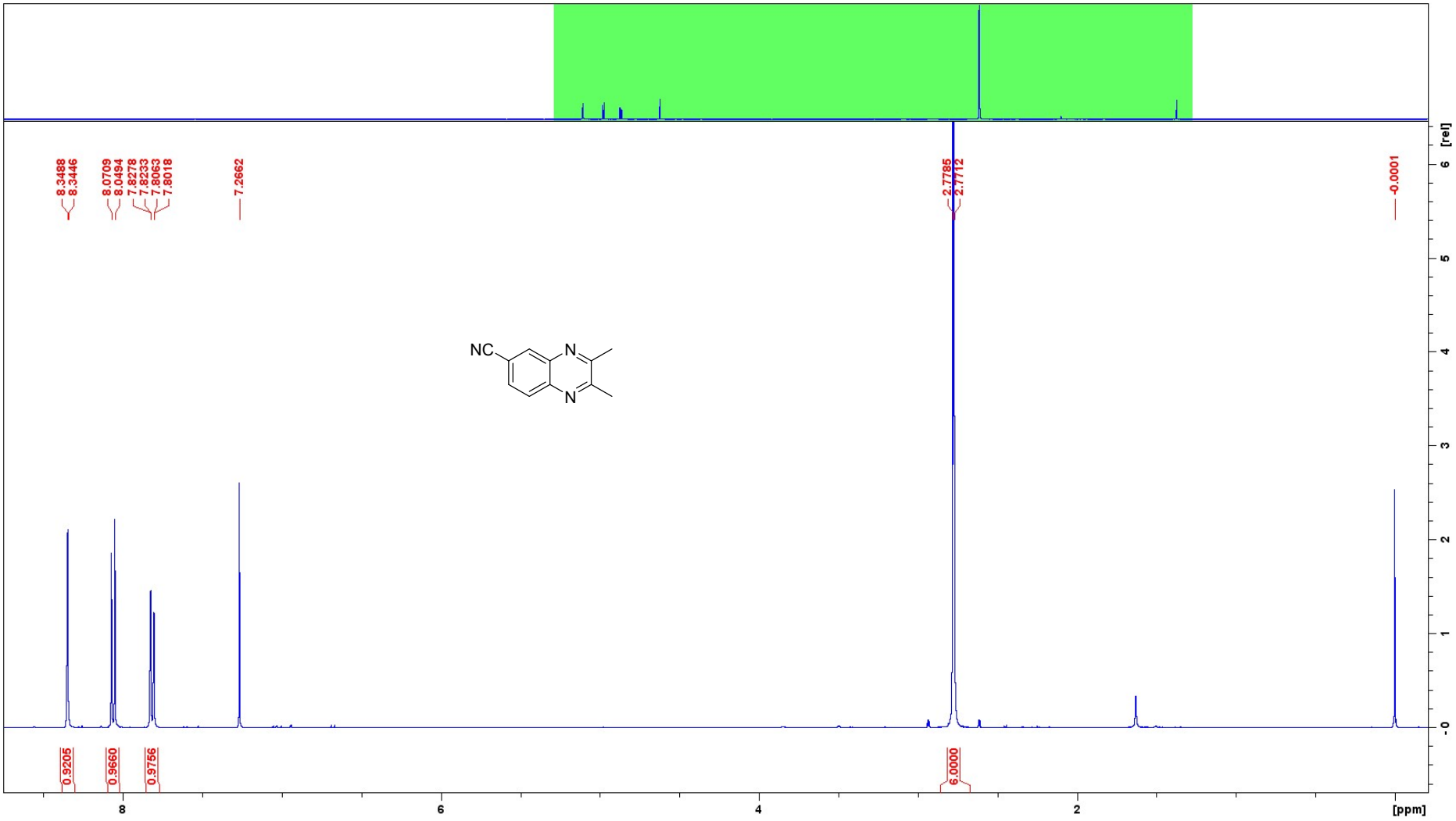

^{13}C NMR ($CDCl_3$) compound **2j**

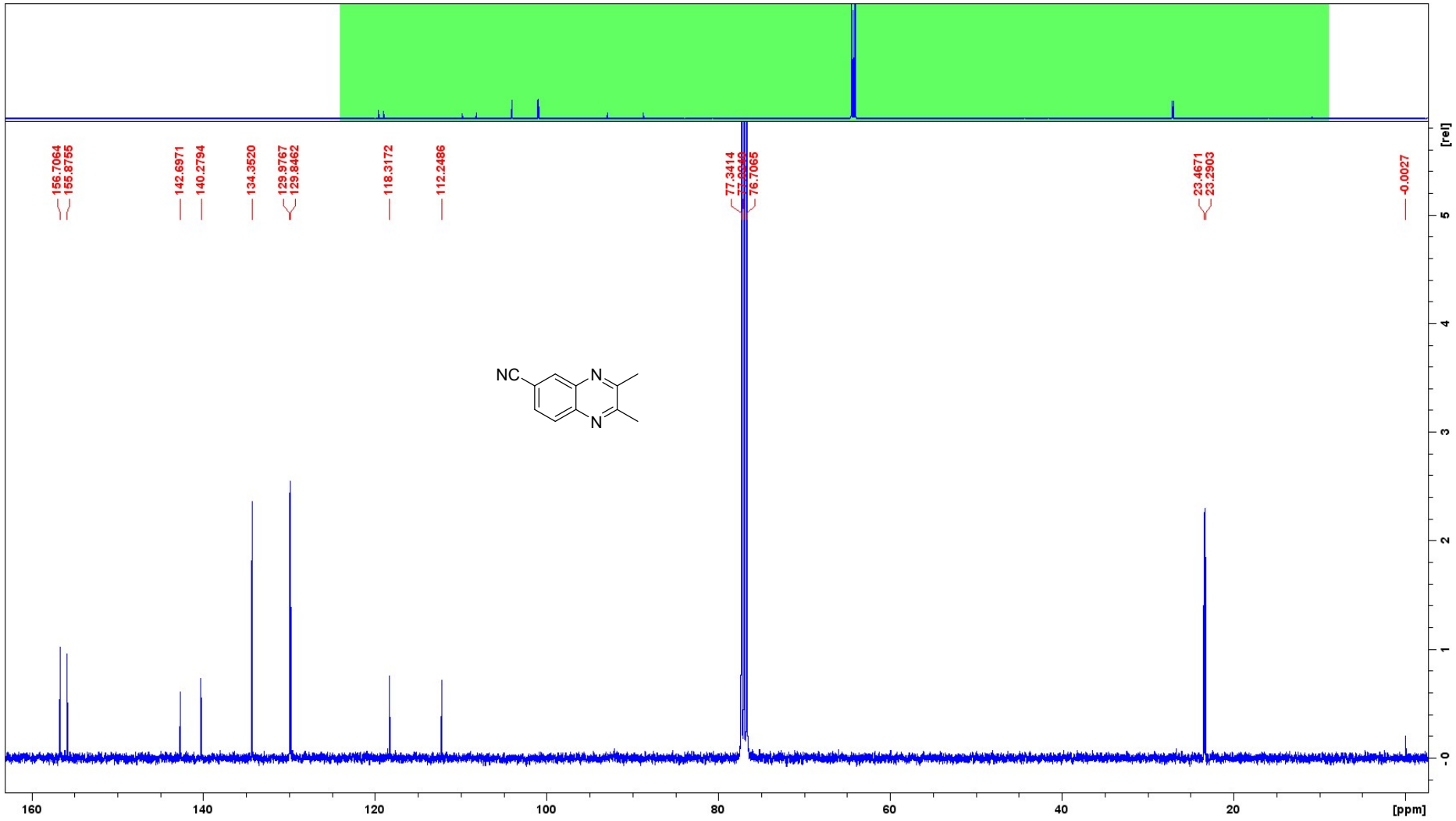

^{1}H NMR ($CDCl_3$) compound **2k**

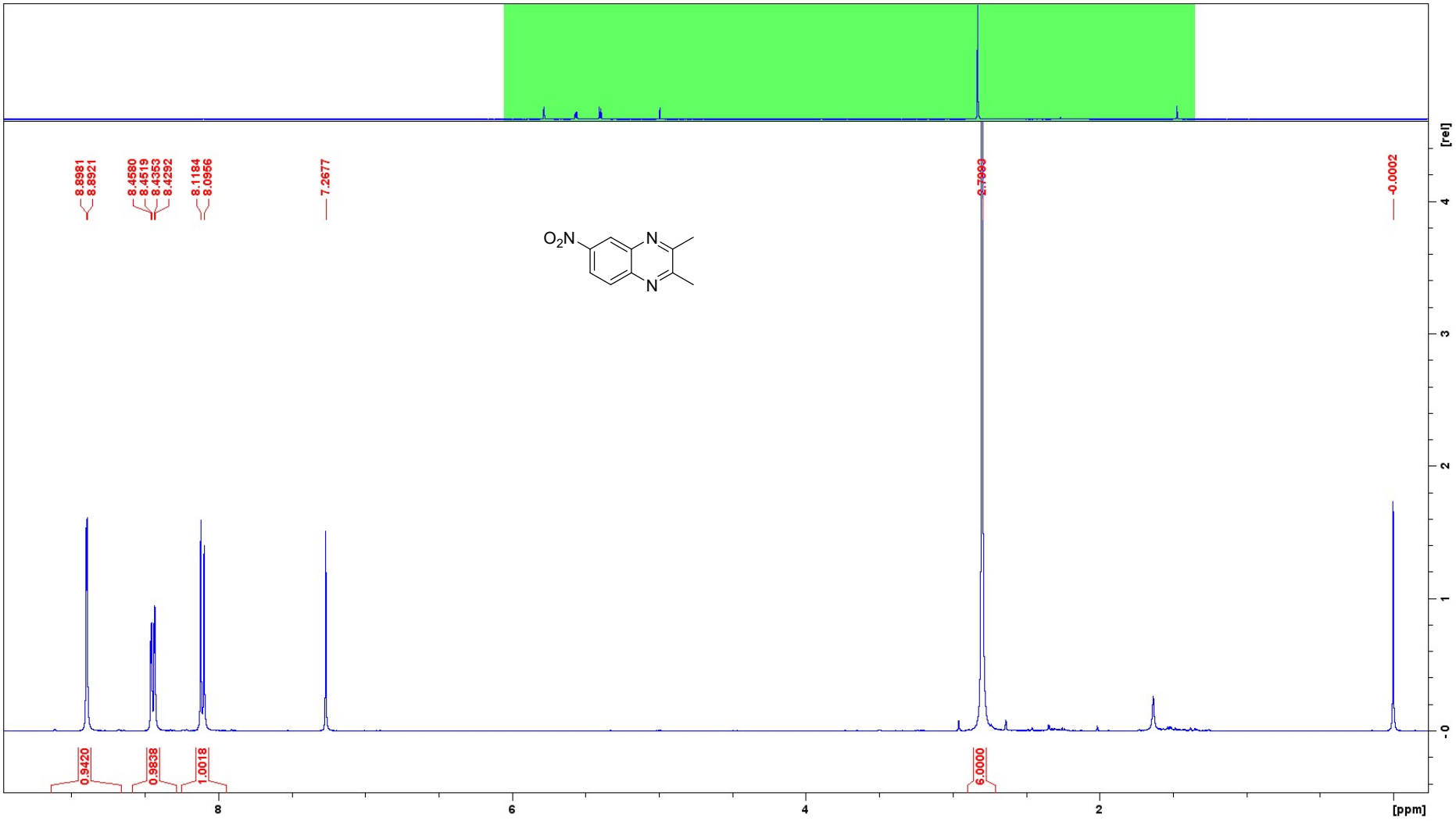

^{13}C NMR ($CDCl_3$) compound **2k**

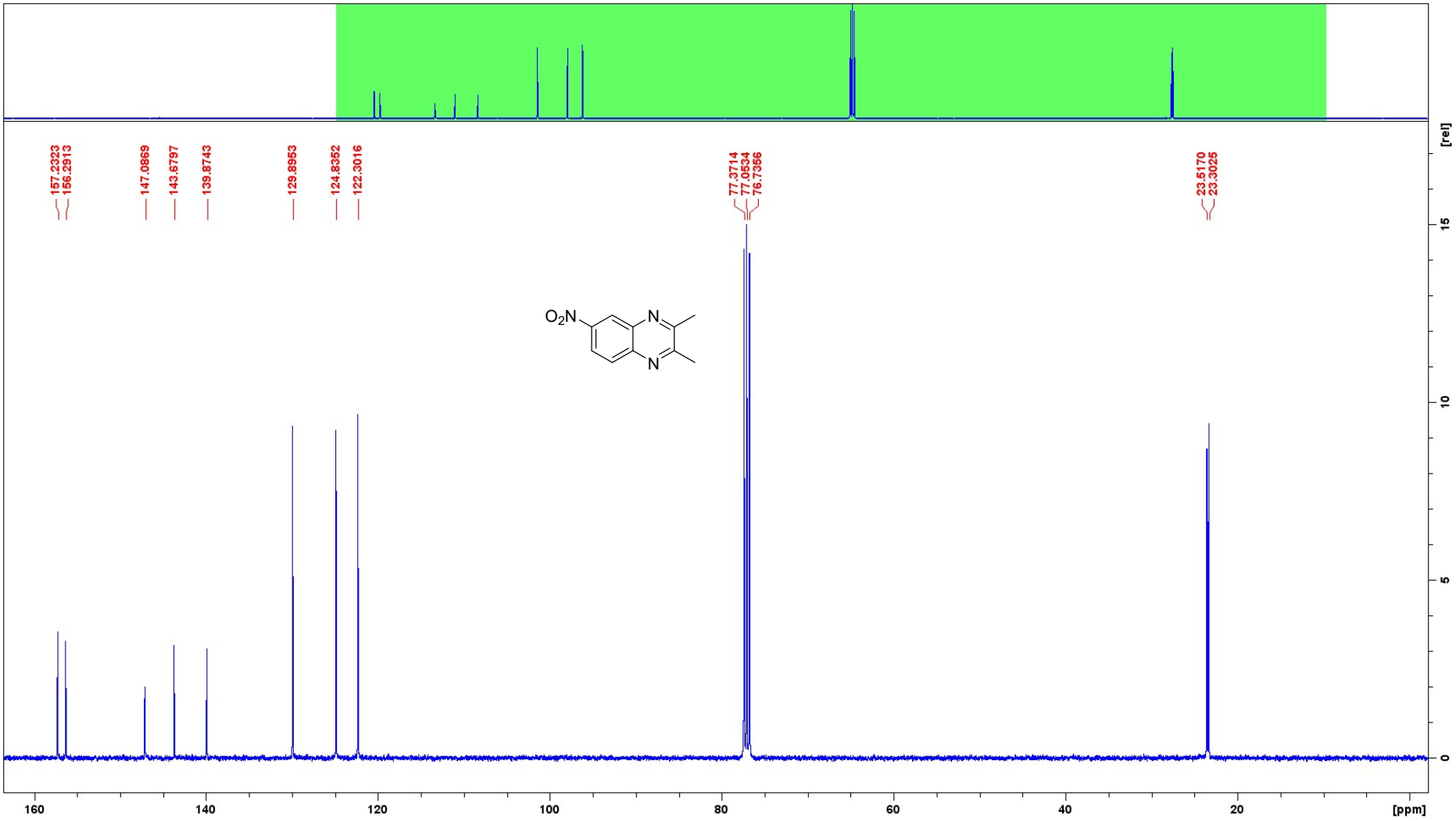

5.2 NMR spectra of transfer hydrogenation products

^{1}H NMR ($CDCl_3$) compound **3a**

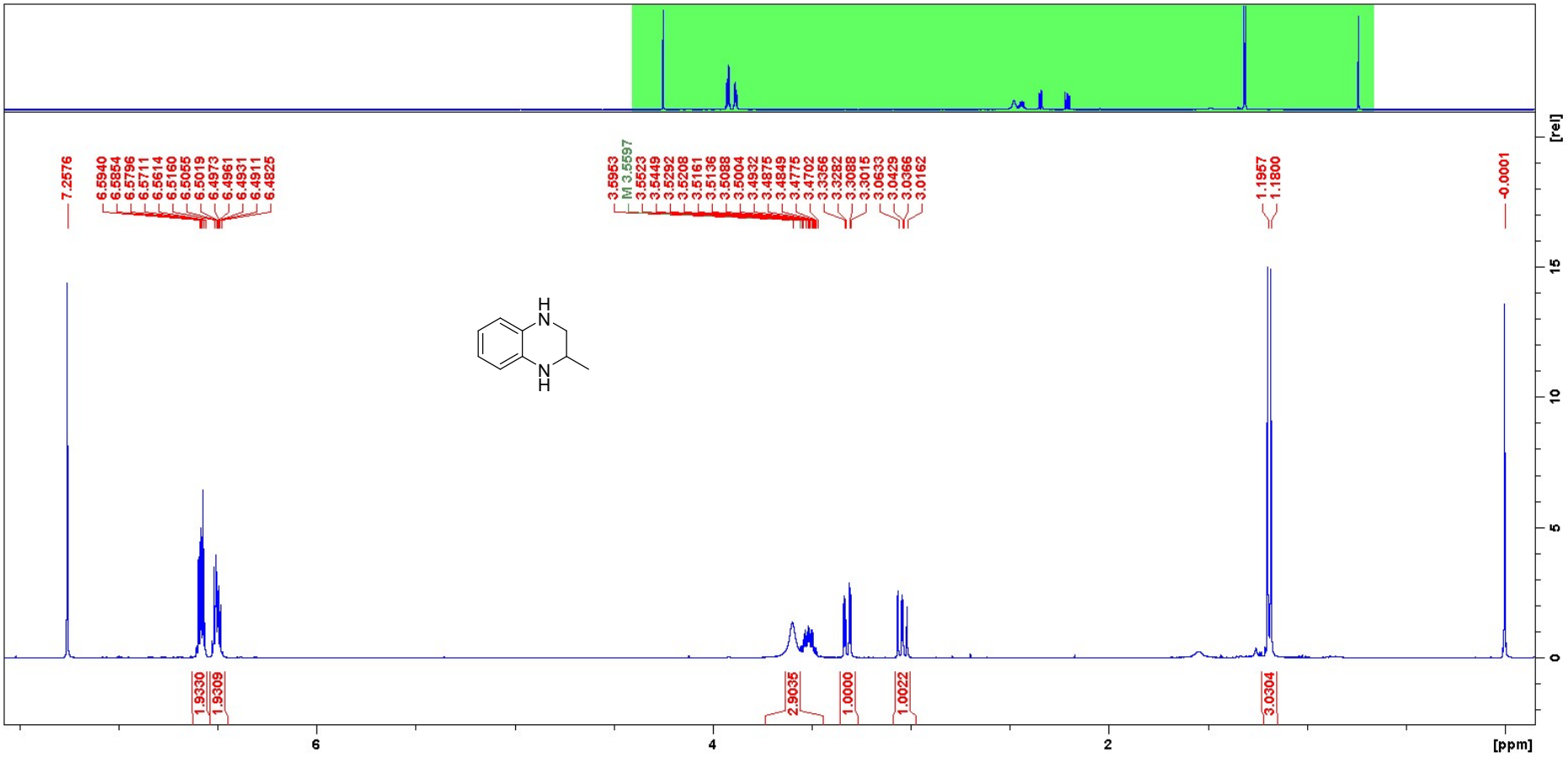

^{13}C NMR ($CDCl_3$) compound **3a**

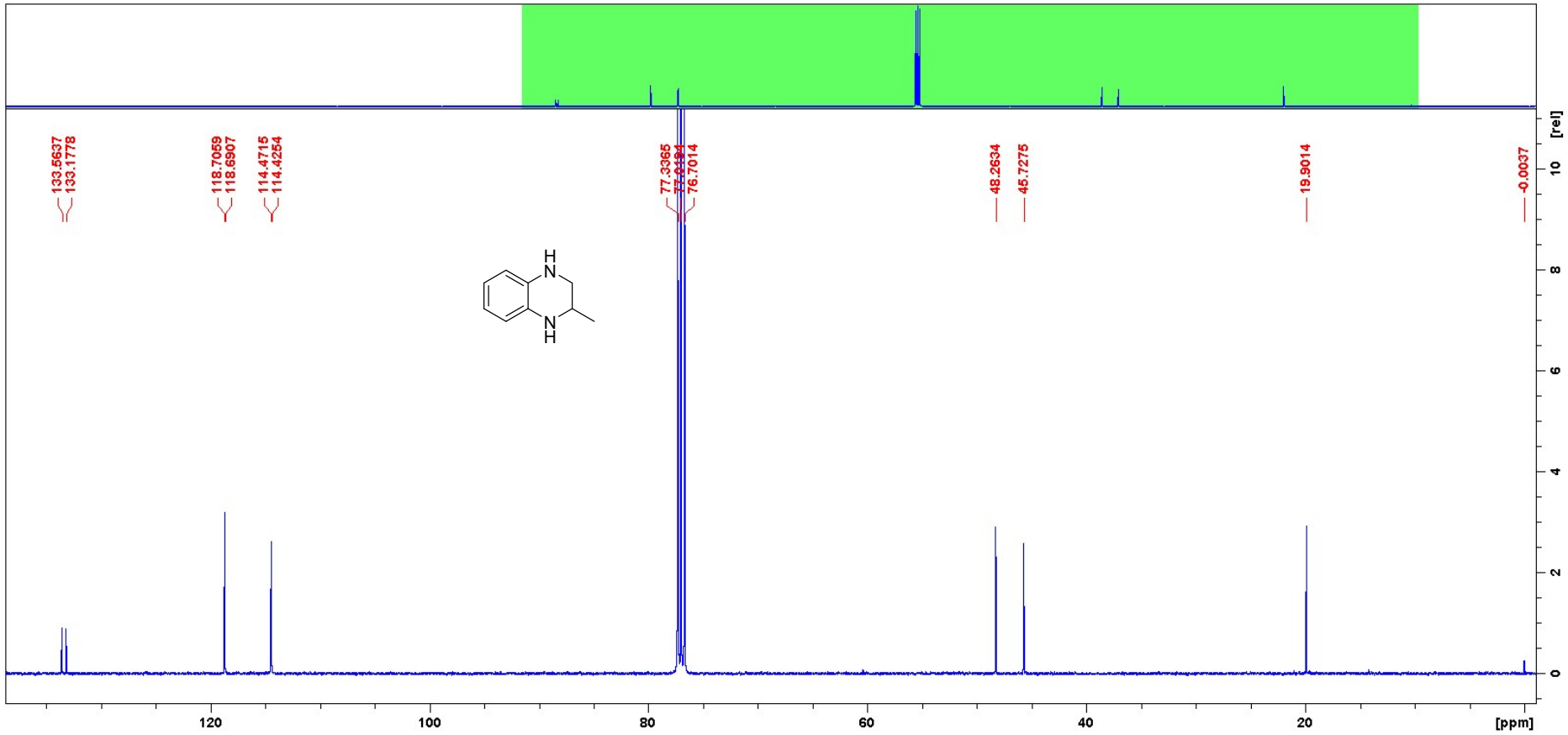

^{1}H NMR ($CDCl_3$) compound **3b**

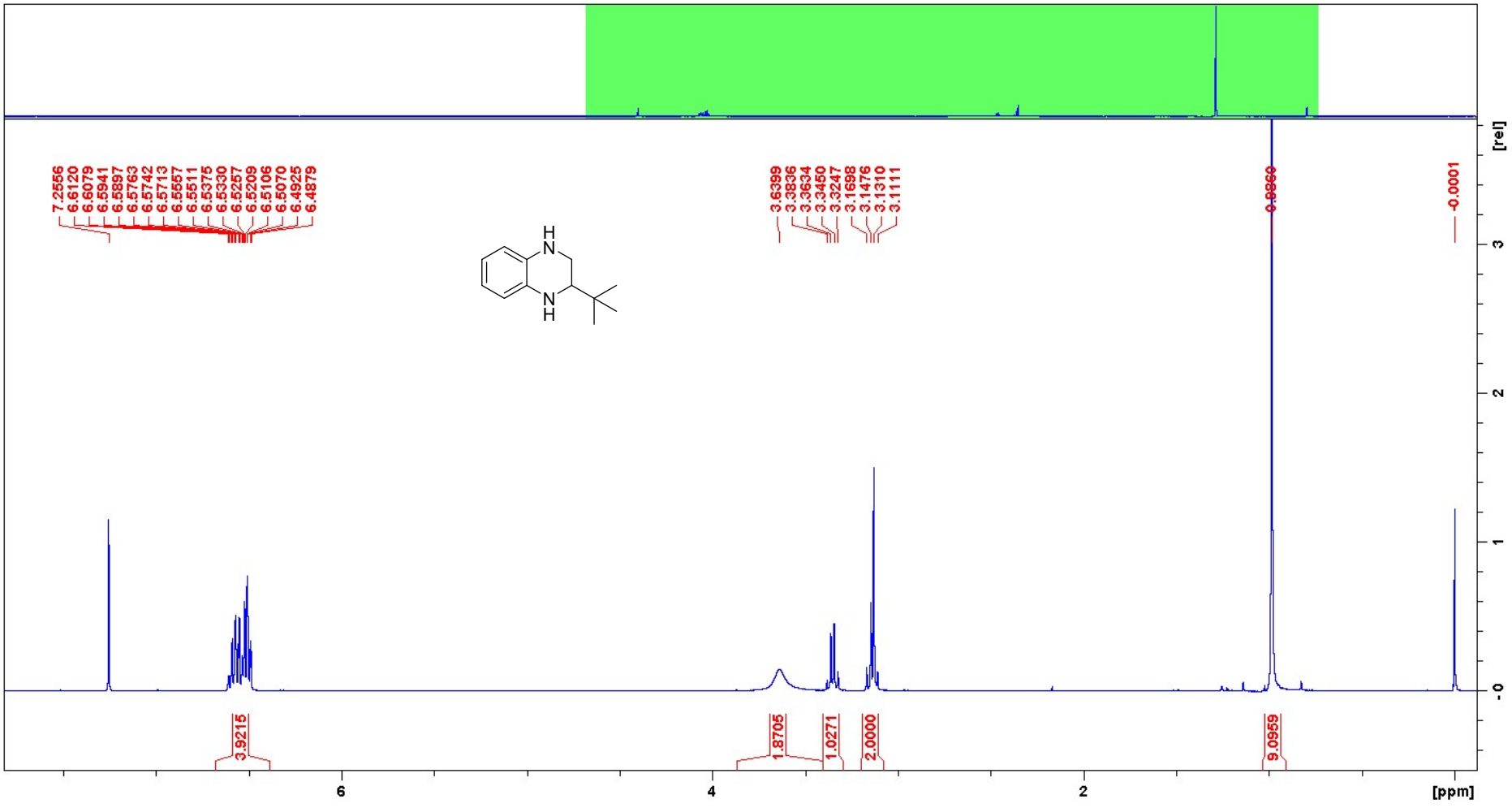

^{13}C NMR ($CDCl_3$) compound **3b**

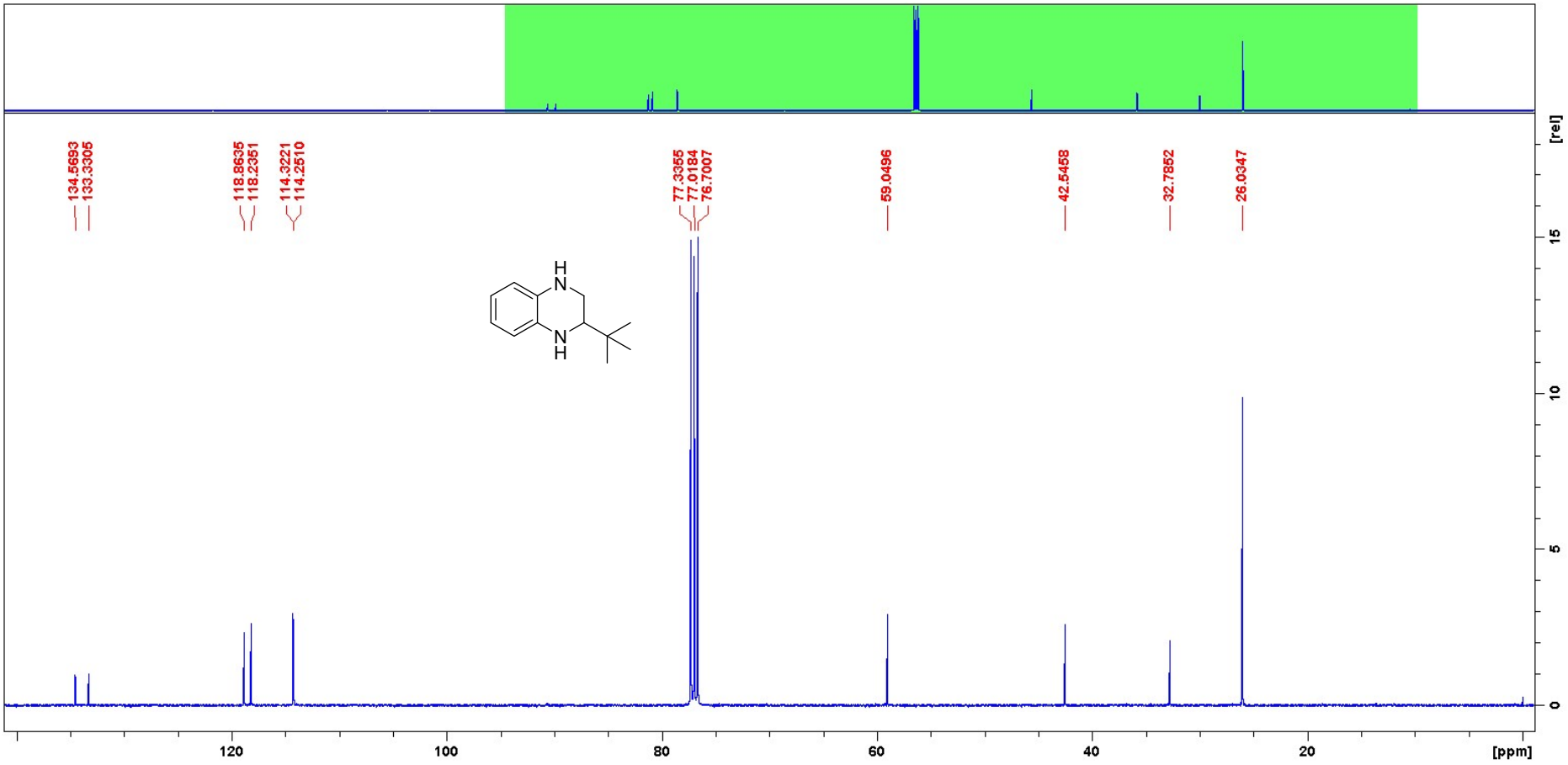

^{1}H NMR ($CDCl_3$) compound **3c**

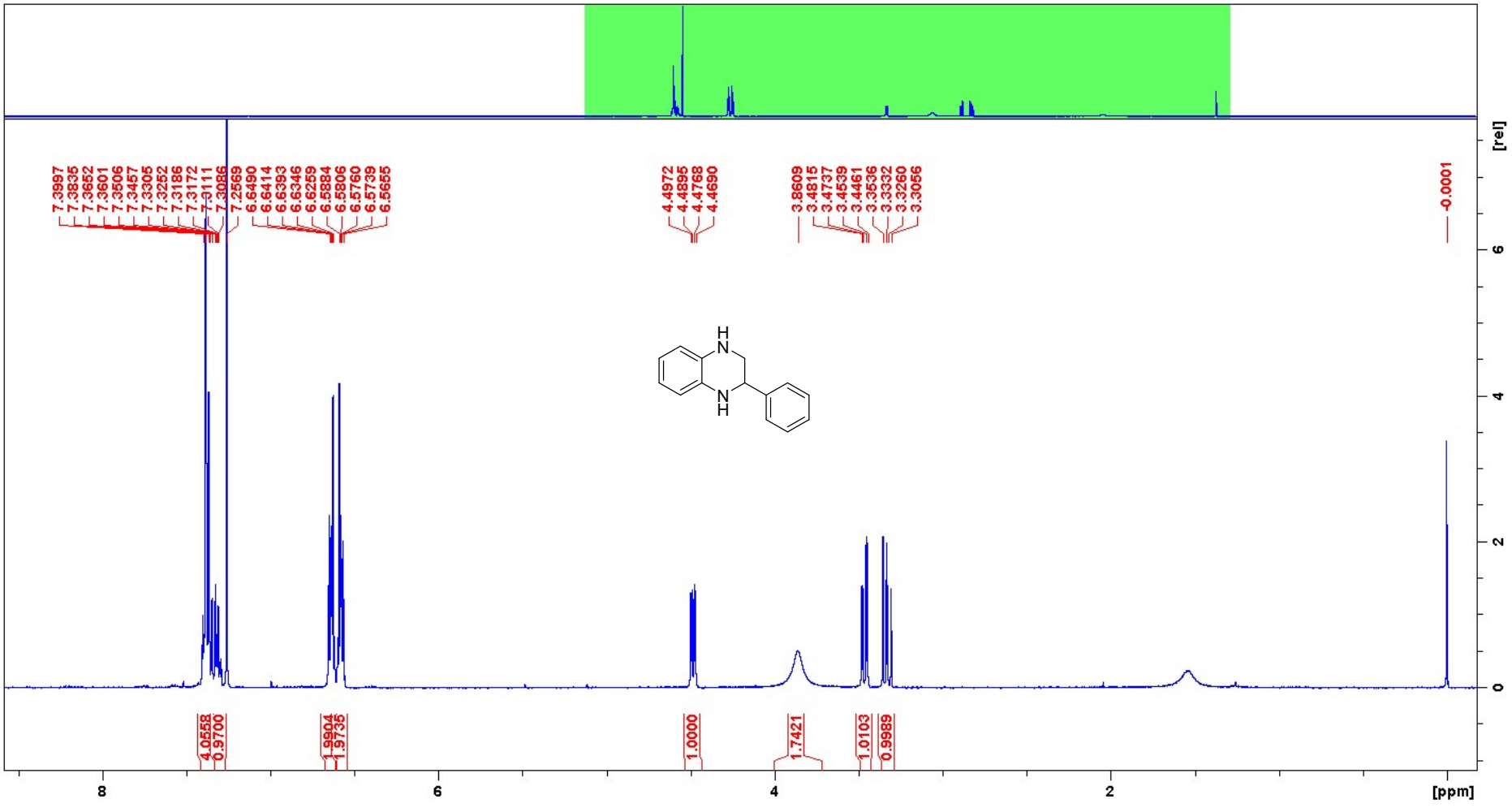

^{13}C NMR ($CDCl_3$) compound **3c**

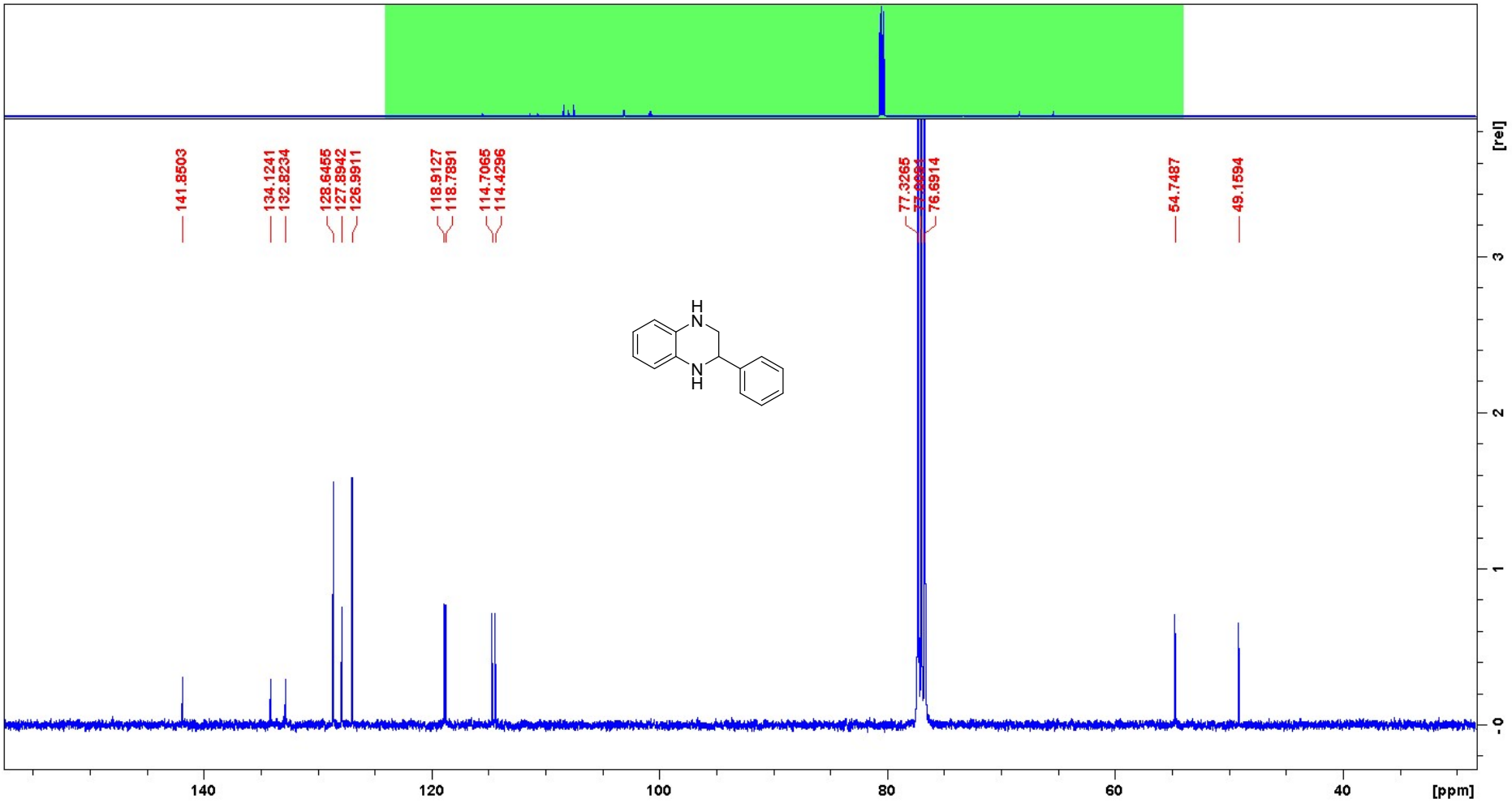

^{1}H NMR ($CDCl_3$) compound **3d**

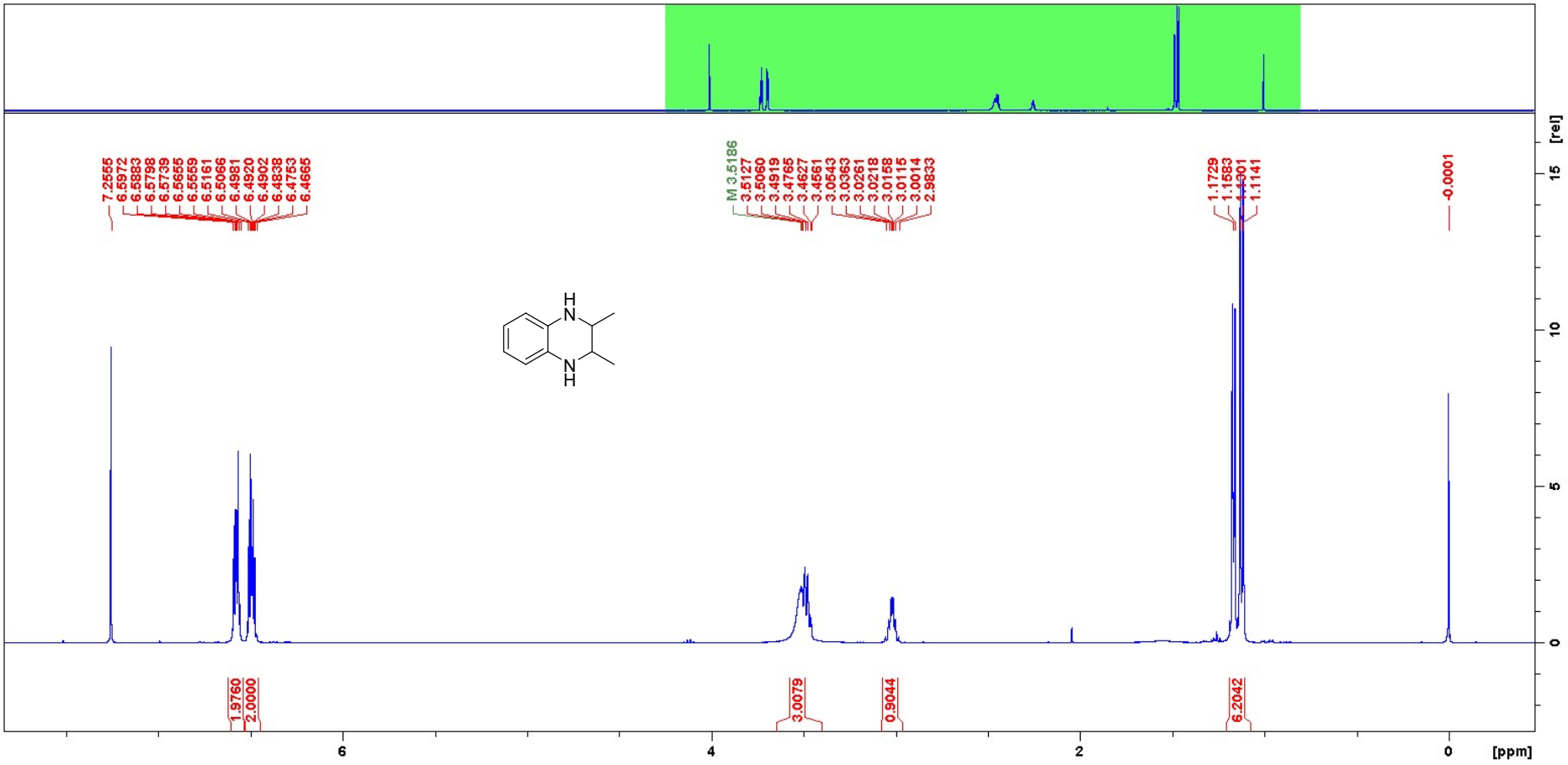

^{13}C NMR ($CDCl_3$) compound **3d**

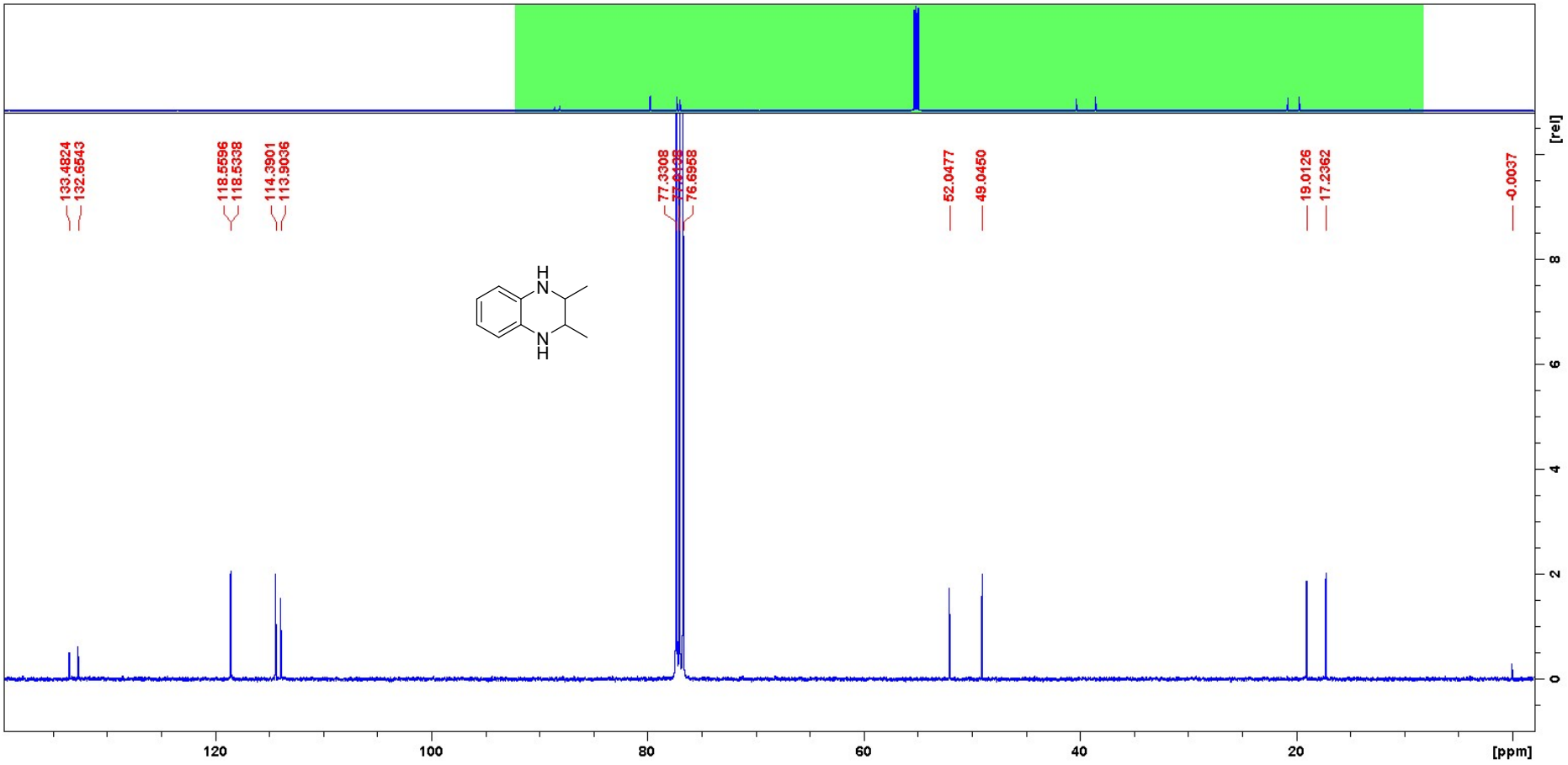

^{1}H NMR ($CDCl_3$) compound ***cis*-3e**

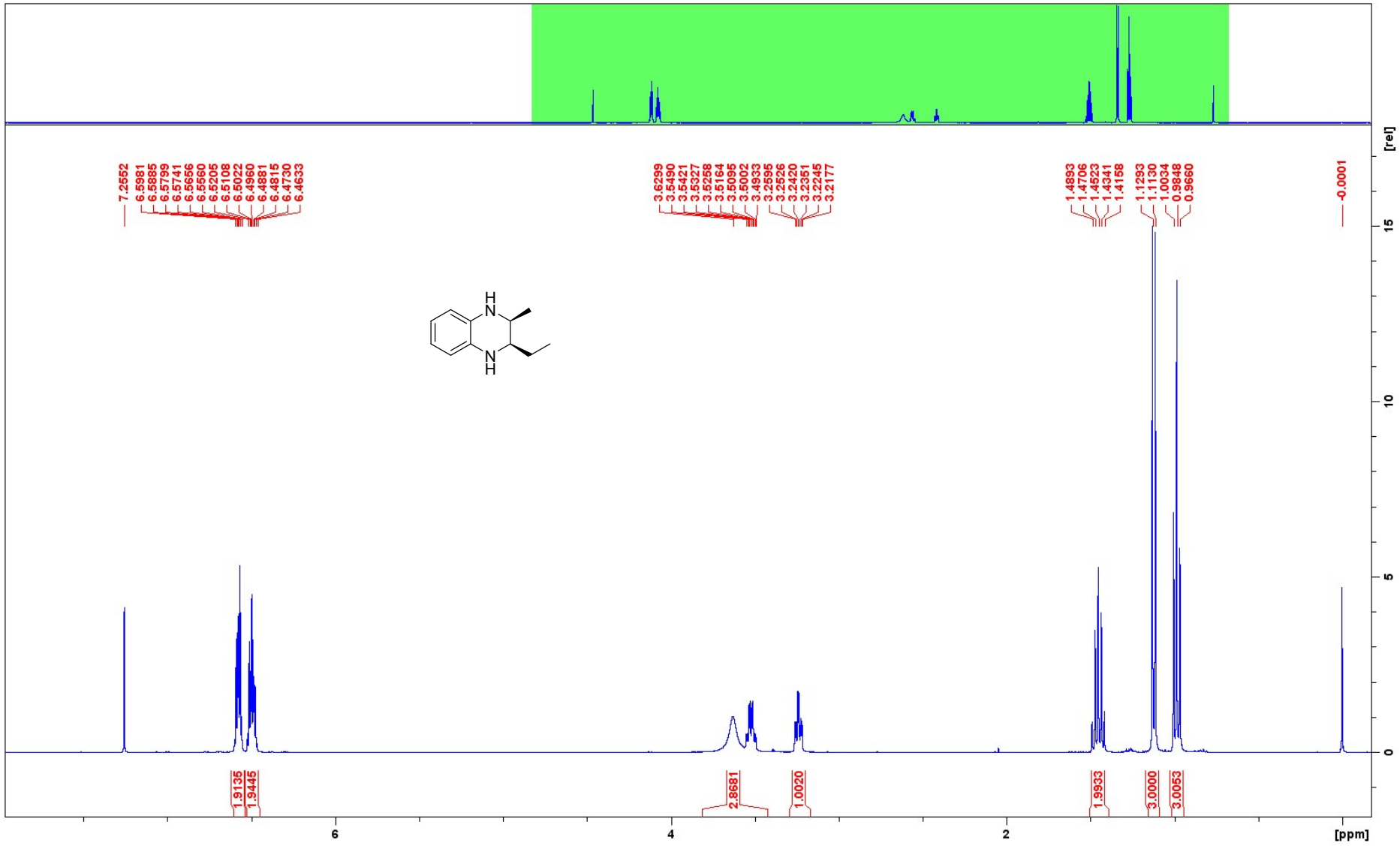

^{13}C NMR ($CDCl_3$) compound ***cis*-3e**

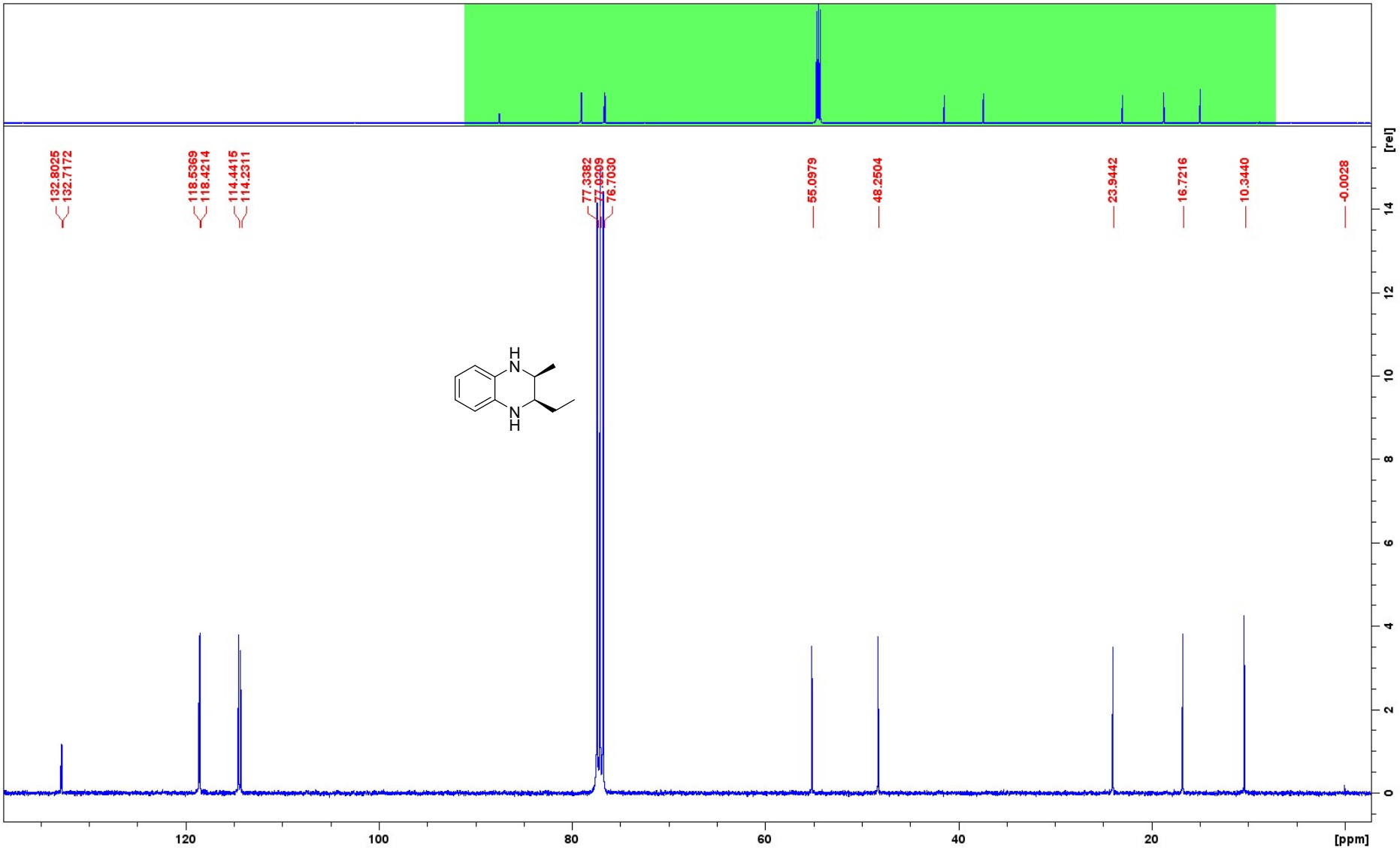

^{1}H NMR ($CDCl_3$) compound ***trans*-3e**

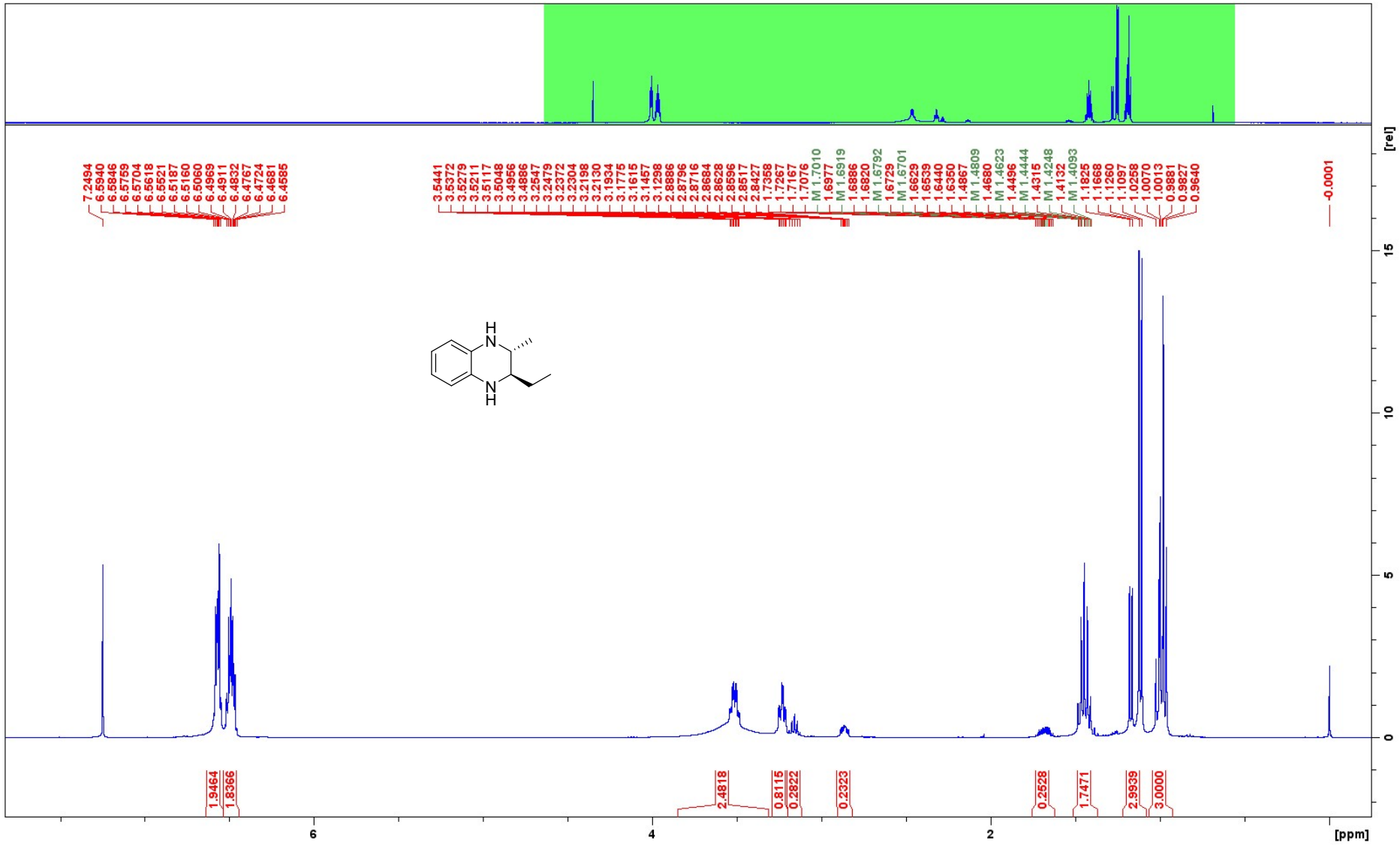

^{13}C NMR ($CDCl_3$) compound ***trans*-3e**

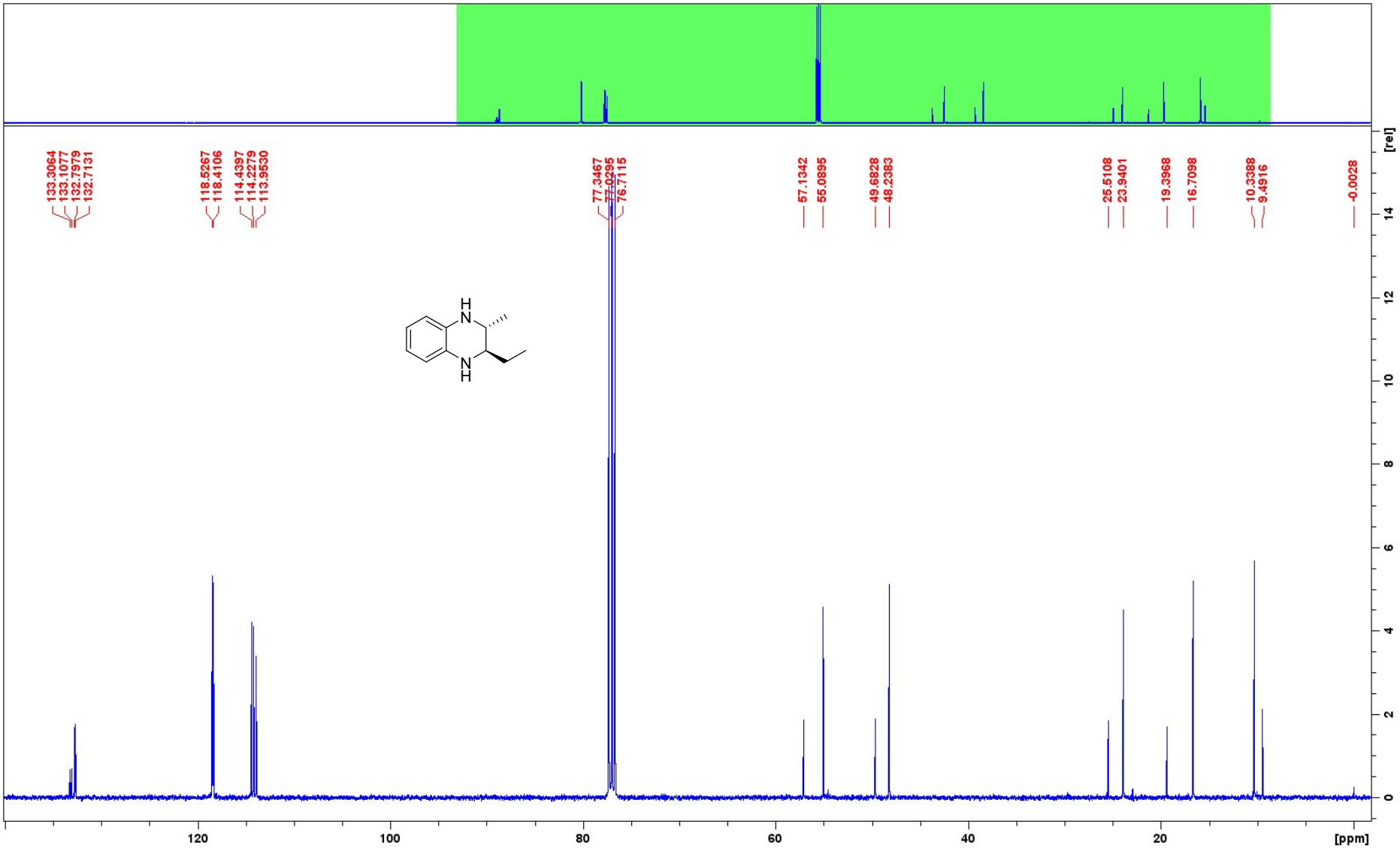

^{1}H NMR ($CDCl_3$) compound ***cis*-3f**

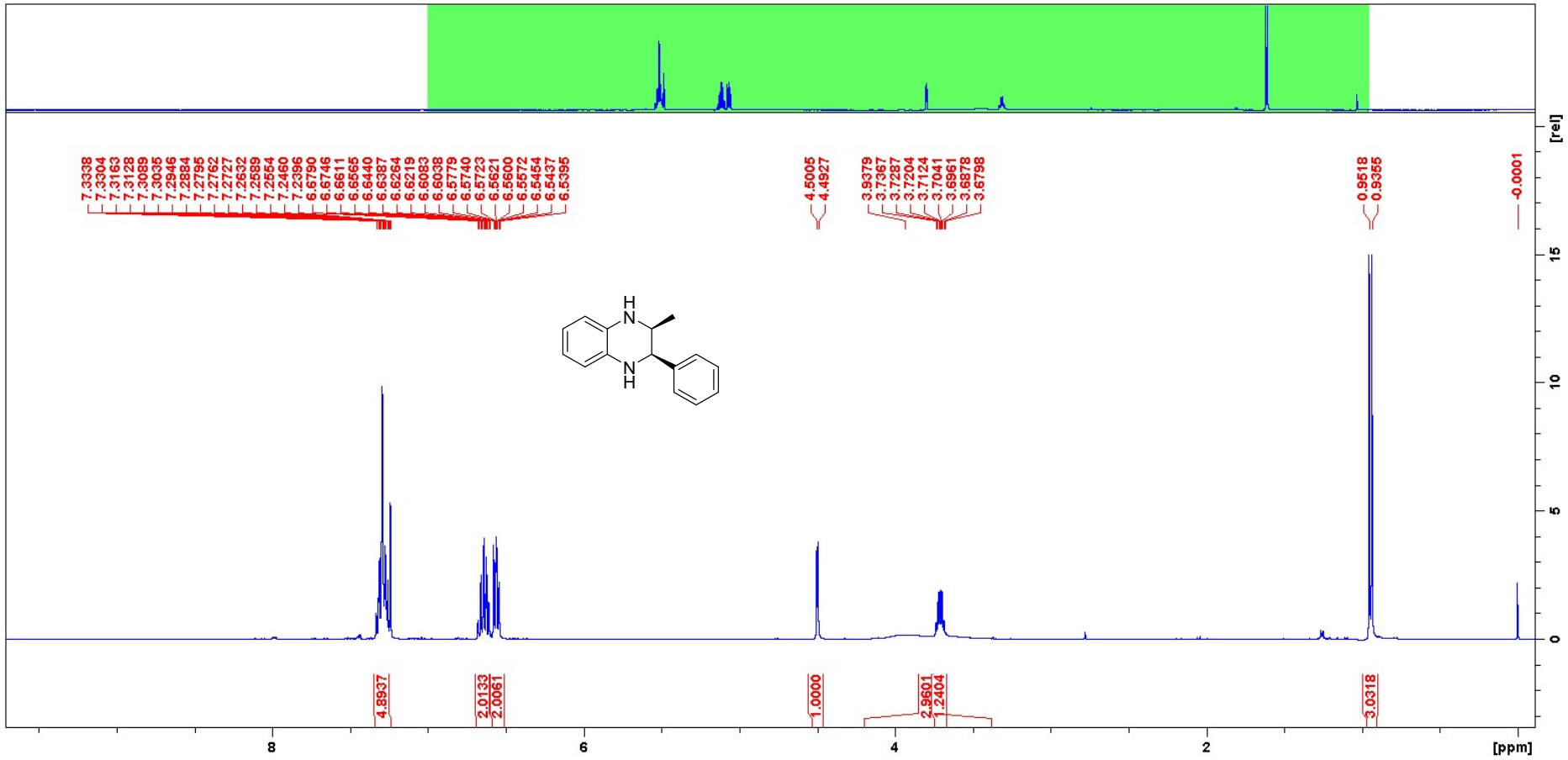

^{13}C NMR ($CDCl_3$) compound ***cis*-3f**

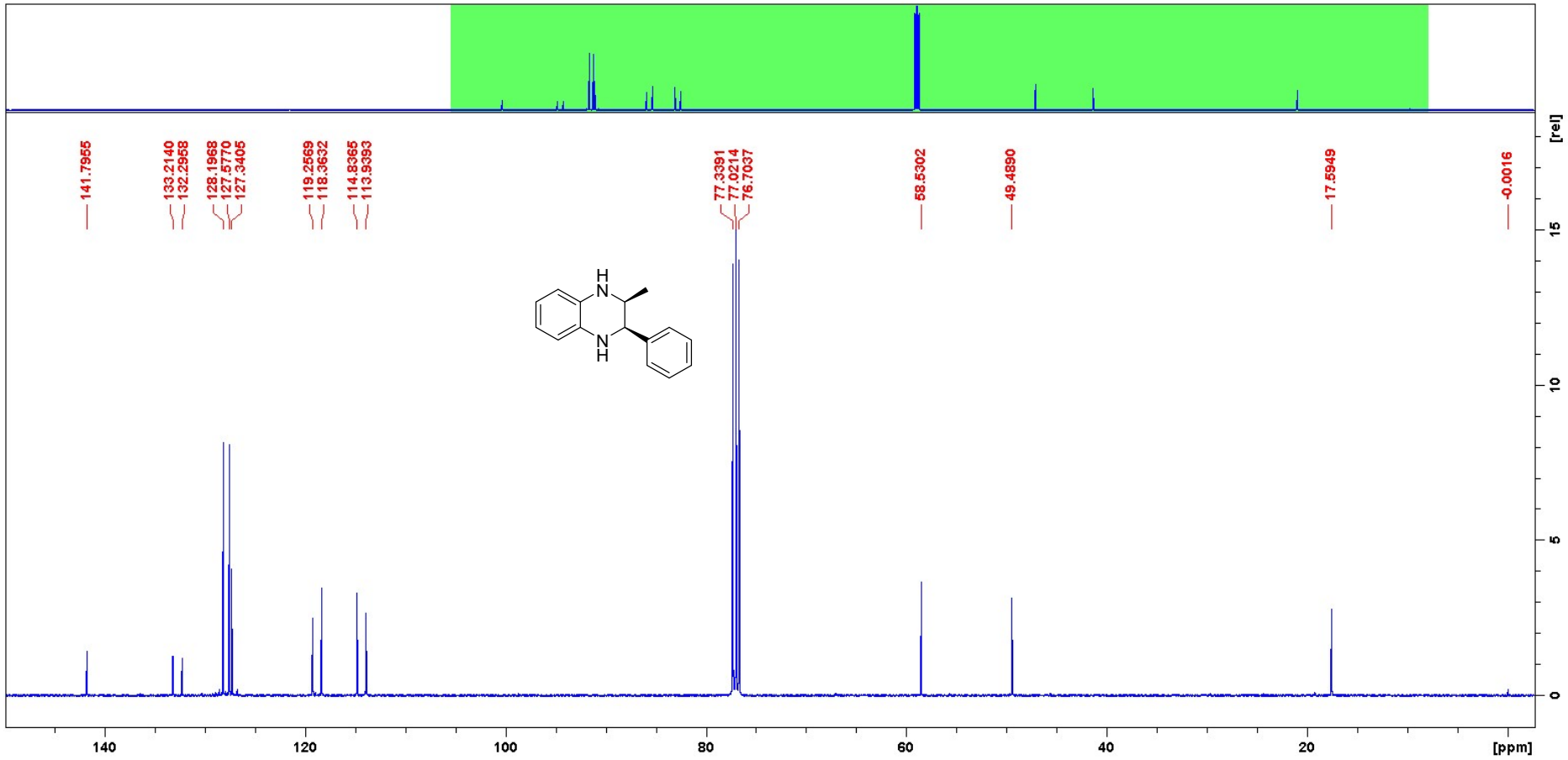

^{1}H NMR ($CDCl_3$) compound ***cis*-3g**

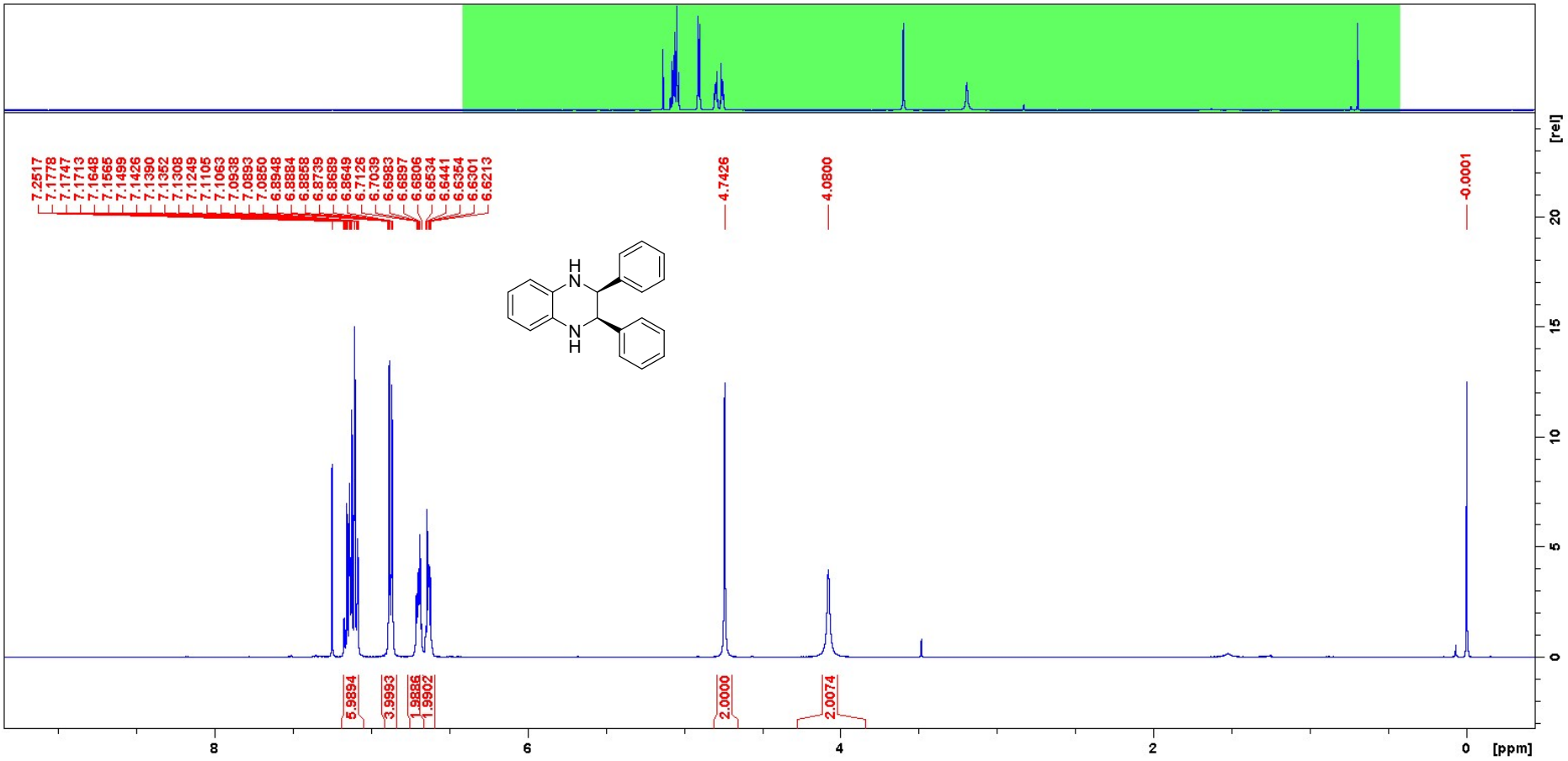

^{13}C NMR ($CDCl_3$) compound ***cis*-3g**

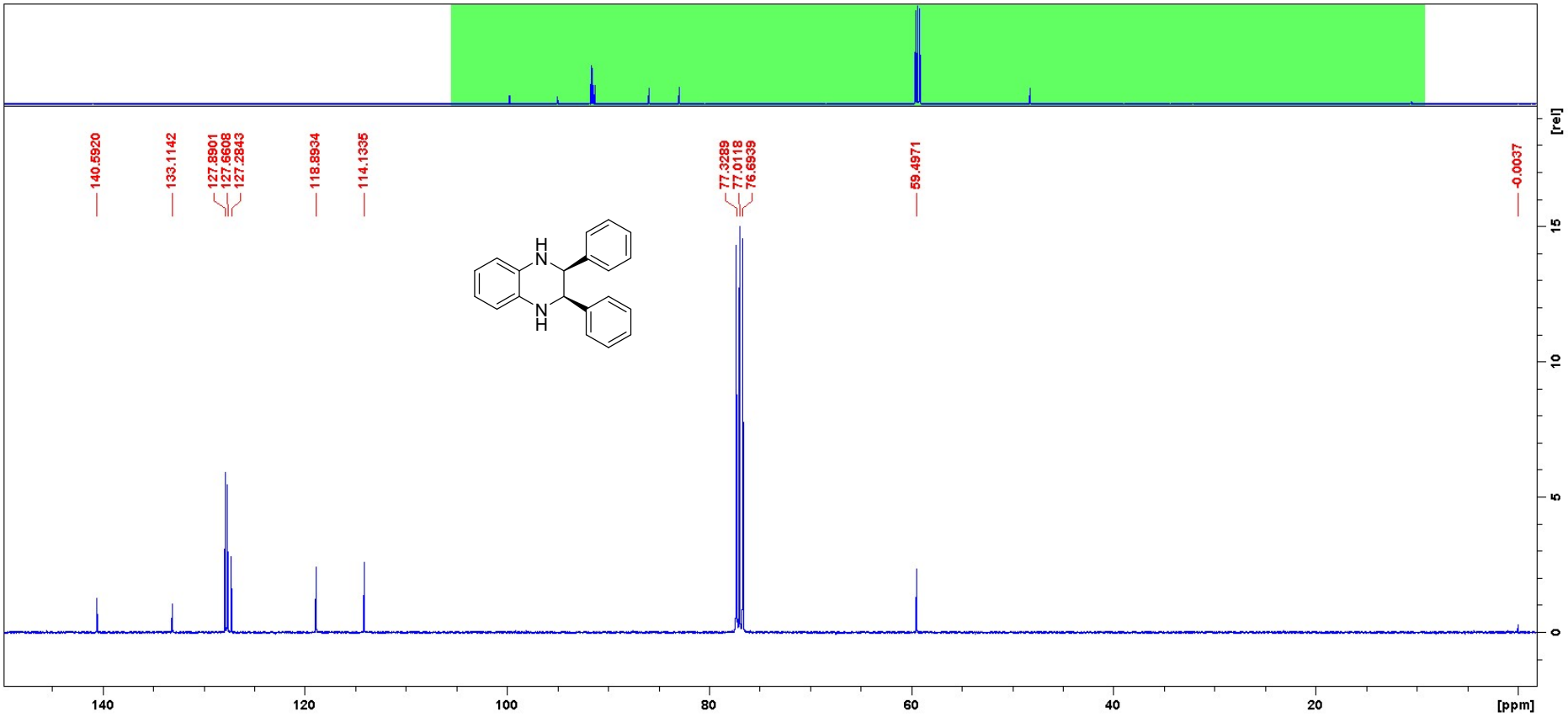

^{1}H NMR ($CDCl_3$) compound ***cis*-3h**

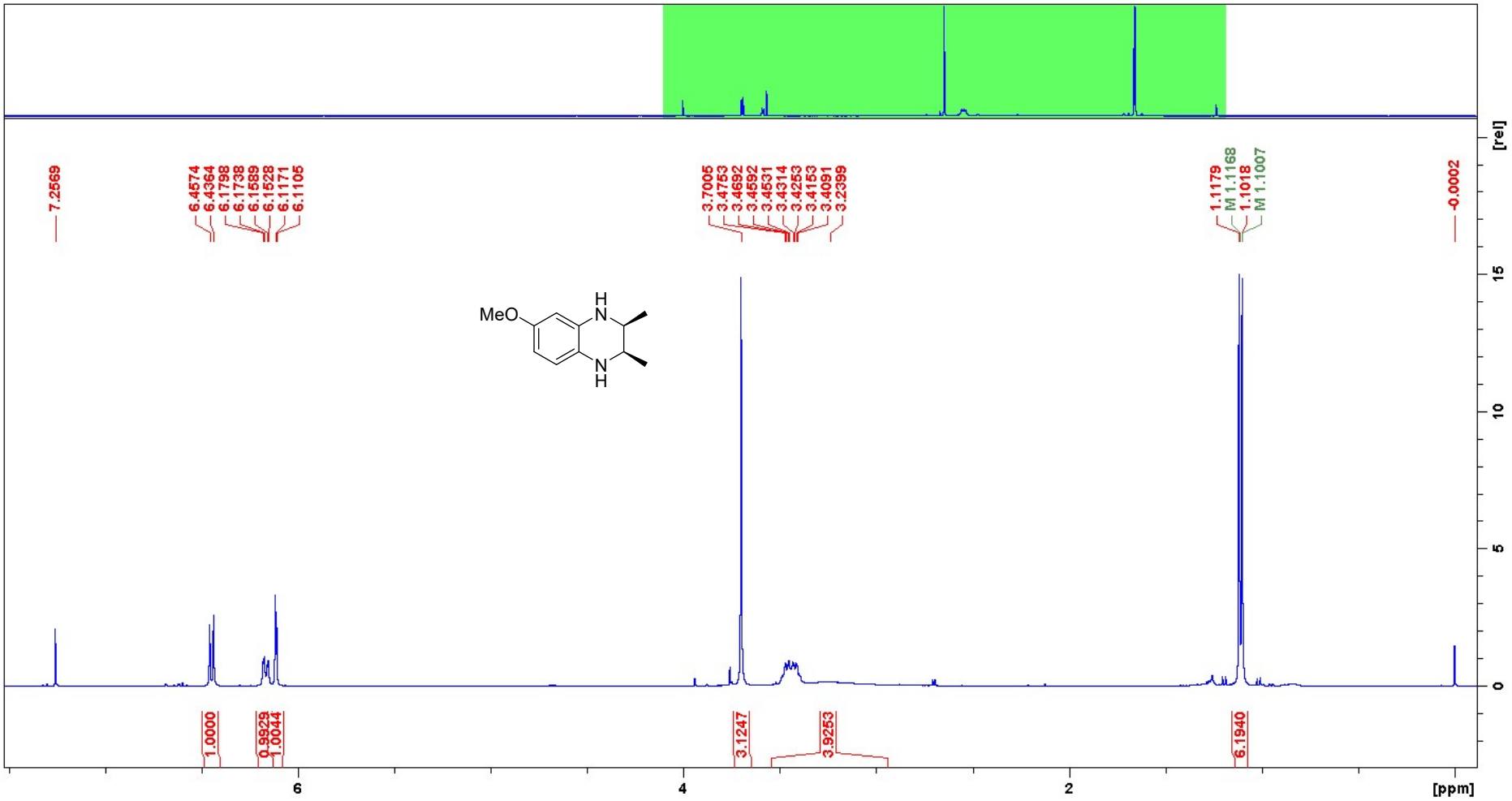

^{13}C NMR ($CDCl_3$) compound ***cis*-3h**

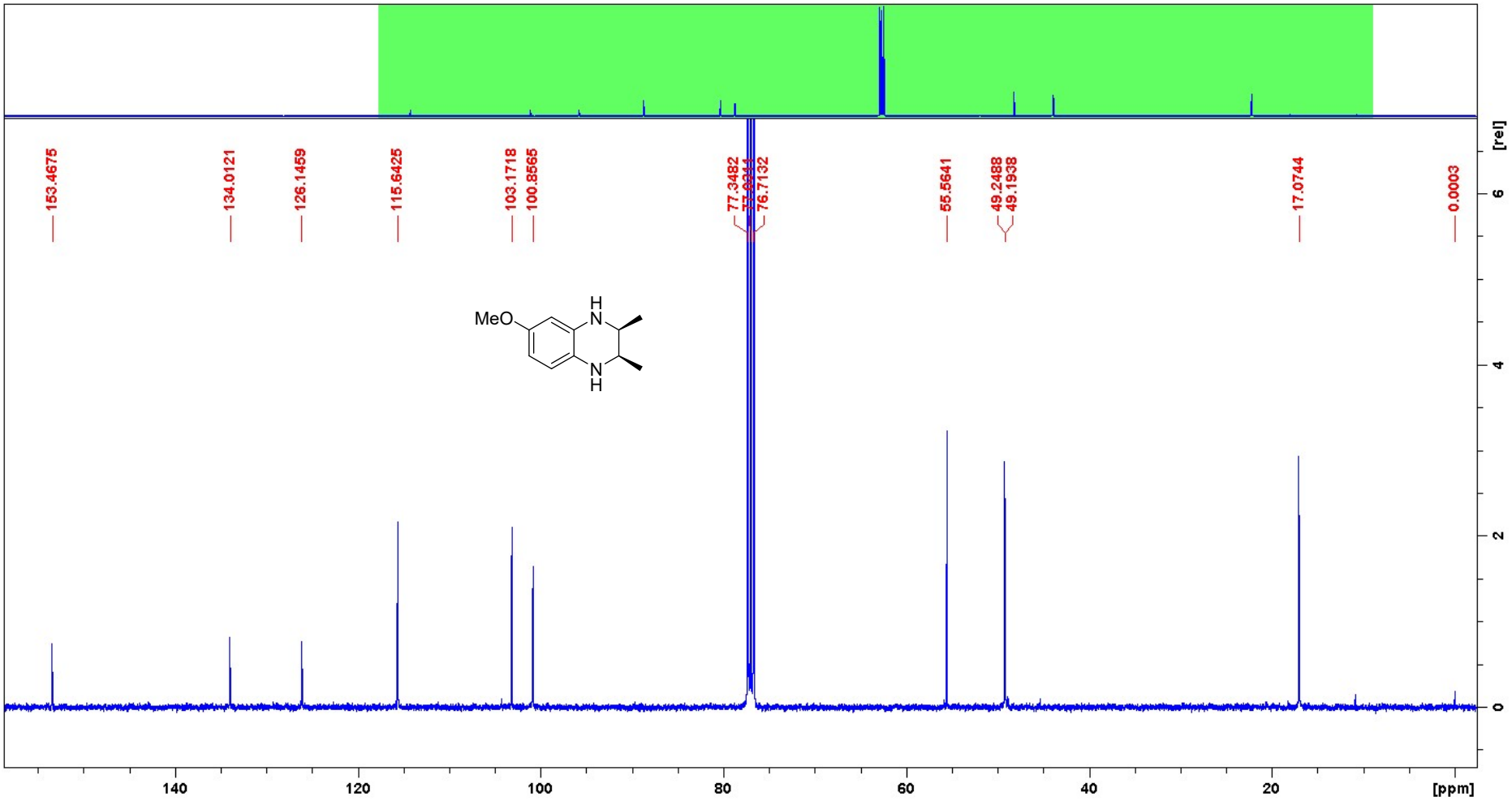

^{1}H NMR ($CDCl_3$) compound ***trans*-3h**

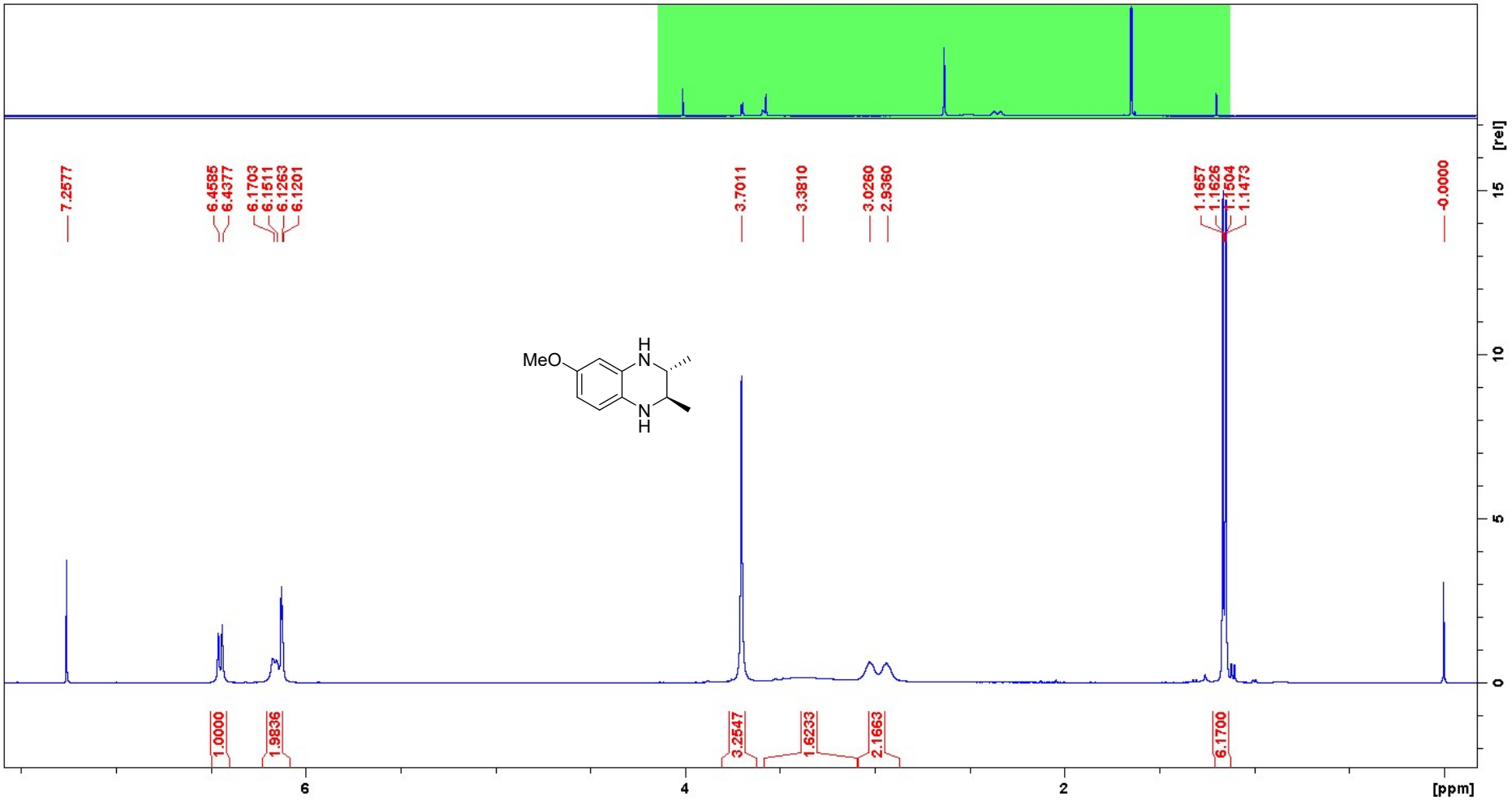

^{13}C NMR ($CDCl_3$) compound ***trans*-3h**

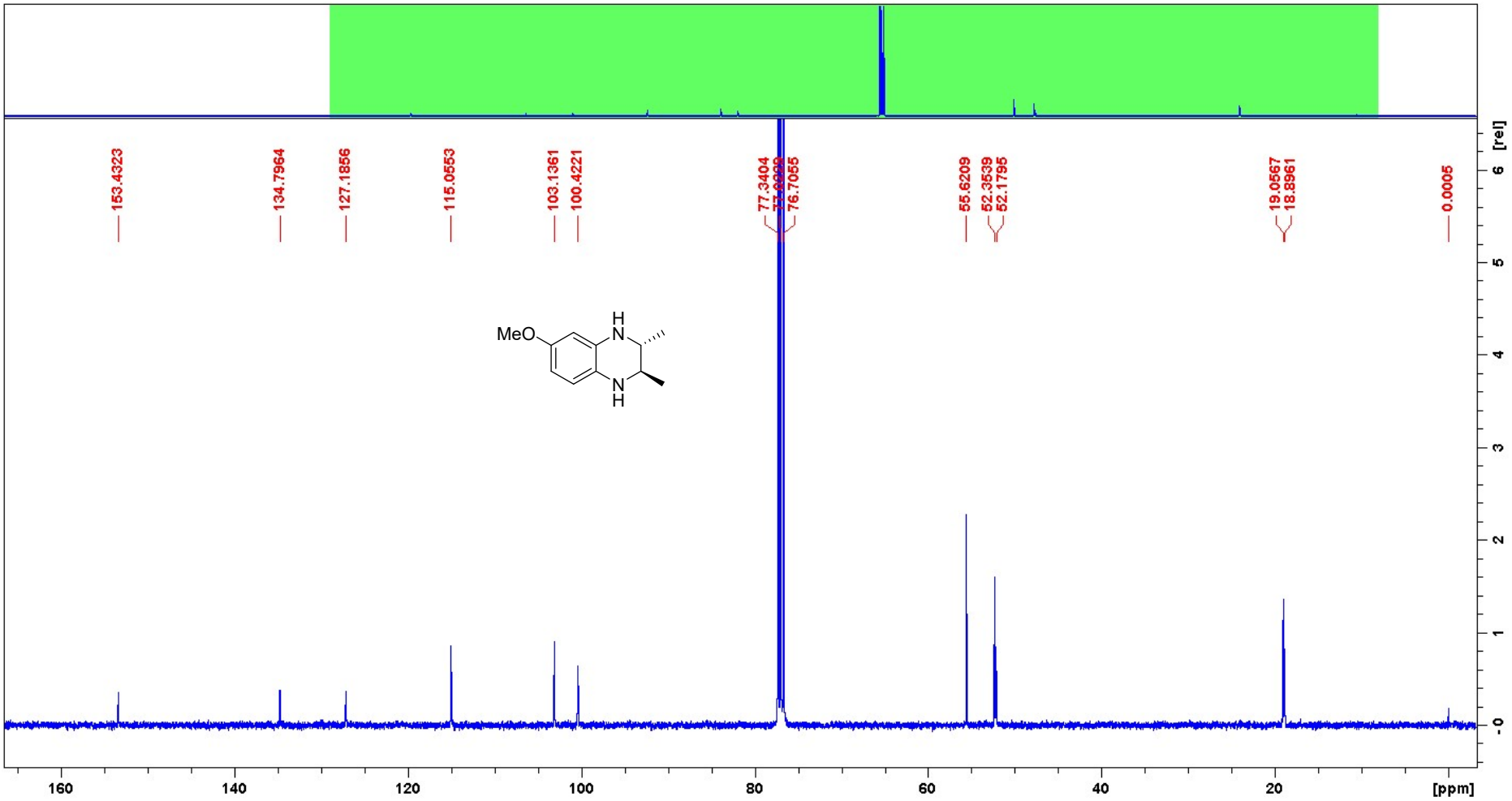

^{1}H NMR ($CDCl_3$) compound **3i**

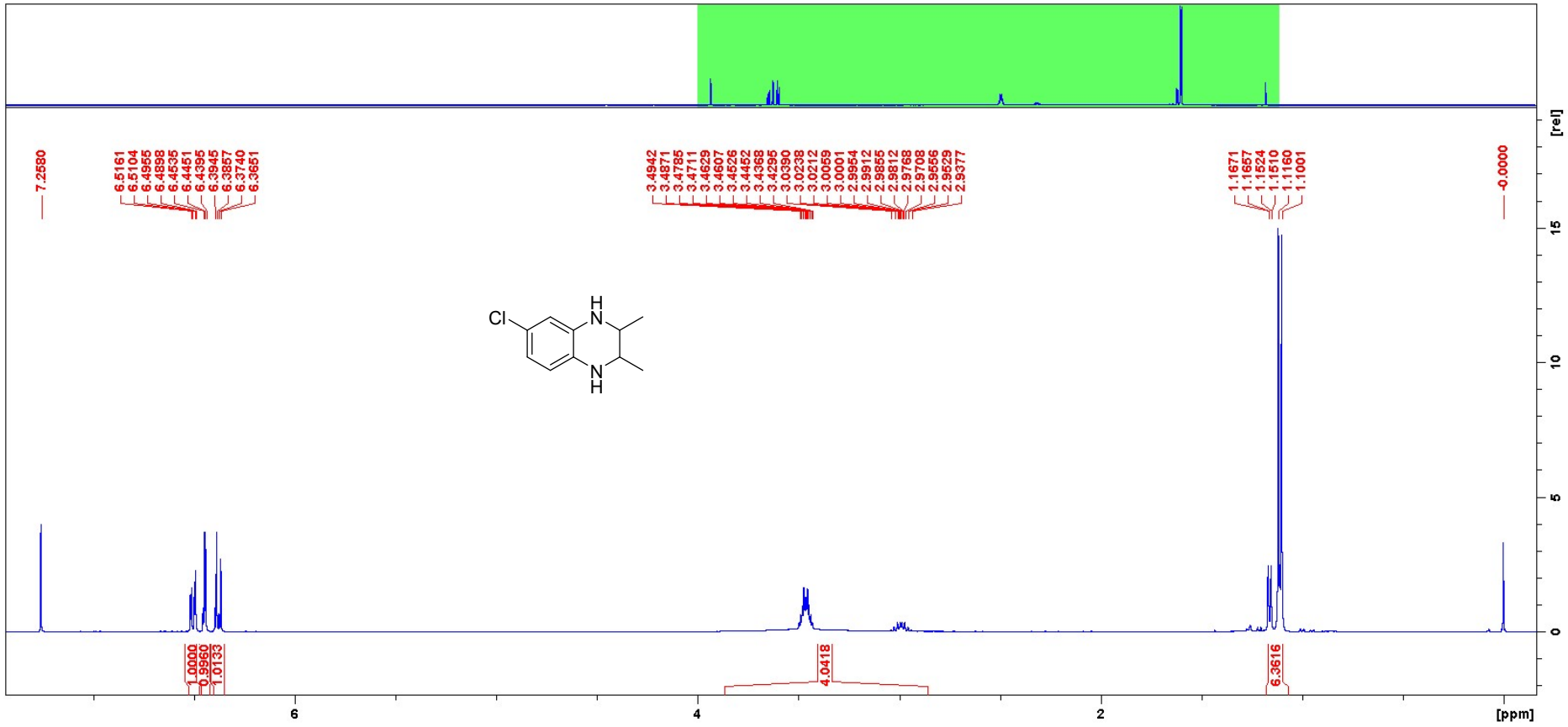

^{13}C NMR ($CDCl_3$) compound **3i**

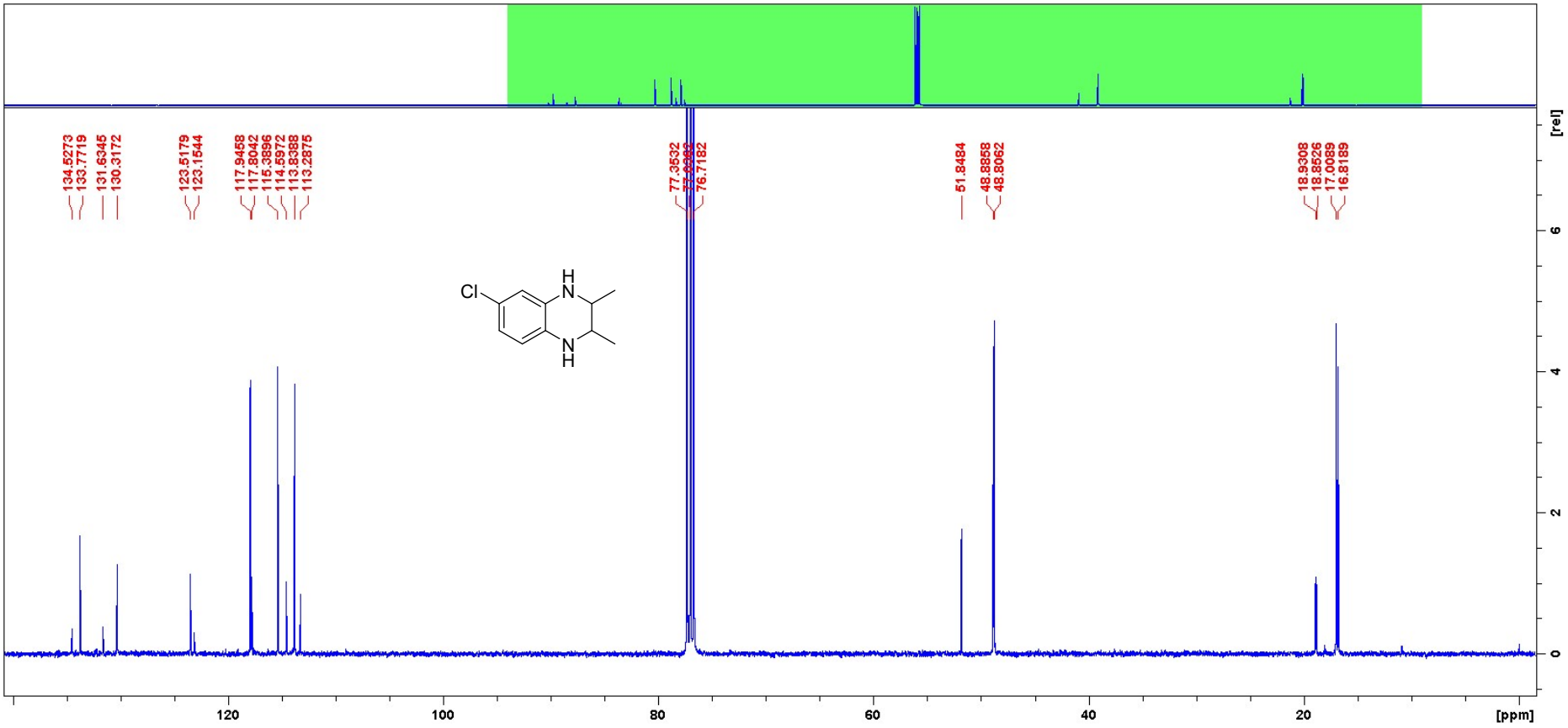

^{1}H NMR ($CDCl_3$) compound **3j**

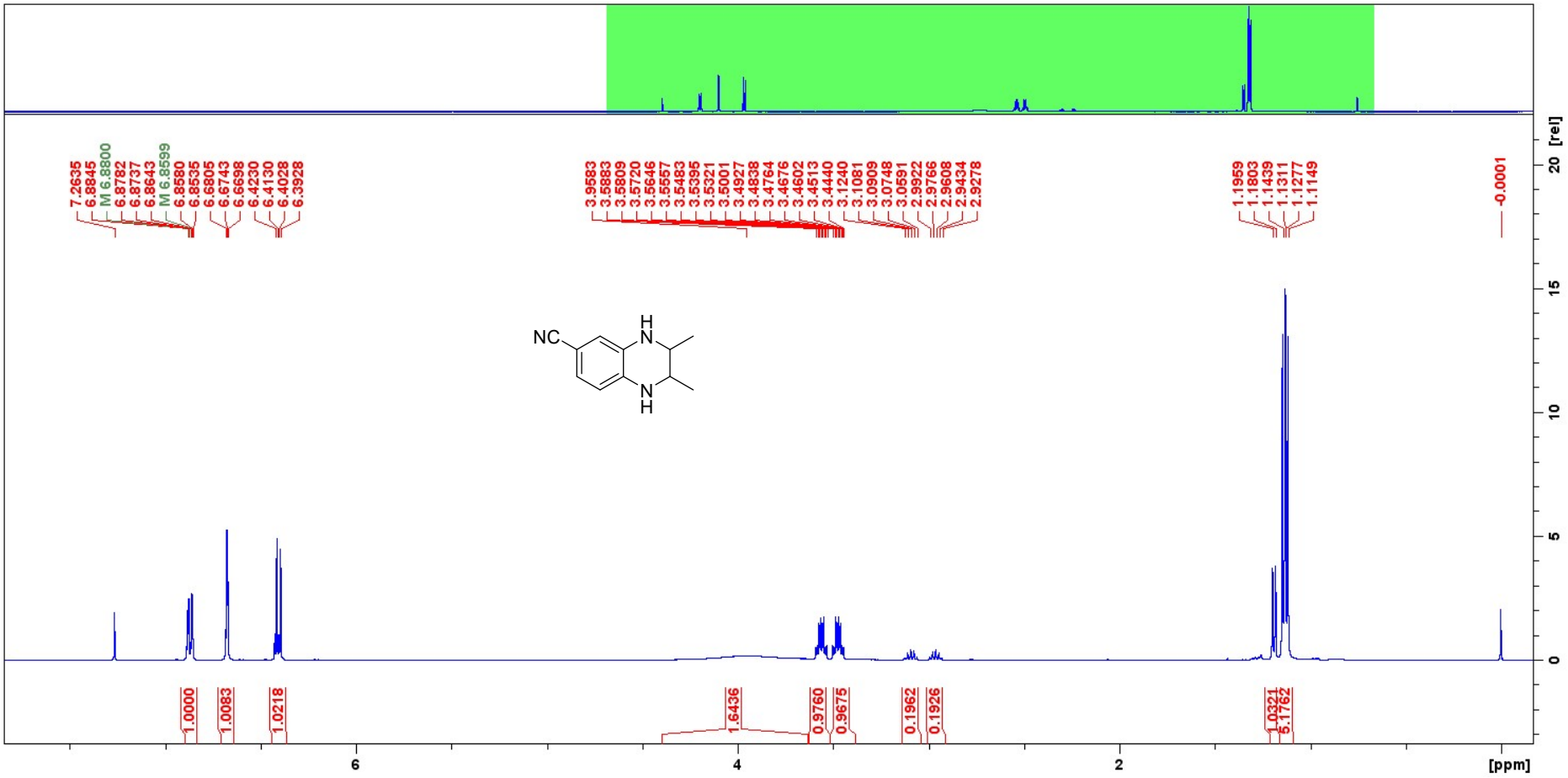

^{13}C NMR ($CDCl_3$) compound **3j**

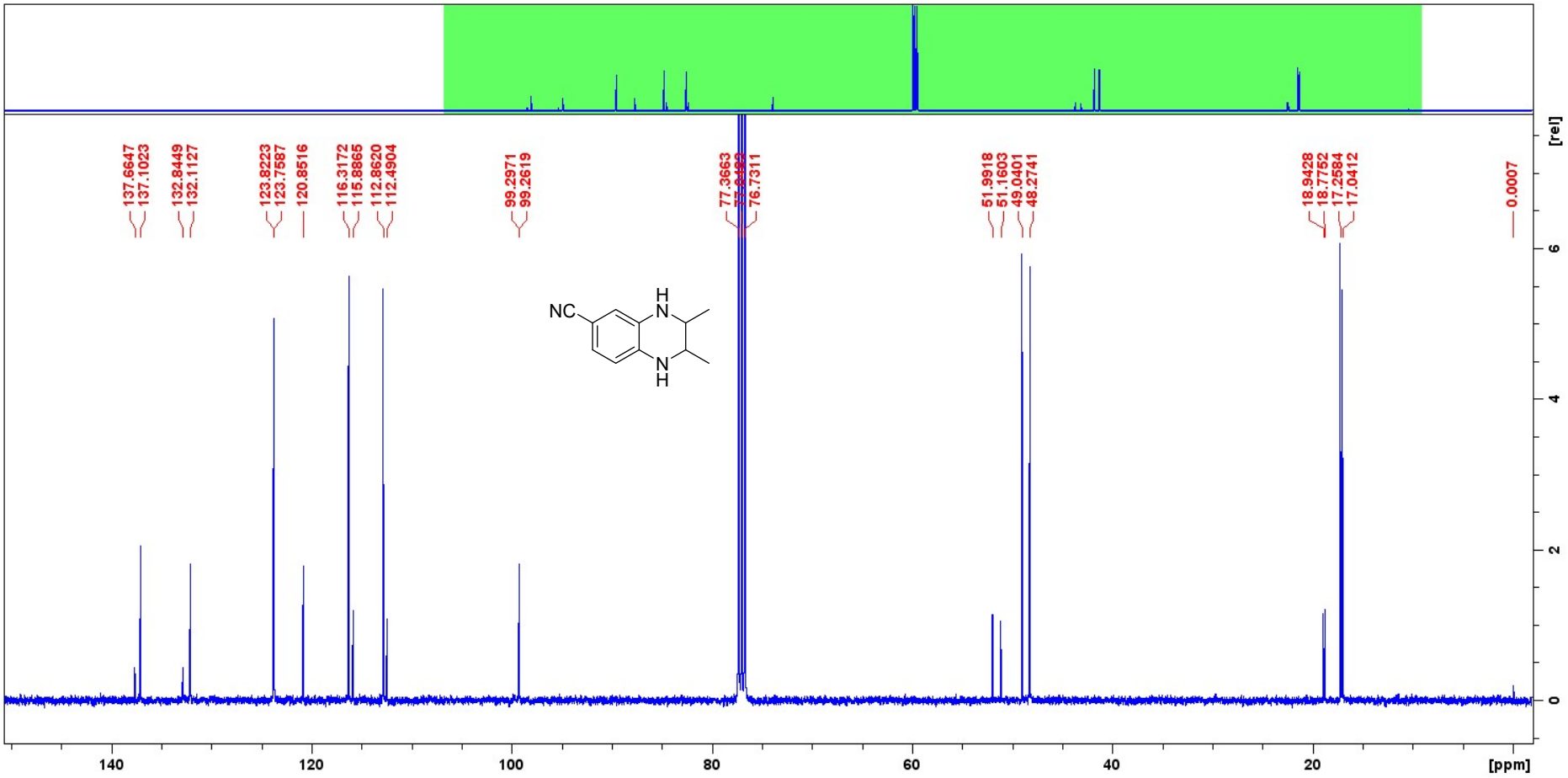

^{1}H NMR ($CDCl_3$) compound **3k**

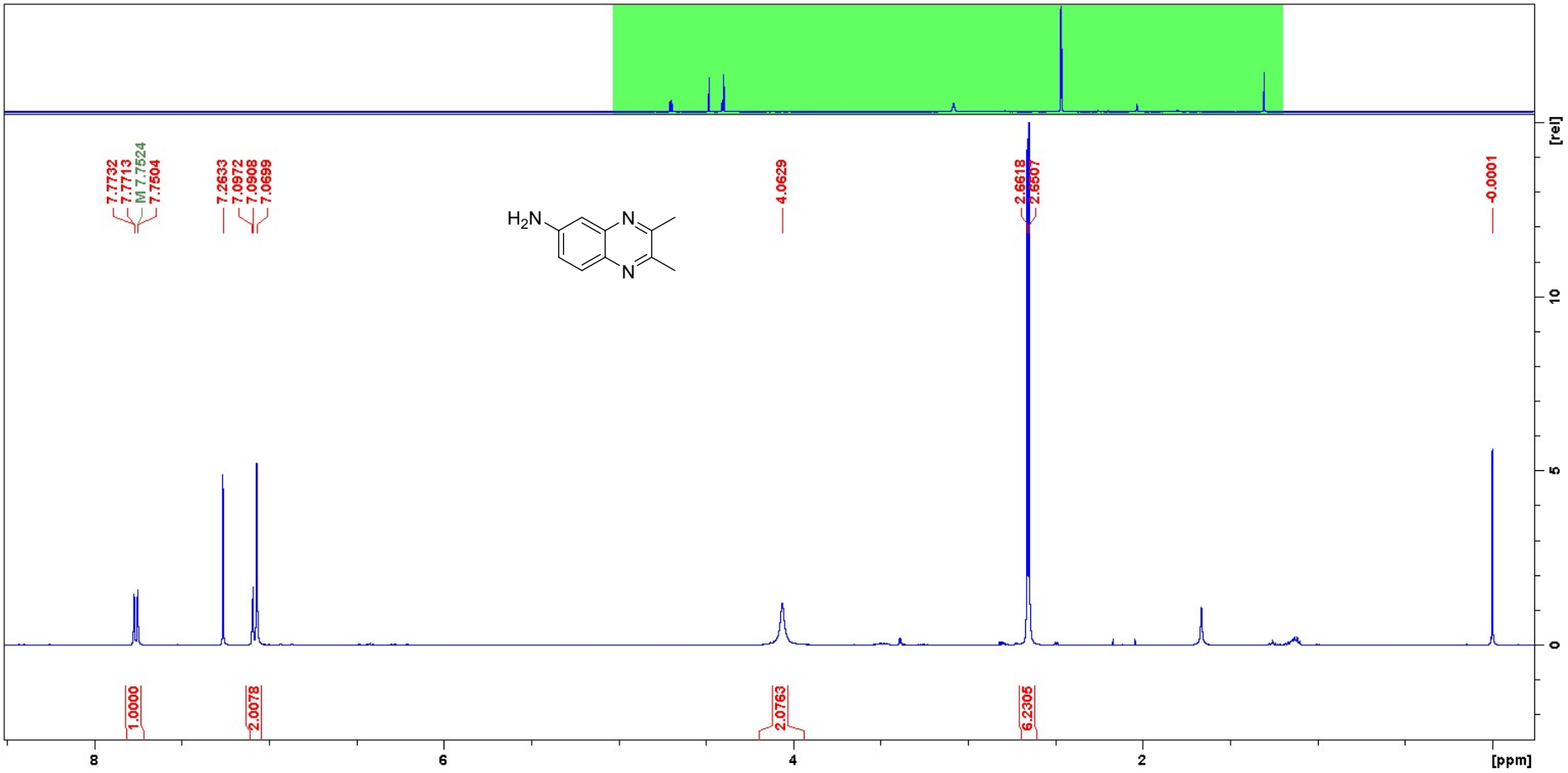

^{13}C NMR ($CDCl_3$) compound **3k**

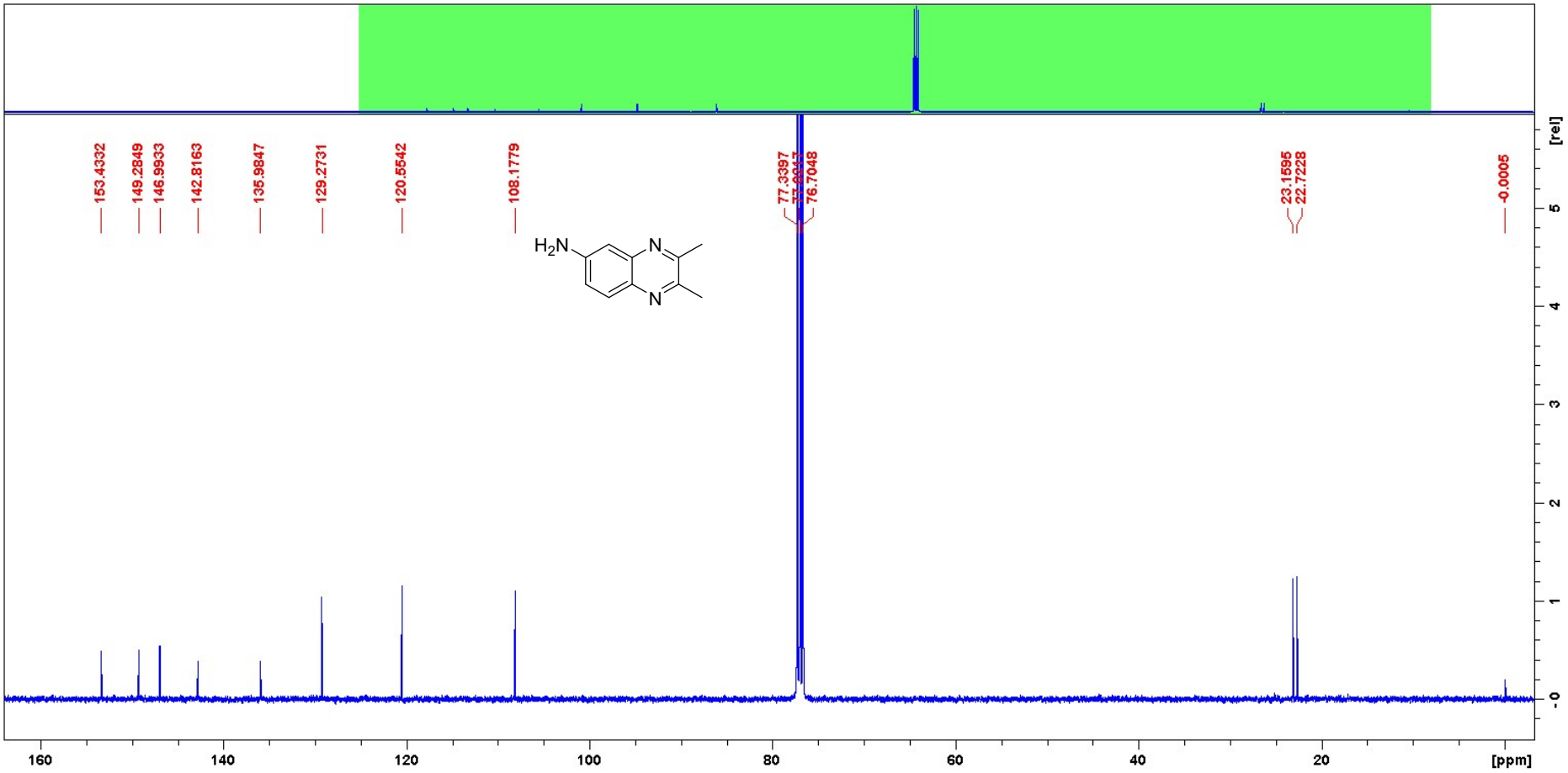

^{1}H NMR ($CDCl_3$) compound **5a**

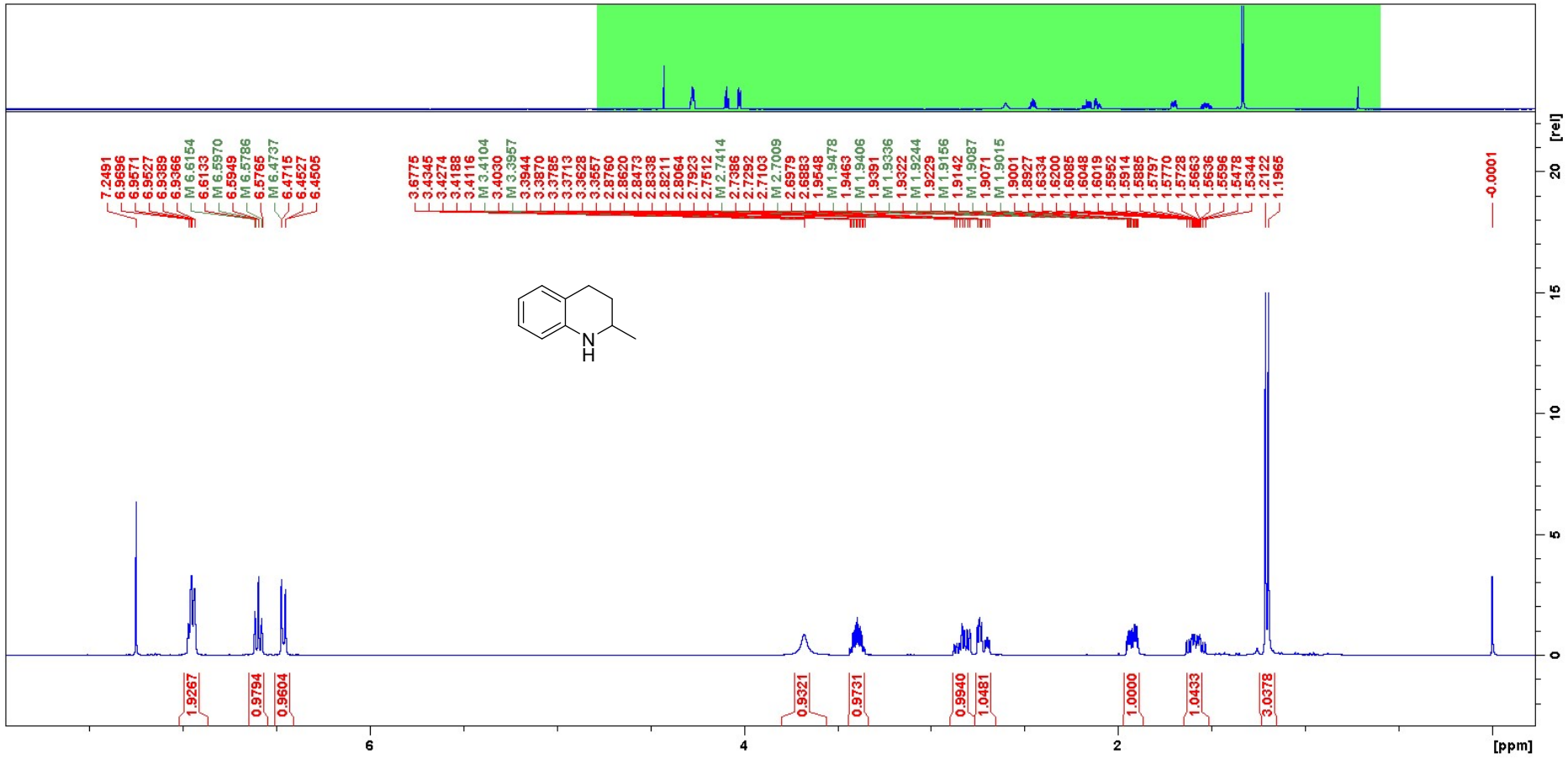

^{13}C NMR ($CDCl_3$) compound **5a**

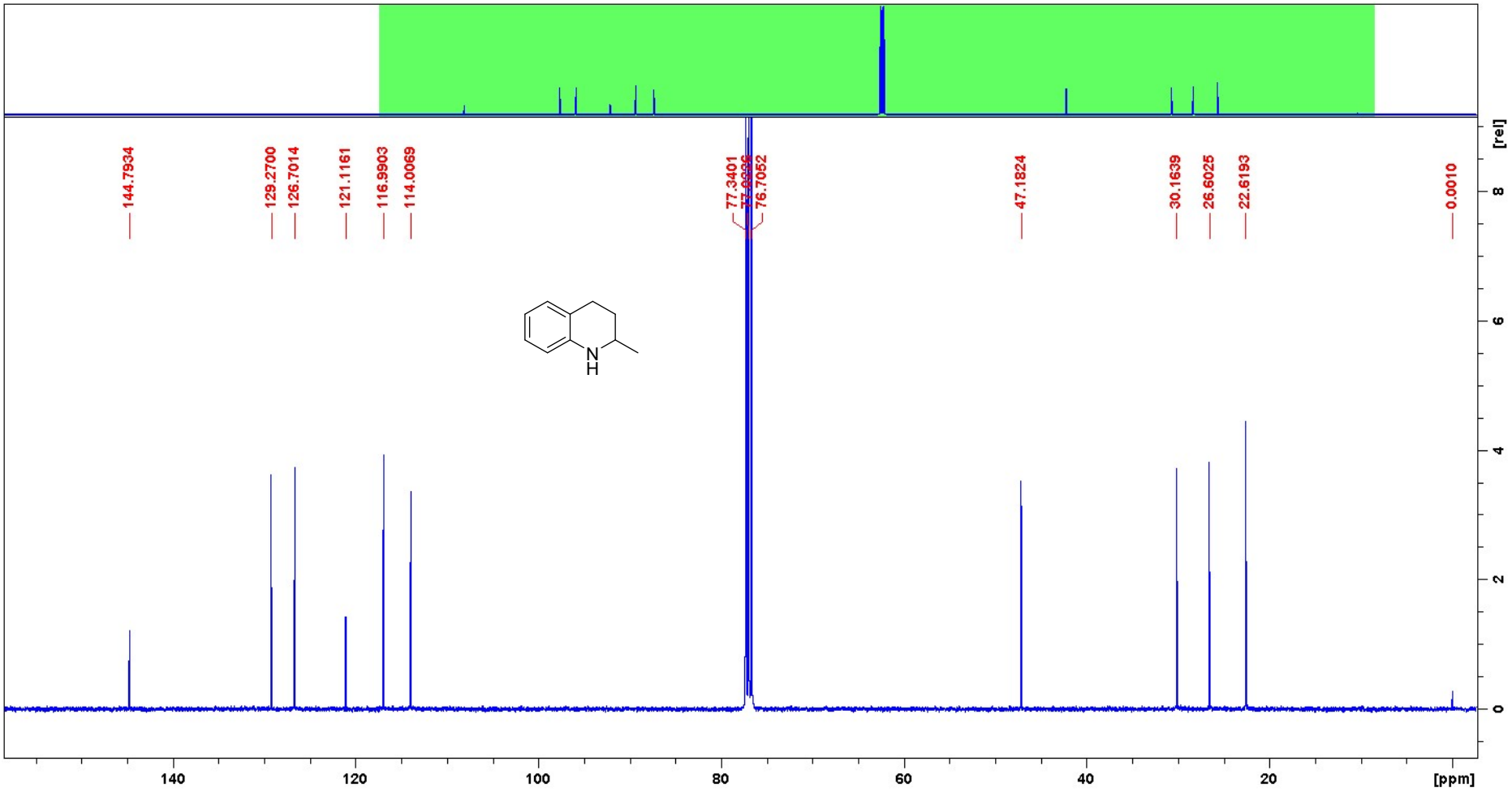

^{1}H NMR ($CDCl_3$) compound **5b**

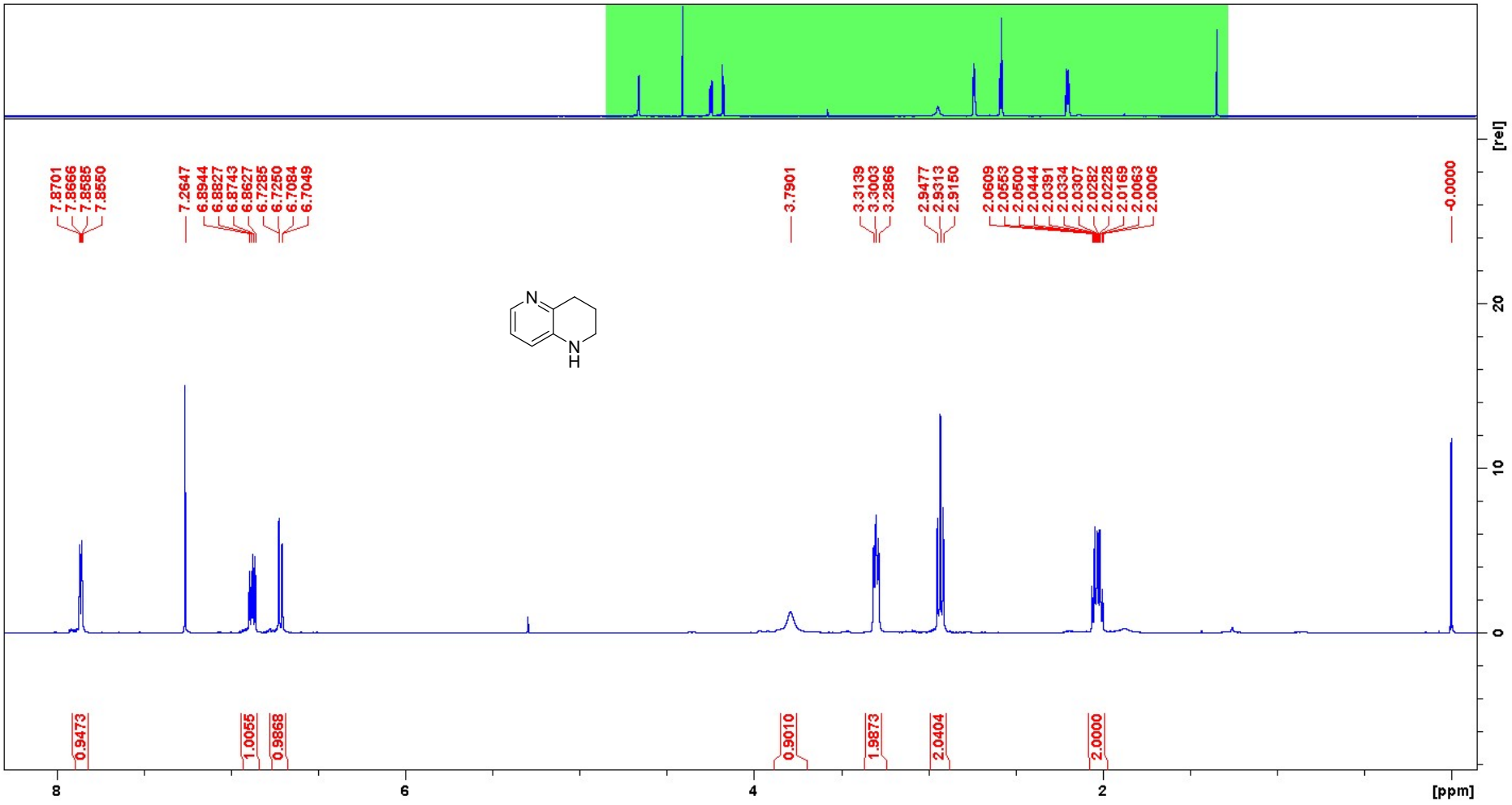

^{13}C NMR ($CDCl_3$) compound **5b**

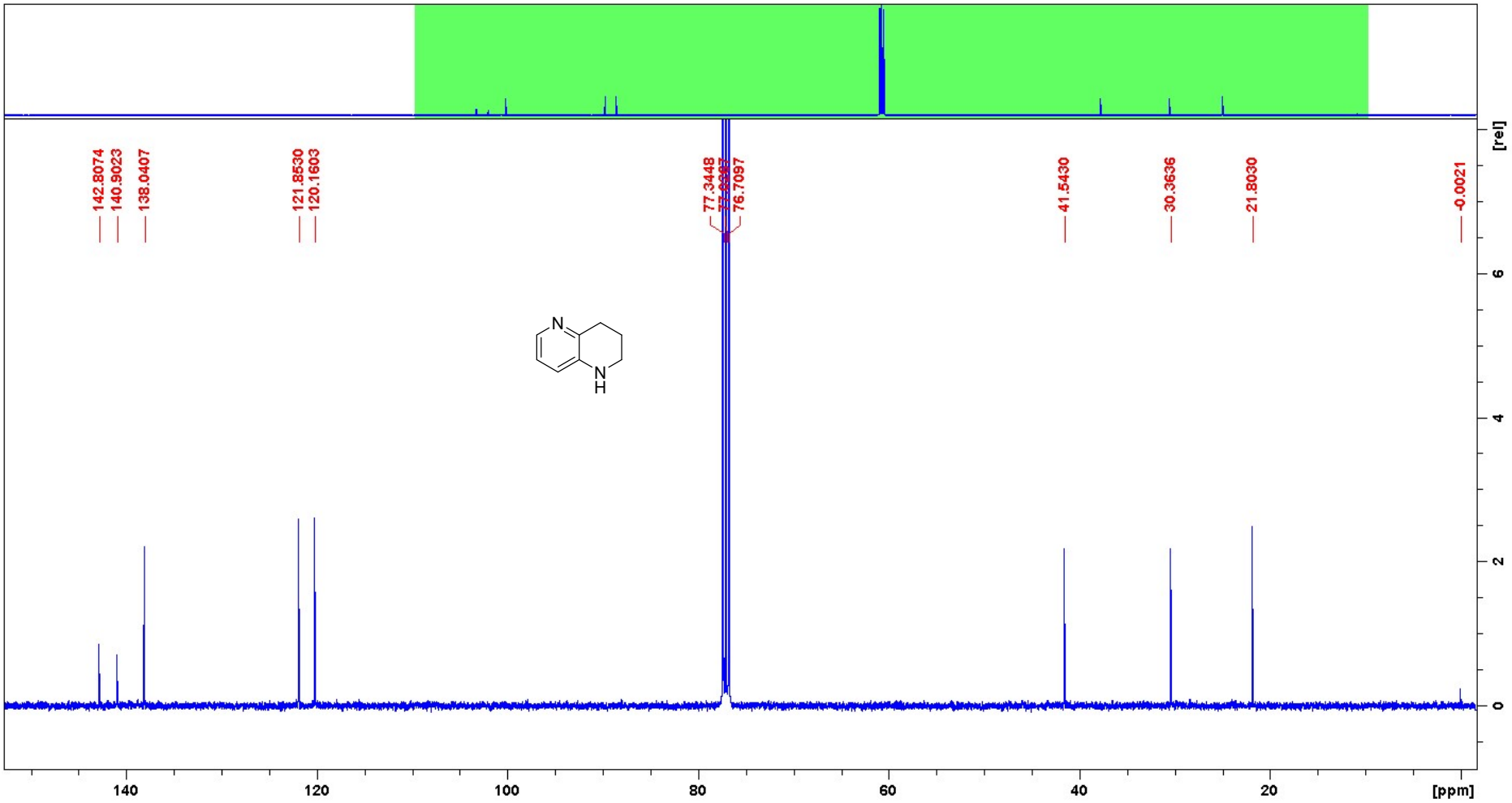

^{1}H NMR ($CDCl_3$) compound **5c**

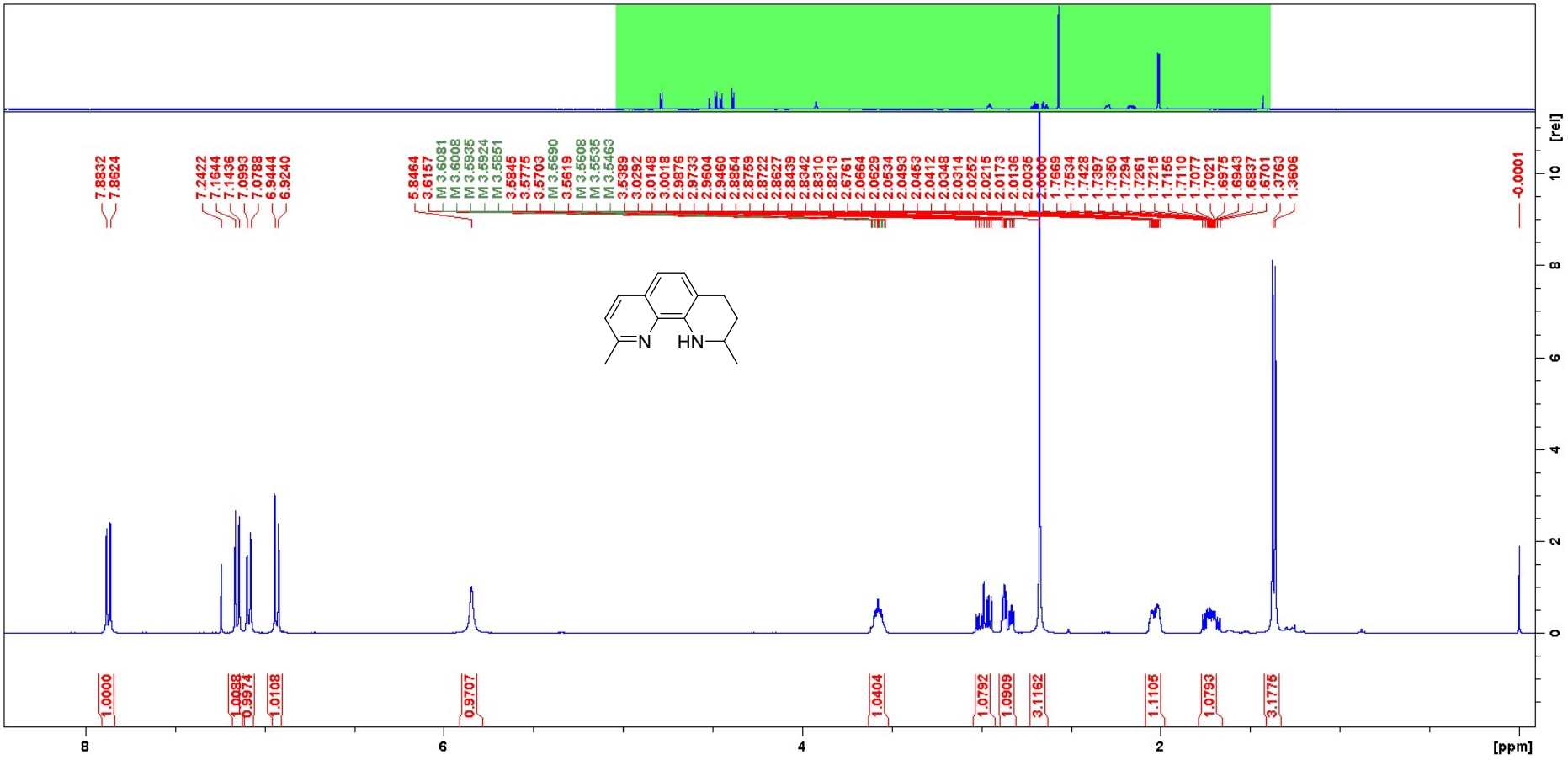

^{13}C NMR ($CDCl_3$) compound **5c**

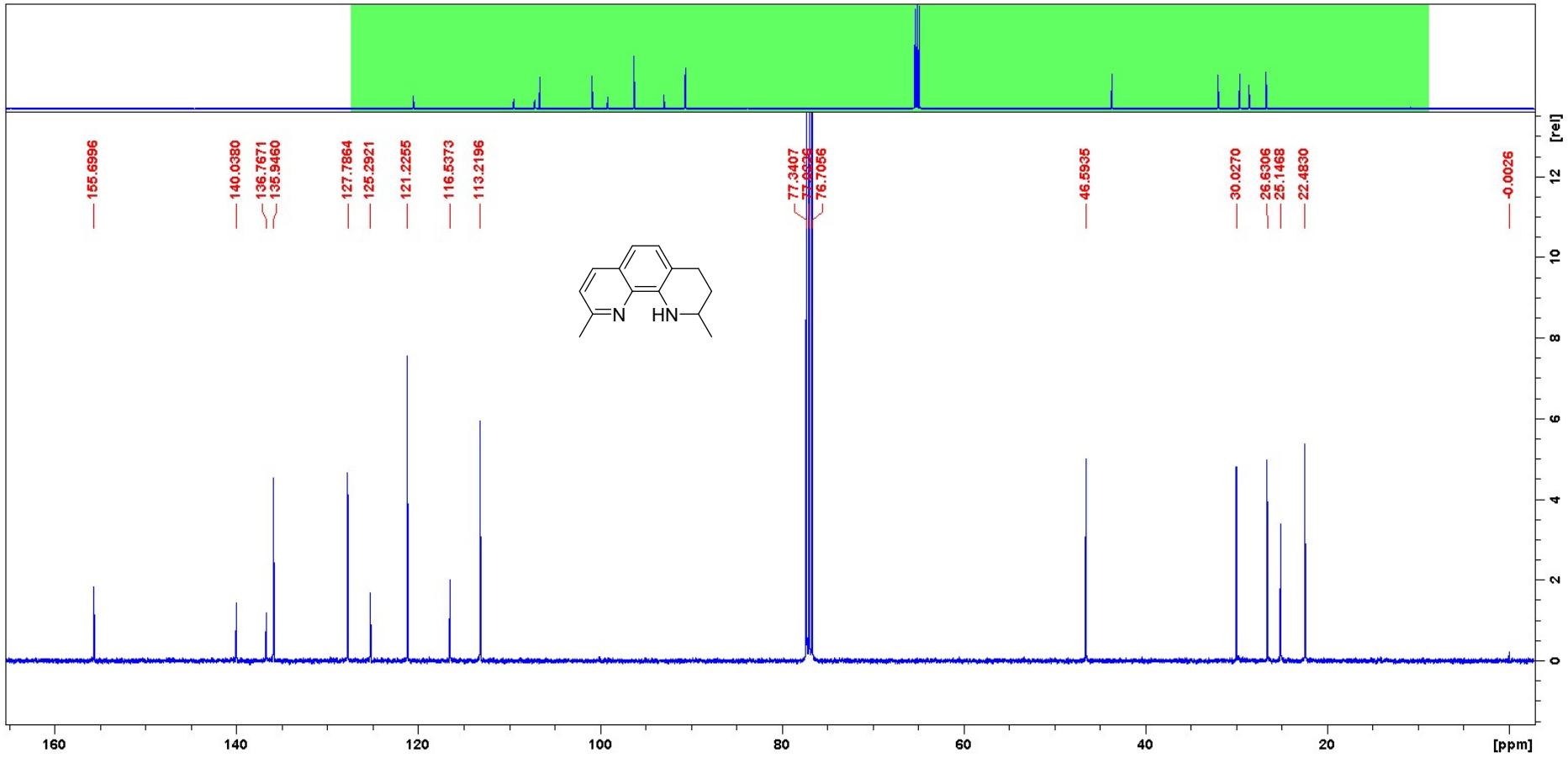

^{1}H NMR ($CDCl_3$) compound **5d**

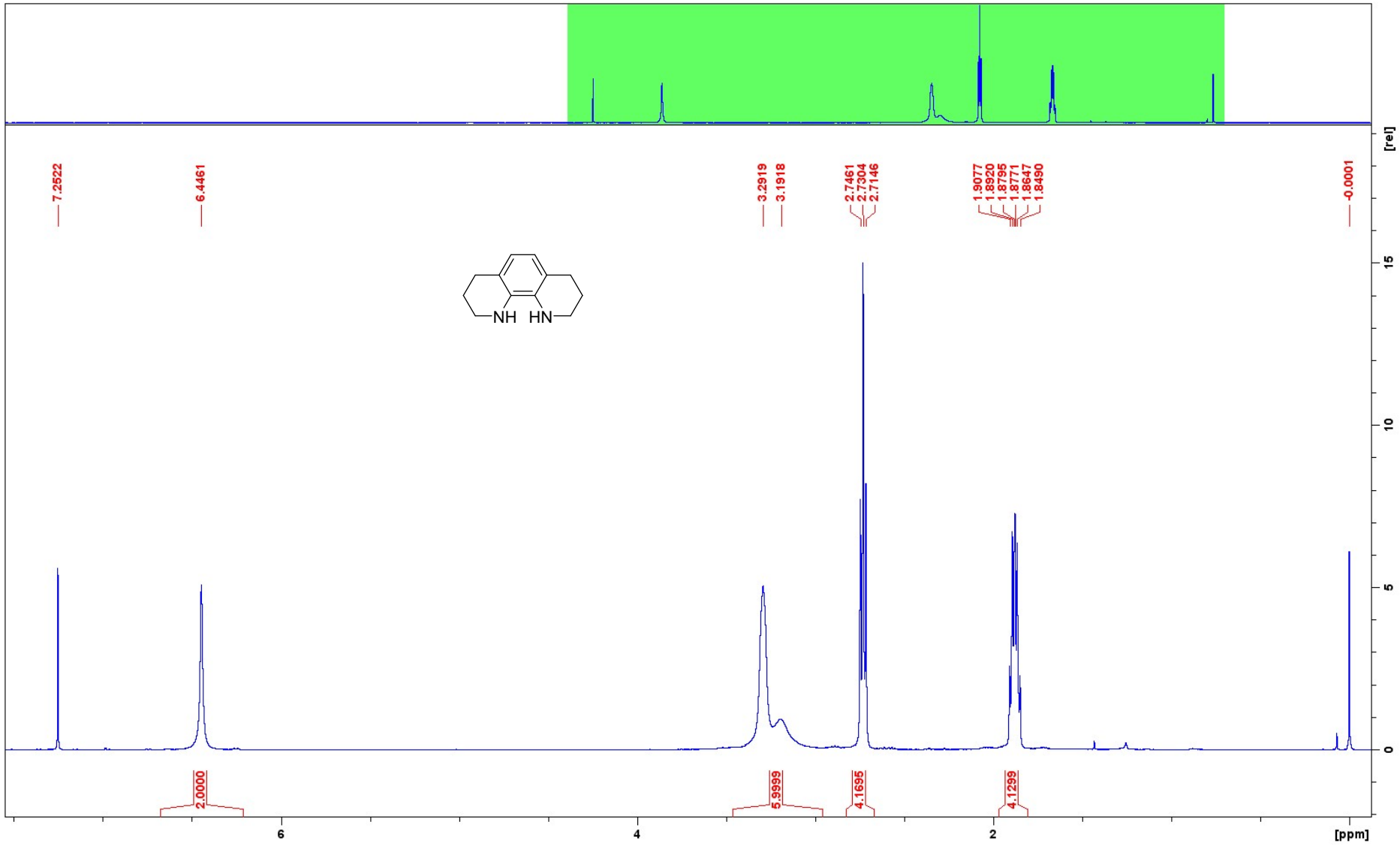

^{13}C NMR ($CDCl_3$) compound **5d**

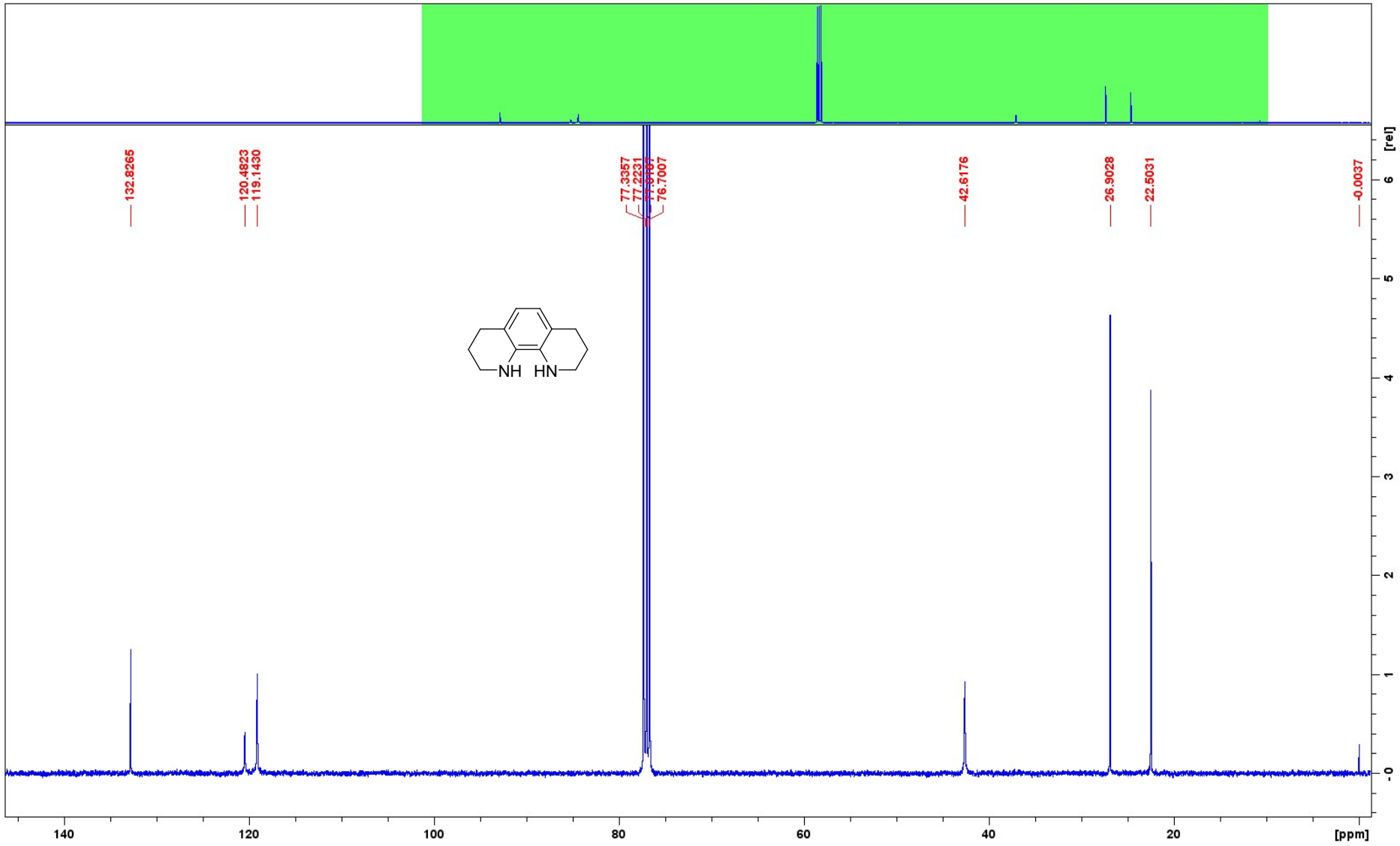

^{1}H NMR ($CDCl_3$) compound **5e**

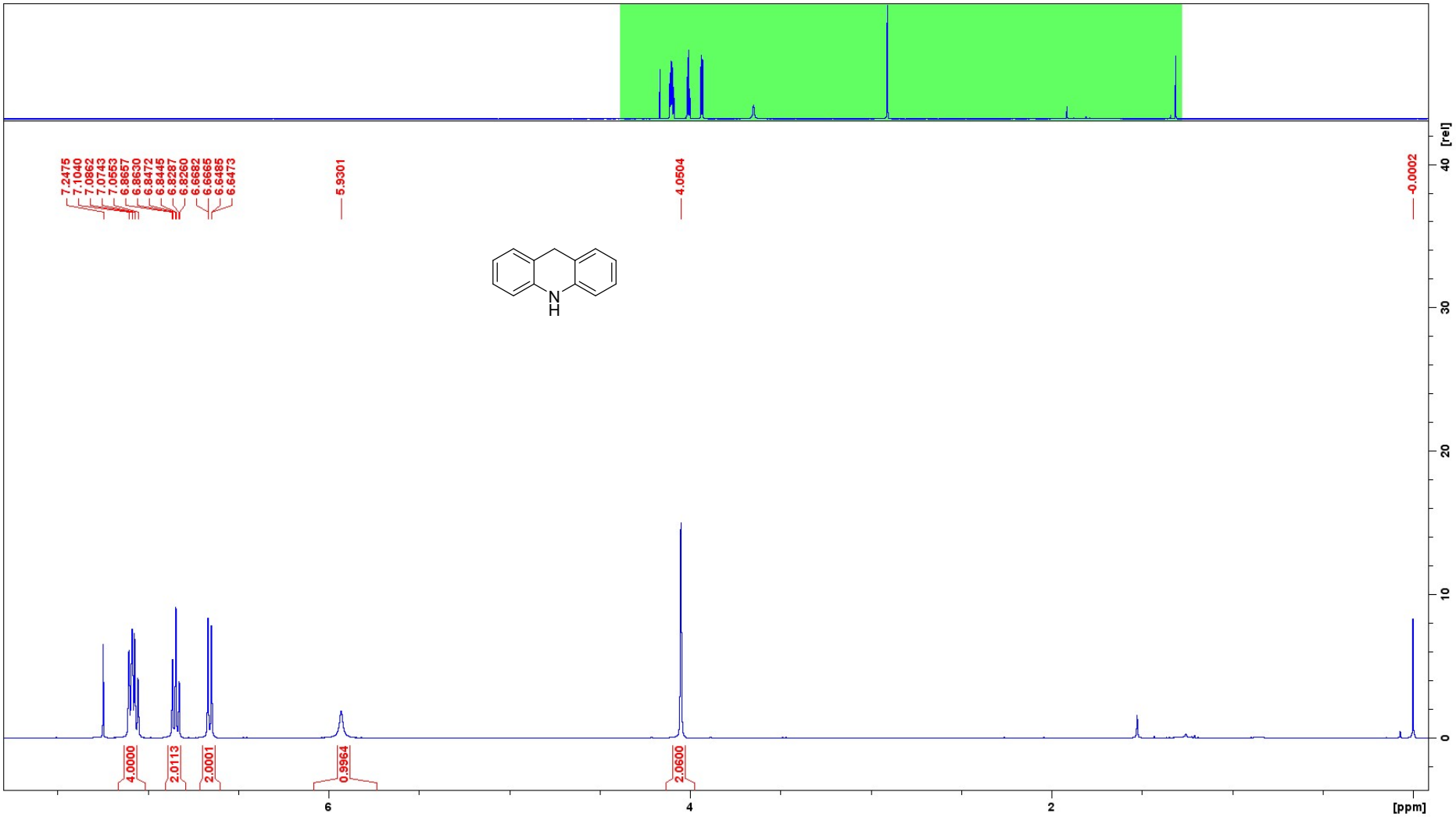

^{13}C NMR ($CDCl_3$) compound **5e**

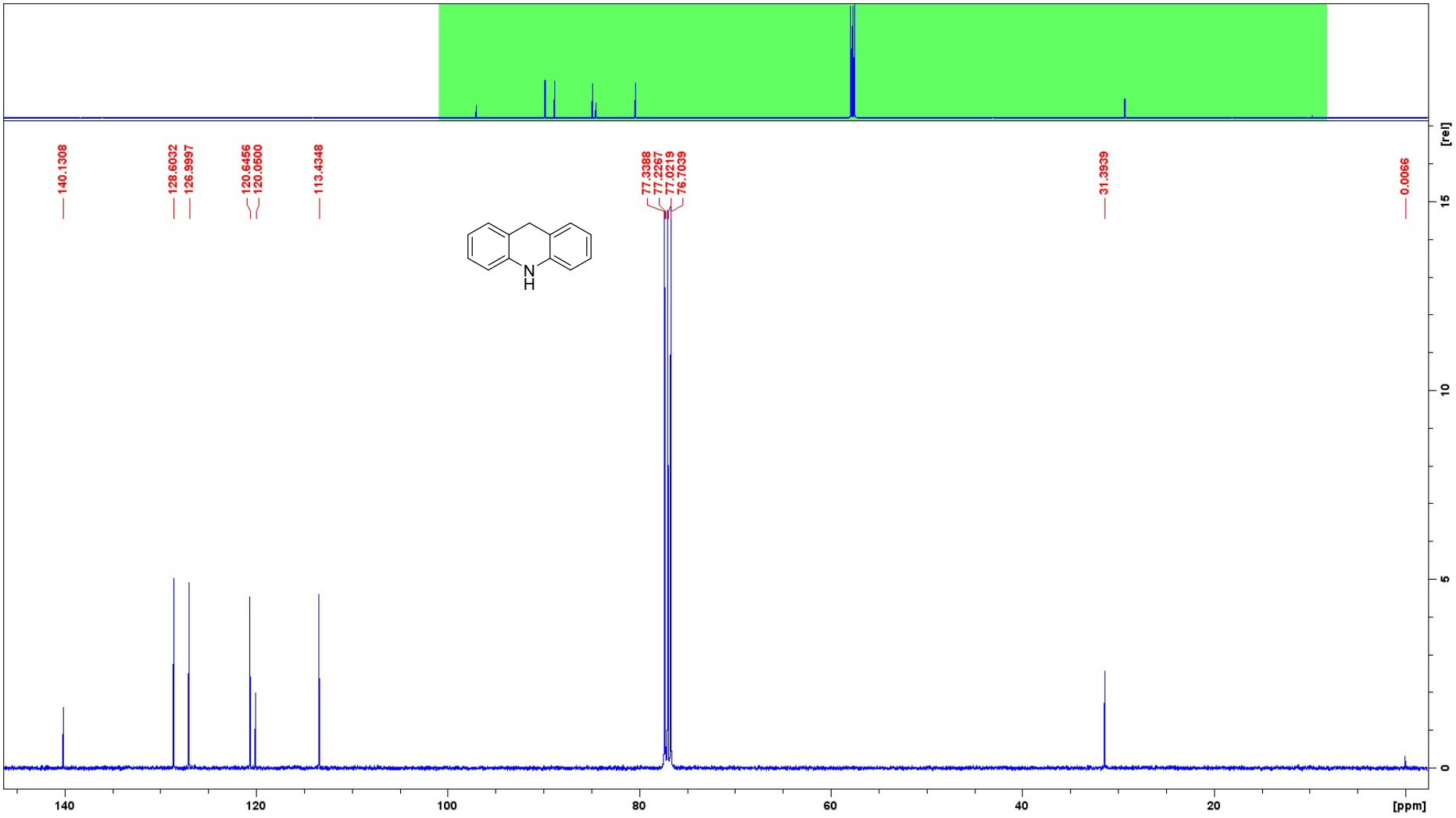

^{1}H NMR ($CDCl_3$) compound **5f**

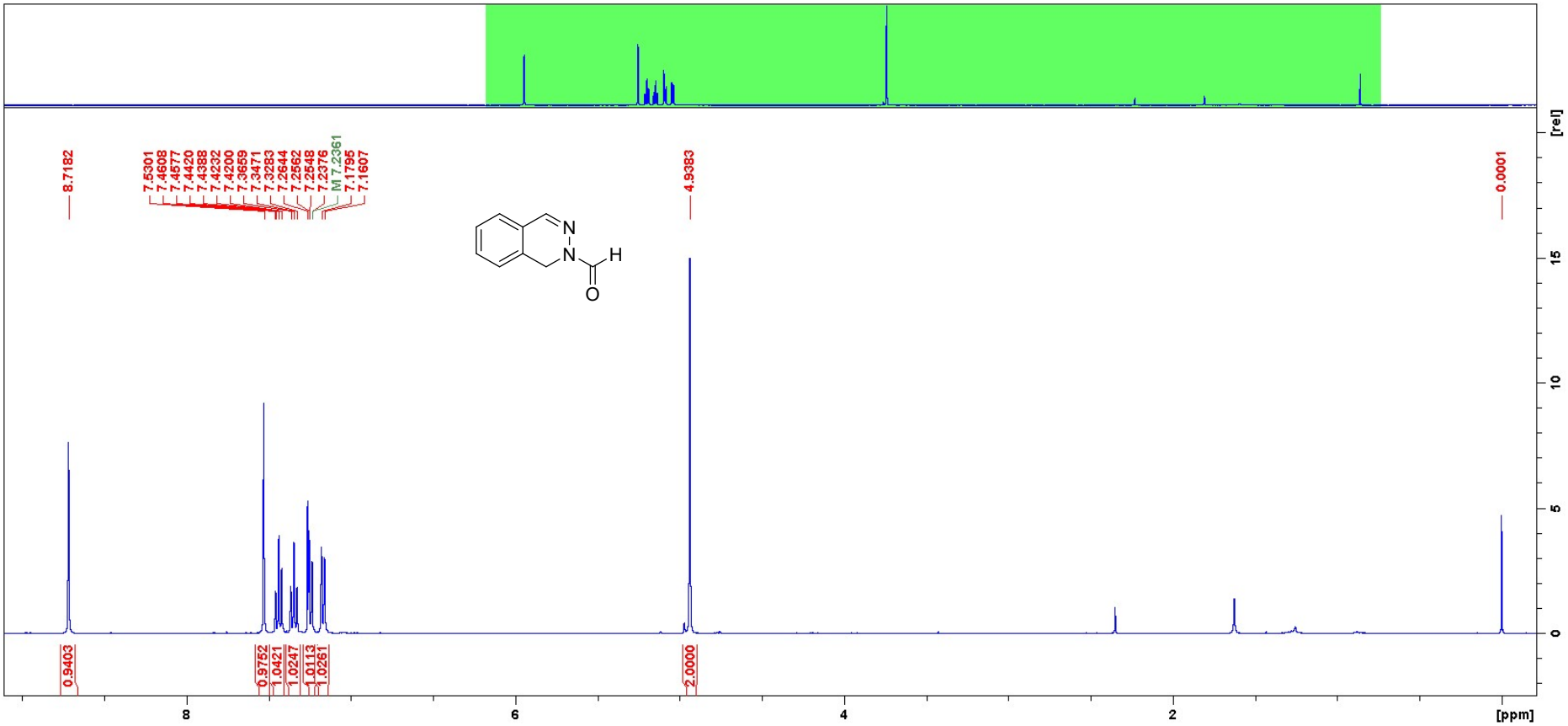

^{13}C NMR ($CDCl_3$) compound **5f**

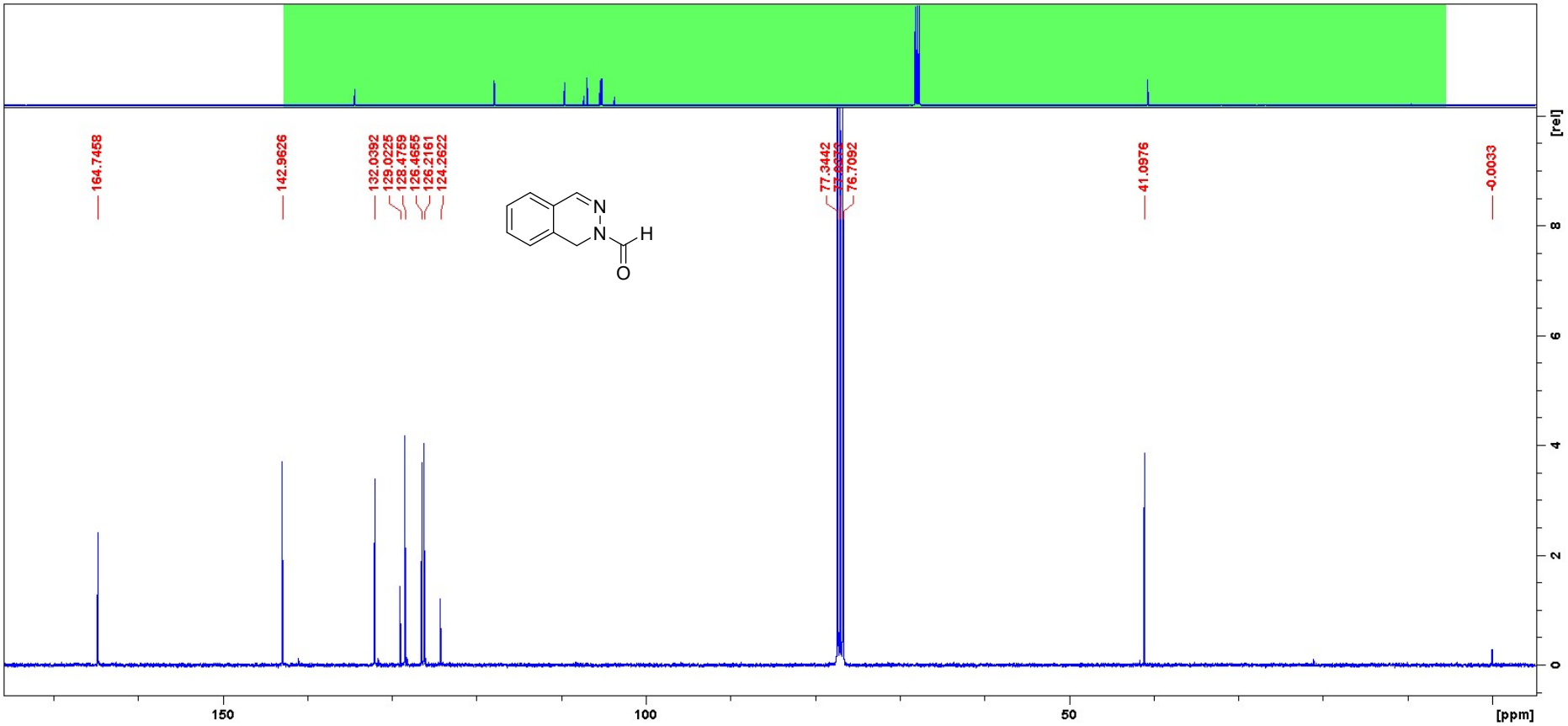

^{1}H NMR ($CDCl_3$) compound **6**

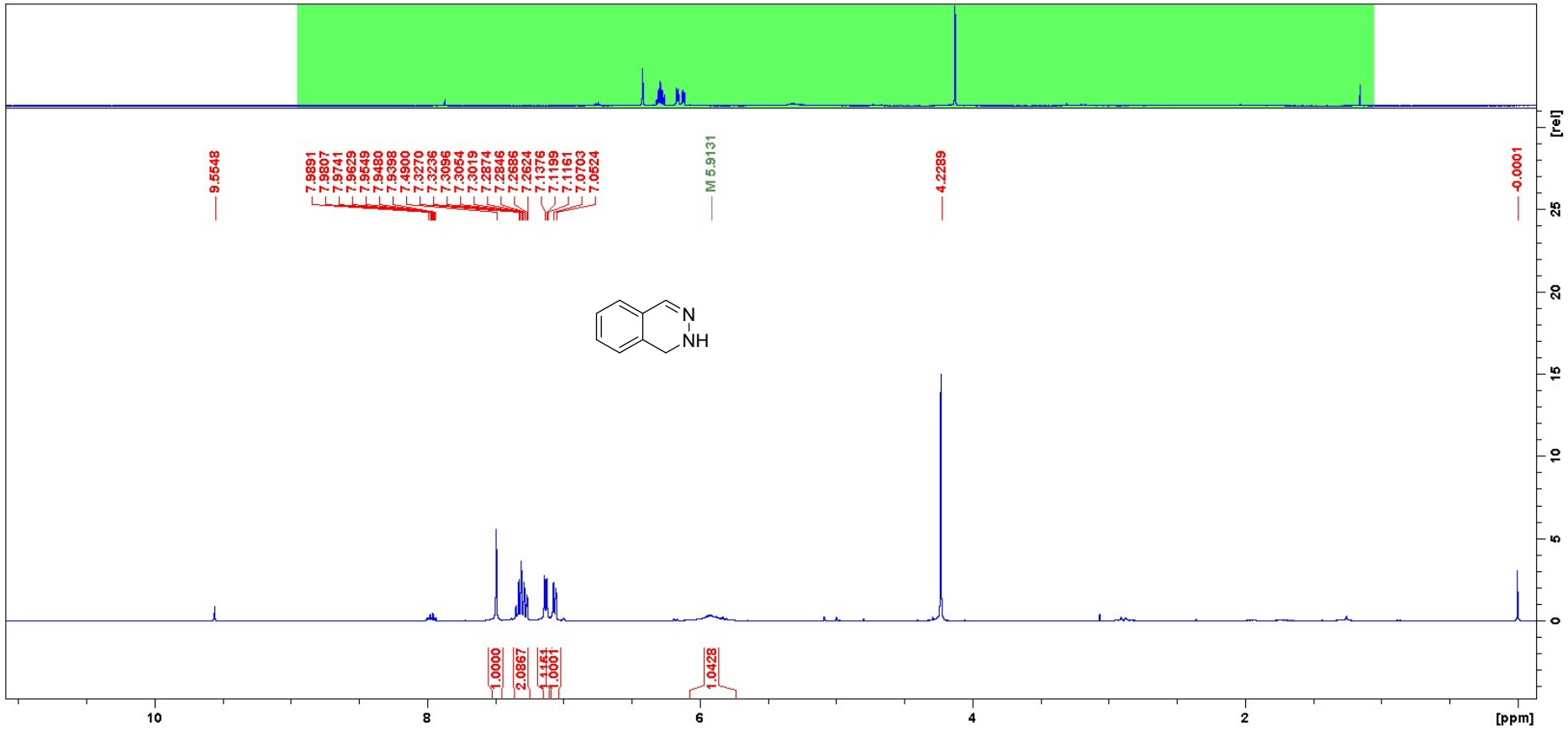

^{13}C NMR ($CDCl_3$) compound **6**

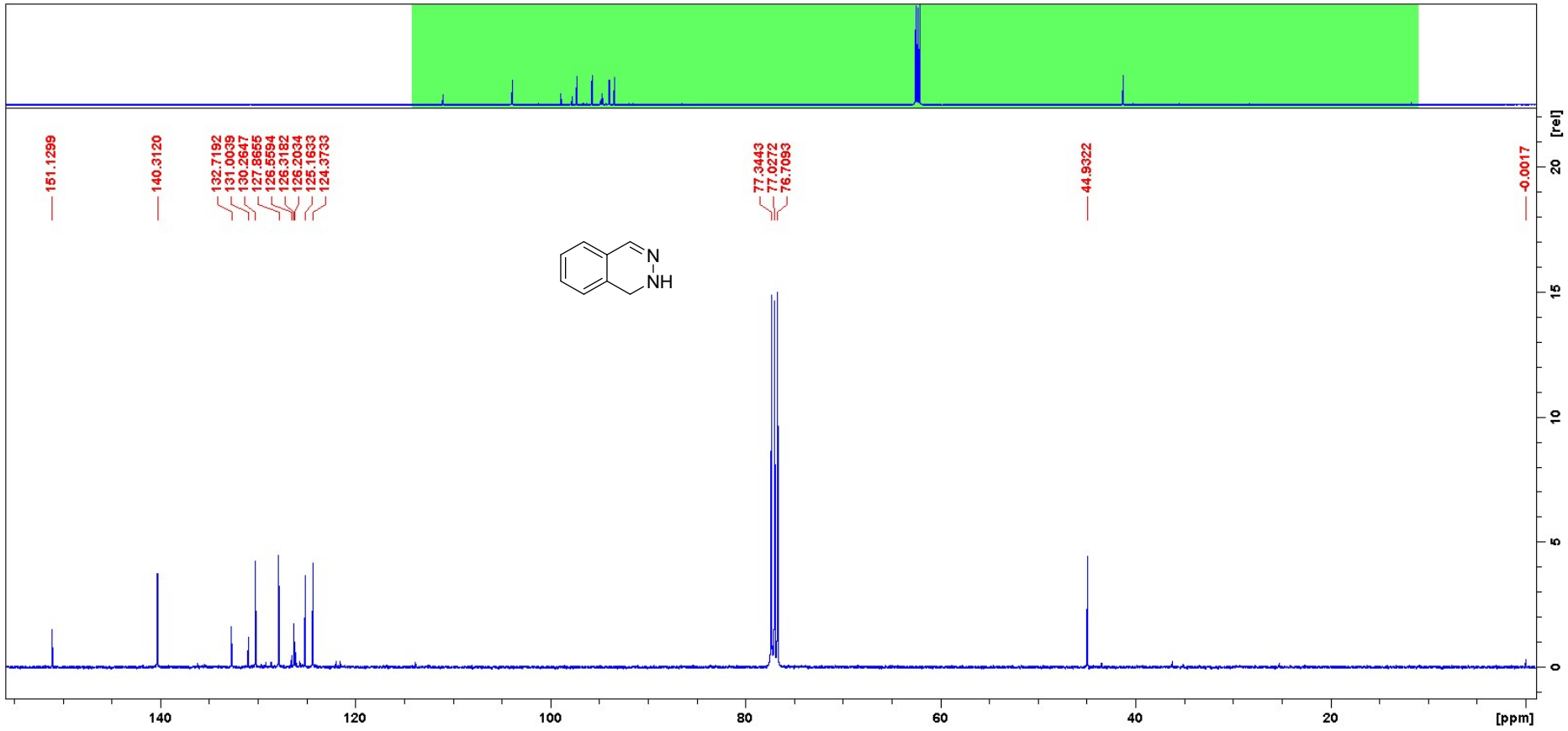

6 References

1 J. Rouquerol, P. Llewellyn and F. Rouquerol, in *Stud. Surf. Sci. Catal.*, eds. P. L. Llewellyn, F. Rodriquez-Reinoso, J. Rouqerol and N. Seaton, Elsevier, Amsterdam, 2007, vol. 160, pp. 49–56.

2 J. Everaert, M. Debruyne, F. Vanden Bussche, K. Van Hecke, T. S. A. Heugebaert, P. Van Der Voort, V. Van Speybroeck and C. V. Stevens, *Synthesis*, 2023, **55**, 333–340.

3 J. M. Veauthier, C. N. Carlson, G. E. Collis, J. L. Kiplinger and K. D. John, *Synthesis*, 2005, 2683–2686.

4 F. Fontana, F. Minisci, M. C. Nogueira Barbosa and E. Vismara, *Tetrahedron*, 1990, **46**, 2525–2538.

5 W. Tang, L. Xu, Q.-H. Fan, J. Wang, B. Fan, Z. Zhou, K.-h. Lam and A. S. C. Chan, *Angew. Chem. Int. Ed.*, 2009, **48**, 9135–9138.

6 M. Darabantu, L. Boully, A. Turck and N. Plé, *Tetrahedron*, 2005, **61**, 2897–2905.

7 J. Peralta-Cruz, M. Díaz-Fernández, A. Ávila-Castro, D. Ortegón-Reyna and A. Ariza-Castolo, *New J. Chem.*, 2016, **40**, 5501–5515.

8 J. Qin, F. Chen, Z. Ding, Y.-M. He, L. Xu and Q.-H. Fan, *Org. Lett.*, 2011, **13**, 6568–6571.

9 Z. Zhang and H. Du, *Angew. Chem. Int. Ed.*, 2015, **54**, 623–626.

10 A. Go, G. Lee, J. Kim, S. Bae, B. M. Lee and B. H. Kim, *Tetrahedron*, 2015, **71**, 1215–1226.

11 G. H. Fisher and H. P. Schultz, *J. Org. Chem.*, 1974, **39**, 635–640.

12 N. Mršić, T. Jerphagnon, A. J. Minnaard, B. L. Feringa and J. G. de Vries, *Adv. Synth. Catal.*, 2009, **351**, 2549–2552.

13 H.-X. Lei, K. Zhang, Y.-X. Qin, R.-J. Dong, D.-Z. Chen, H. Zhou and X.-H. Sheng, *J. Mol. Struct.*, 2021, **1228**, 129485.

14 S. Li, W. Meng and H. Du, *Org. Lett.*, 2017, **19**, 2604–2606.

15 W. Yoshihisa, O. Tetsuo, T. Yasushi, H. Takao and T. Yasuo, *Bull. Chem. Soc. Jpn.*, 1984, **57**, 2440–2444.

16 J. R. Cabrero-Antonino, R. Adam, K. Junge, R. Jackstell and M. Beller, *Catal. Sci. Technol.*, 2017, **7**, 1981–1985.

17 C. Bianchini, V. Dal Santo, A. Meli, S. Moneti, R. Psaro, L. Sordelli and F. Vizza, *Inorg. Chim. Acta*, 2008, **361**, 3677–3680.

18 W. M. Czaplik, J.-M. Neudörfl and A. J. von Wangelin, *Green Chem.*, 2007, **9**, 1163–1165.

19 J. Wu, C. Wang, W. Tang, A. Pettman and J. Xiao, *Chem. Eur. J.*, 2012, **18**, 9525–9529.

20 F. Chen, B. Sahoo, C. Kreyenschulte, H. Lund, M. Zeng, L. He, K. Junge and M. Beller, *Chem. Sci.*, 2017, **8**, 6239–6246.

21 C.-K. Sha and C.-P. Tsou, *J. Chin. Chem. Soc.*, 1991, **38**, 183–186.

22 O. V. Dolomanov, L. J. Bourhis, R. J. Gildea, J. A. K. Howard and H. Puschmann, *J. Appl. Crystallogr.*, 2009, **42**, 339–341.

23 G. Sheldrick, *Acta Crystallogr. Sect. A*, 2015, **71**, 3–8.

24 G. Sheldrick, *Acta Crystallogr. Sect. C*, 2015, **71**, 3–8.